# Investigating QseBC and PmrAB two-component system cross-interactions

By

Kirsten Raquel Guckes

Dissertation

Submitted to the Faculty of the

Graduate School of Vanderbilt University

in partial fulfillment of the requirements

for the degree of

DOCTOR OF PHILOSOPHY

in

Microbiology and Immunology

May, 2017

Nashville, Tennessee

Approved:

Eric P. Skaar, Ph.D., M.P.H.

Jonathan M. Irish, Ph.D.

Thomas Stricker, M.D., Ph.D.

Oscar Gomez, M.D., Ph.D.

Maria Hadjifrangiskou, Ph.D.

For Logan, Mom, Dad, and Alex

ACKNOWLEDGEMENTS

I would like to express my gratitude to my advisor, Dr. Maria Hadjifrangiskou, for her guidance and training, which were instrumental in both the completion of this thesis as well as my development as a young scientist. I am grateful to my thesis committee for their support and direction in both the advancement of my thesis project and my career goals. I am thankful to my fellow Hadjifrangiskou lab mates, both current and emeritus, for their scientific and personal support throughout my graduate career. I would also like to thank my fellow Vanderbilt University Interdisciplinary Graduate Program colleagues for their friendship.

TABLE OF CONTENTS

LIST OF FIGURES

Figure Page

LIST OF TABLES

Table Page

LIST OF ABBREVIATIONS

AE – Attaching and effacing lesions

AI – Autoinducer

CR – Congo Red dye

CRE – Carbapenem resistant *Enterobacteriaceae*

EMSA – Electrophoretic mobility shift assay

EHEC – Enterohemorrhagic *E. coli*

ExPEC – Extra-intestinal pathogenic *E. coli*

FRET – Förster resonance energy transfer

GFP – Green fluorescent protein

LPS – Lipopolysaccharide

PMB – Polymyxin B

PmrAB – Polymyxin resistance AB

PTS – Phosphotransferase system

qPCR – quantitative polymerase chain reaction

QseBC – Quorum sensing *E. coli* BC

SNP – Single nucleotide polymorphism

T6SS – Type VI secretion system

TCS – Two-component system

TLR – Toll-like receptor

UTI – Urinary Tract Infection

UPEC – Uropathogenic *Escherichia coli*

YESCA – Yeast extract-Casamino Acids

# CHAPTER I

# INTRODUCTION

## Introduction

Bacteria encounter and deftly respond to a myriad of environmental signals, yet only have the genomic capacity to encode a finite number of signaling systems that intercept stimuli and transduce them to the bacterial cell interior. This work describes one mechanism by which bacteria expand their response inventory, using few two-component systems (TCSs). Using uropathogenic *E. coli* (UPEC) as a model pathogen that occupies multiple host niches, but encodes only 35 TCSs, we demonstrate that signaling systems can interact to mediate responses to stressors, such as cationic polypeptides. The research in this dissertation focuses on the cross-interactions between two closely related bacterial two-component signaling systems, PmrAB and QseBC, and the downstream effects, resulting from the interactions. Chapter II describes the discovery that PmrAB and QseBC interact, using a panel of mutants and biochemical approaches in the absence of signal. Chapter III provides evidence of QseBC-PmrAB cross-interaction during exposure to the signal ferric iron to mediate tolerance to polymyxin B. Chapter IV describes the regulatory mechanism used to control the expression of the QseBC two-component system and begins to investigate the conservation of this control mechanism in different phylotypes of *E. coli*. The ferric iron mediated QseBC-PmrAB global regulon is discussed in Chapter V. This thesis offers novel insight into the way bacteria use two-component system signaling to respond to relevant stimuli and highlights the significance of two-component system interactions in a human pathogen.

## Bacterial Two-component Systems

Bacteria must be able to efficiently sense and respond to their environment, especially those that live symbiotically within a host. The host environment can be harsh for both pathogens and commensals alike, and must be equipped to respond to variation in nutrient availability, evasion of the immune response, and competition with other bacteria. Two-component systems (TCSs) are one of the primary mechanisms that bacteria utilize to accomplish this goal. Over 98 percent of sequenced bacterial genomes contain at least one putative TCS (Laub & Goulian, 2007; Stock, Robinson, & Goudreau, 2000). The number of TCSs per genome correlates with the number of environmental niches that a particular bacterial species is known to encounter. For example, *Helicobacter pylori*, a strict gastric pathogen, possess three intact TCSs, while *Pseudomonas aeruginosa*, which can be colonize and infect a multitude of environments from plants to various damaged human tissues, possess an average of 60 TCSs (MiST Database). In their simplest form, TCSs are comprised of a sensor histidine kinase, which detects the changing environment, and a response regulator, which mediates the resulting alterations in bacterial behavior to respond to the environmental stressor (Stock et al., 2000).

### *Mechanism of signal transduction*

The typical sensor histidine kinase is a membrane embedded protein, located within the lipid bilayer of the bacterial cell membrane (Stock et al., 2000). These proteins canonically possess distinct domains: a sensing domain that typically lies extracytoplasmically, at least one transmembrane domain that spans the lipid bilayer, as well as a dimerization phosphotransfer

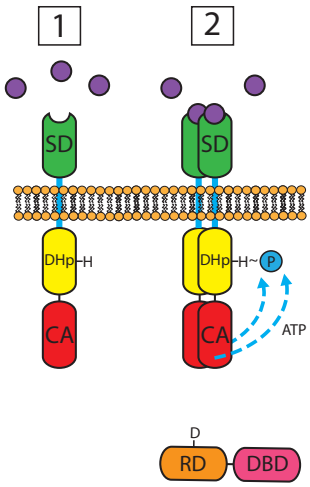


**Figure 1. Model of classical two-component system autophosphorylation**

The sensor kinase is shown here with the sensing domain (SD) in green, the transmembrane domain in blue, the dimerization and phosphotransfer domain (DHp) containing the conserved histidine residue in yellow, and the catalytic domain (CA). The response regulator is shown with the receiver domain (RD) containing the conserved aspartate residue in orange, and the DNA binding domain (DBD) in pink. [1] The system is unstimulated where both the sensor kinase and the response regulator likely exist as monomers without the presence of signal. [2] The sensor kinase detects the presence of signal, inducing dimerization and autophosphorylation at the conserved histidine of at least one of the sensor kinase monomers. The front blue arrow depicts autophosphorylation in *cis*, while the back blue arrow depicts autophosphorylation in *trans*.

domain and a catalytic domain, both of which reside in the cytoplasm ((Capra & Laub, 2012; Stock et al., 2000) and Fig. 1). Sensor kinases function as dimers, although whether they exist as monomers or dimers prior to signal detection remains unclear. Upon detection of a signal, the sensor kinase will hydrolyze ATP to autophosphorylate at a conserved histidine residue within the phosphotransfer domain. This can occur either *in cis*, where one monomer is using its own catalytic domain to hydrolyze ATP to phosphorylate the conserved histidine, or it can occur *in trans* where the ATP catalytic domain of one monomer facilitates the phosphorylation of the conserved histidine residue of the second monomer ((Capra & Laub, 2012; Gao & Stock, 2013; Stock et al., 2000) and Figure 1).

The partner, or cognate, response regulator then docks onto an interaction surface within the sensor kinase (Capra et al., 2010; Skerker et al., 2008). Once the kinase and regulator have established contact, the regulator catalyzes the transfer of the phosphoryl group from the histidine of the sensor kinase to a conserved aspartate on the response regulator ((Capra et al., 2010; Skerker et al., 2008) and Figure 2). The interaction surface between the sensor and regulator is composed of a series of amino acid residues that allow for specificity between the two proteins. The residues responsible for this stringent molecular recognition are referred to as co-evolving residues, because change in one or more residues on the kinase leads to compensatory changes in the residues of the response regulator to maintain high affinity interactions between the cognate pair and prevent interactions with other TCSs (Capra et al., 2012; Capra et al., 2010; Skerker et al., 2008) .

Once phosphorylated, the response regulator dimerizes and assumes a conformation that

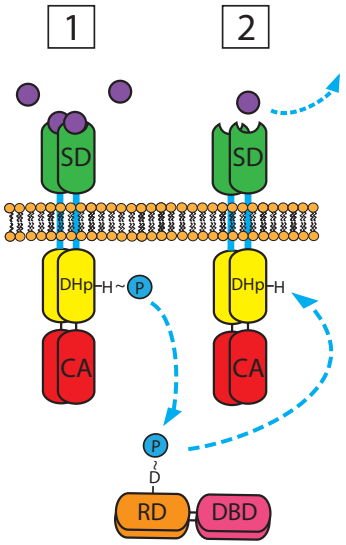


**Figure 2. Model of classical two-component system phosphotransfer and de-phosphorylation**

[1] The phosphoryl group is then transferred onto the conserved aspartate on the response regulator, causing dimerization and activation of that protein. [2] In many cases, sensor kinases exhibit phosphatase activity, removing the phosphoryl group from the response regulator, thereby allowing for re-sensitization of the system when a new system is detected.

allows its output domain to become functional; in most cases, this manifests as DNA binding, leading to a change in gene expression (Stock et al., 2000). Some TCSs are able to auto-regulate their own expression, meaning that the response regulator binds the promoter region of the operon that encodes the TCS, activating transcription. In these cases, the TCS transcript levels peak around 15 minutes after the bacteria have been exposed to the stimulating signal (Shin, Lee, Huang, & Groisman, 2006). Afterwards, transcript levels decrease as the bacteria respond to the stressor, requiring less of the TCS transcript to be made. This is known as an activation surge (Nairismagi et al., 2012; Shin et al., 2006).

Once the stimulus is no longer detected by the sensor kinase, the system "resets," so that it can appropriately respond to future incoming signals. To accomplish this, the sensor kinase can mediate the removal of the phosphoryl group from the response regulator in one of two ways: Either the kinase also exhibits activity or the kinase performs reverse phosphotransfer, where the phosphoryl group is transferred from the aspartate within the response regulator back to the conserved histidine of the sensor kinase ((Stock et al., 2000) and Figure 2).

*Evolution of two-component system fidelity and cross-interactions*

TCSs can be acquired via horizontal gene transfer or from gene duplication events and between bacteria. In the case of gene duplication, the interacting surfaces of the new TCS would have significant overlap with the interacting surfaces of the pre-existing TCS, allowing for phosphotransfer events to occur between non-cognate pairs (Figure 3). Therefore, newly acquired systems open the opportunity for cross-interactions between TCSs, which can lead to response outputs that are not appropriate for the signal that is detected. Thus, to maintain specific interactions between cognate partner proteins, evolutionary pressure selects for co-

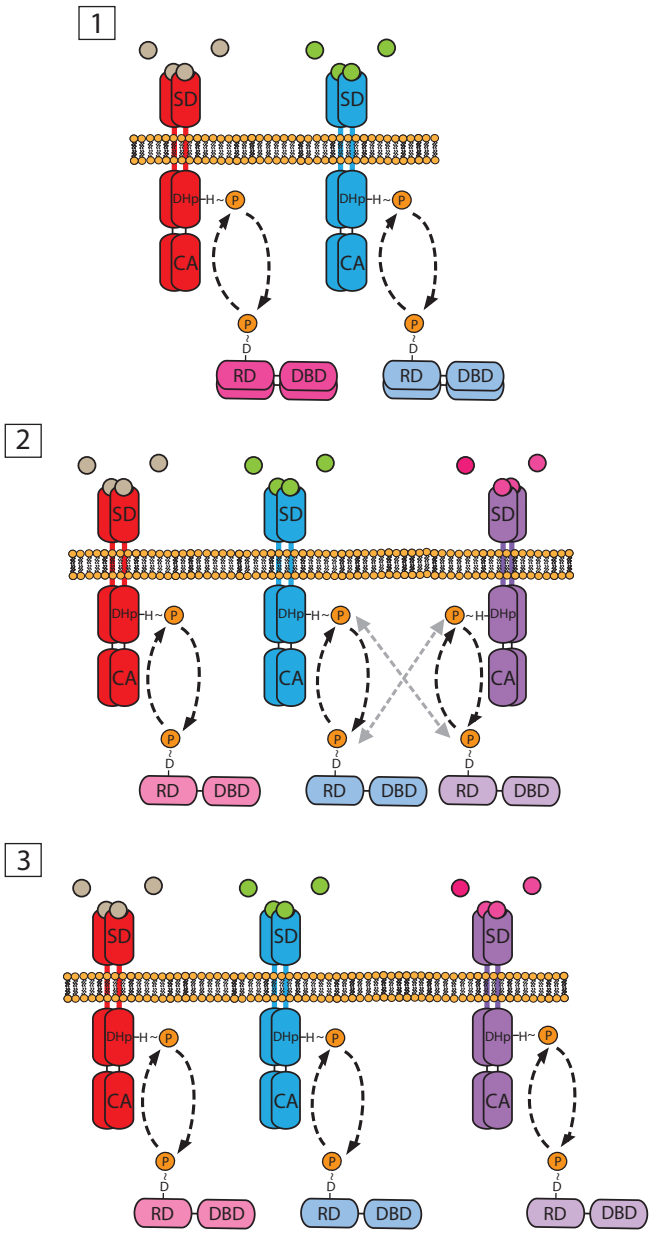


**Figure 3. Evolution of two-component systems.**

As the bacteria acquire new systems, cross-interactions between non-cognate partners acts as an intermediary stage during the course of evolution before divergence is achieved. Box 1 indicates two non-interacting two-component systems (red and blue) before the gene duplication event. Box 2 indicates the cross-interactions between non-cognate protein pairs after a gene duplication event of the blue system, giving rise to the purple TCS. Even as the bacteria detect different signals, the outputs are uncontrolled, as the sensor kinases cannot discriminate between response regulators. Box 3 indicates the post-divergence state, where each two-component system has moved into its own sequence space and cross-interactions have been eliminated.

evolving residues on the sensor kinase and response regulator of one TCS pair to diverge from those of the pre-existing TCS. The selection for mutations that maintain specificity between cognate partners and the selection against mutations that allow for interactions with non-cognate partners is described as the TCS movement through 'sequence space' ((Capra & Laub, 2012) and Figure 3).

Intrinsic mechanisms, such as co-evolving residues, maximize specificity within TCSs and minimize interactions with other TCSs. However, there have been reports of non-cognate interactions between TCS constituents with a beneficial outcome for the bacterium. A handful of previous studies have described sensor kinases that are capable of phosphorylating both their cognate partner, as well as a non-cognate response regulator in wild-type bacterial cells (Drepper et al., 2006; Matsubara, Kitaoka, Takeda, & Mizuno, 2000; Mika & Hengge, 2005; Rabin & Stewart, 1993). These examples can be found in multiple bacterial species, including *Bacillus subtilis* (Howell, Dubrac, Noone, Varughese, & Devine, 2006), *E. coli* (Matsubara et al., 2000), and *Rhodobacter capsulatus* (Drepper et al., 2006). In these examples, cross-regulation between TCSs is critical to mediate an appropriate response to environmental stress.

Specifically, in *R. capsulatus,* the interacting NtrBC and NtrXY TCSs have been reported to cross-interact in order to mediate nitrogen responses. Bacteria lacking the NtrC response regulator, or both NtrY and NtrB sensor kinases cannot properly utilize molecular nitrogen ($N_2$) or urea as a nitrogen source. This suggests interactions between non-cognate partners NtrY and NtrC are critical in wild-type cells (Drepper et al., 2006). However, the exact signal that initiates NtrY - NtrC interactions is unknown.

In non-pathogenic K12 lineages of *E. coli*, two interacting TCSs, NarPQ and NarLX regulate nitrate metabolism. NarX and NarQ are the sensor kinases, where NarX preferentially

senses nitrate, while NarQ senses both nitrate and nitrite. Both NarQ and NarX are able to phosphorylate the response regulators NarL and NarP (Noriega, Lin, Chen, Williams, & Stewart; Rabin & Stewart, 1993). Interestingly, in response to signal, NarQ has a slight kinetic preference for the non-cognate NarL, even though it can still phosphorylate its cognate response regulator, NarP. On the other hand, activated NarX maintains strong kinetic preference for the cognate NarL, which allows NarX to de-phosphorylate NarL when nitrate is absent (Noriega et al.; Rabin & Stewart, 1993; Schröder, Wolin, Cavicchioli, & Gunsalus, 1994). Cross-interactions such as these have been proposed to act as a way to fine-tune molecular responses to the multitude of signals that bacteria must adapt to in ever changing environments. However, very little work has been performed on this subject, especially in pathogenic bacteria.

## Two-component System Signaling in Pathogenesis

The mammalian host encompasses multiple micro-environments with various stimuli bacteria must respond to in order to establish infection. Therefore, not surprisingly, TCSs have been found to be vital for virulence in multiple pathogens. In *Pseudomonas aeruginosa* the AlgR/FimS TCS controls multiple critical virulence factors, including biofilm formation, motility, and the Ysc type III secretion system (T3SS) (Belete, Lu, & Wozniak, 2008; Konyecsni & Deretic, 1988; Lizewski, Lundberg, & Schurr, 2002; Morici et al., 2007; Overhage, Lewenza, Marr, & Hancock, 2007; Whitchurch, Alm, & Mattick, 1996; Yu, Mudd, Boucher, Schurr, & Deretic, 1997). Although this system is central to signaling required for full virulence, the signal that stimulates the system is still unknown. Not many signals have been identified for TCSs that contribute to virulence of a pathogen. For instance, a deletion of the LisR/LisK, AgrA/AgrC, or VirR/VirS TCS in *Listeria monocytogenes* lead to attenuation; however, there is no known signal

for any of these TCSs (Autret, Raynaud, Dubail, Berche, & Charbit, 2003; Cotter, Emerson, Gahan, & Hill, 1999; Mandin et al., 2005). The PmrAB TCS in *Salmonella enterica* presents a rare case where the stimulus has been well characterized (Richards, Strandberg, Conroy, & Gunn, 2012; Wosten, Kox, Chamnongpol, Soncini, & Groisman, 2000). Ferric iron is able to stimulate the PmrB sensor kinase, leading to the phosphorylation of the PmrA response regulator, which then promotes the expression of genes involved in lipopolysaccharide (LPS) modifications (Kato, Chen, Latifi, & Groisman, 2012; Wosten et al., 2000).

PmrAB is also unique in that it indirectly interacts with another TCS, PhoPQ. The PhoQ sensor kinase is stimulated by low magnesium and cationic polypeptides, leading to PhoP phosphorylation, which is important for *Salmonella enterica* virulence (Bijlsma & Groisman, 2005; Groisman, 2001). In *Salmonella*, PhoP upregulates the expression of *pmrD*, which encodes an accessory protein that interacts with the response regulator PmrA. This physical interaction prevents PmrA from being dephosphorylated by its cognate sensor kinase PmrB and locks the PmrAB system in an activated state (Kato & Groisman, 2004). PmrD is negatively regulated by PmrAB, closing this regulatory circuit and preventing over-activation of the system (Guckes et al., 2013; Kato & Groisman, 2004). Notably, this interaction between the PhoPQ and PmrAB TCSs does not involve cross-phosphorylation between non-cognate sensors and regulators.

The QseBC TCS has been shown to be important to the pathogenesis of multiple bacterial species including various *E. coli* pathotypes, *Salmonella enterica*, and *Francisella tularensis* (Bearson & Bearson, 2008; Bearson, Bearson, Lee, & Brunelle, 2010; Clarke, Hughes, Zhu, Boedeker, & Sperandio, 2006; Kostakioti, Hadjifrangiskou, Pinkner, & Hultgren, 2009; Rasko et al., 2008). In all of these pathogens, deletion of *qseC* leades to severe virulence attenuation in

animal models of infection (Bearson & Bearson, 2008; Bearson et al., 2010; Clarke et al., 2006; Rasko et al., 2008). However, the mechanism of QseBC TCS signaling has been reported differently for two different *E. coli* pathotypes (Clarke et al., 2006; Clarke & Sperandio, 2005; Sperandio, Torres, Jarvis, Nataro, & Kaper, 2003). One hypothesis for this discrepancy is that the bacteria have evolved different signal transduction pathways driven by the different selection pressures found in distinct niches occupied by enterohemorrhagic *E. coli* (EHEC) and uropathogenic *E. coli* (UPEC) during pathogenesis.

*QseBC signaling in EHEC and UPEC*

EHEC is an enteric pathogen that causes bloody diarrhea and hemolytic-uremic syndrome (HUS), which can lead to life-threatening kidney failure due to the destruction of red blood cells (Stahl et al., 2015). The bacteria are typically transmitted from fecal-oral contamination (Nguyen & Sperandio, 2012). Once introduced to the host, EHEC must overcome obstacles including destructive enzymes in saliva, acid stress in the stomach, and bile salts in the small intestine (House et al., 2009; Nguyen & Sperandio, 2012). Upon entrance into the large intestine, the bacteria must penetrate the physical mucosal barrier to fully adhere to the intestinal epithelium (Nguyen & Sperandio, 2012). Upregulation of virulence factors such as those involved in flagella- mediated motility and attaching and effacing (AE) lesions allow the bacteria to successfully infect the host (Nakanishi et al., 2009). During infection, EHEC produce an exotoxin called Shiga toxin, which binds to cells in the gastrointestinal tract and inhibits protein synthesis by impairing ribosomes (Pacheco & Sperandio, 2012). This leads to apoptosis and pro-inflammatory responses within the gut (Pacheco & Sperandio, 2012). In addition to the physical and biochemical barriers associated with colonizing the mammalian gut, EHEC must also

overcome a biological barrier, competing for nutrients and space with commensal bacteria. The quorum sensing *E. coli* BC TCS was initially proposed to aid EHEC in communicating with commensal gut microbiota (Sperandio et al., 2003; Sperandio, Torres, & Kaper, 2002).

Initial studies led to the hypothesis that EHEC QseBC was used to sense and respond to bacterial signals as a means to communicate via quorum signaling (Sperandio et al., 2003; Sperandio et al., 2002). It was also reported that QseC was not sensing the previously characterized autoinducer (AI)-2 but in fact sensing a novel molecule, AI-3 (Sperandio et al., 2003). However, it was also determined that QseC could respond to the hormones epinephrine and norepinephrine which offered a platform for EHEC to potentially communicate host cells to coordinate virulence factor expression (Sperandio et al., 2003; Sperandio et al., 2002). EHEC QseC was reported to enhance phosphotransfer to cognate response regulator QseB in the presence of epinephrine (Clarke et al., 2006). QseC was proposed to bind epinephrine as a direct ligand, although biochemical evidence supporting this hypothesis is lacking (Clarke et al., 2006). Early reports concluded that because the deletion of the *qseC* caused a decrease in motility and the expression of flagellin, QseBC is a positive regulator of motility (Sperandio et al., 2002). As a result it was proposed that QseB is a classical TCS in which loss of the sensor kinase leads to the inability to activate the response regulator.

UPEC is the main causative agent of one of the most common bacterial infections: urinary tract infections (UTIs) (Hooton & Stamm, 1997). UTIs manifest as either infection of the bladder, cystitis, or of the kidneys, pyelonephritis (Foxman, 2010). They are among the most common primary diagnosis for female emergency visits and are responsible for roughly 3 billion dollars in healthcare costs per year in the US alone (Foxman, 2010). Outside the hospital setting, UTIs disproportionately affect women, with about 50% having at least one UTI during their

lifetime. Among these women who contract a UTI, about 24% will experience a second episode within 6 months of the first (Foxman, 2014).

The gut acts as a reservoir for UPEC, where the bacteria colonize but do not symptomatically infect the host (Moreno et al., 2008). Upon exit from the gut, the bacteria ascend the urethra and enter the bladder. To establish bladder infection, the bacteria must overcome the primary host defense against UTI, urination (Foxman, 2010). To prevent expulsion from the urinary tract, UPEC have evolved a multitude of strategies, including the expression of adhesive organelles that allow the bacterial cells to adhere to the bladder epithelium (Foxman, 2014; Mulvey et al., 1998). This initial adhesion step is crucial to UPEC pathogenesis and triggers the bacteria to become internalized by the superficial umbrella cells of the bladder (Bower, Eto, & Mulvey, 2005). Once inside the epithelial cell, UPEC are able to escape into the cytoplasm where they are able to replicate to form clonal populations of aggregated bacteria known as intracellular bacterial communities (IBCs) (Anderson et al., 2003; Justice et al., 2004). IBCs offer the bacteria a mechanism by which to evade host immune responses and stresses from antibiotic exposure (Anderson et al., 2003; Hannan, Mysorekar, Hung, Isaacson-Schmid, & Hultgren, 2010). The IBC matures and grows in size, until it erupts and filamentous bacteria are able to escape from the bladder cell. Using flagella-based motility, the bacteria either infect other bladder epithelial cells or ascend to the kidney (Wright, Seed, & Hultgren, 2005).

Similar to studies in EHEC, work focusing on UPEC QseC demonstrated that the loss of the sensor QseC leads to severe attenuation of UPEC in murine models of acute and chronic UTI (Hadjifrangiskou et al., 2012; Kostakioti et al., 2009). However, a detailed genetic analysis revealed that UPEC mutants lacking the QseB response regulator or the entire QseBC TCS are not defective in the acute infection stages (Kostakioti et al., 2009). In UPEC, deletion of *qseC*

also resulted in low motility compared to WT, but deletion in *qseB* or the entire *qseBC* operon had no effect on motility (Kostakioti et al., 2009). It was shown that in UPEC, a deletion in *qseC* led to an accumulation of phosphorylated QseB, which leads to a down regulation of flagella expression and motility (Hadjifrangiskou et al., 2011; Kostakioti et al., 2009). This contradicts what has been reported in EHEC, making QseB a repressor of motility in UPEC (Kostakioti et al., 2009; Sperandio et al., 2002). Another intriguing observation was the accumulation of phosphorylated QseB in the absence of *qseC*, suggesting that QseB can be activated by a moiety other than its cognate sensor kinase (Hadjifrangiskou et al., 2011; Kostakioti et al., 2009).

**Unanswered questions in two-component system biology**

The differences reported in the QseBC TCS signal transduction between UPEC and EHEC provide a platform for investigating questions widely relevant to TCS biology. One such question being how bacteria are able to utilize TCS cross-interactions to fine-tune responses to relevant environmental stimuli. Given the divergent phenotypes observed with QseB and QseC cognate partners, we hypothesized that in the absence of QseC, something else activates QseB. Chapter II describes an additional sensor kinase, PmrB, that is able to phosphorylate QseB, defining the molecular mechanism of cross-interactions between two TCSs in UPEC (Guckes et al., 2013).

Often, the signals that TCSs respond to are difficult to identify, making it extremely difficult to investigate the relevance of a particular TCS to bacterial fitness or virulence in the case of pathogens. Chapter III describes QseBC and PmrAB cross-interactions and corresponding phenotypic output in the form of antibiotic tolerance in response to the stimulating

signal ferric iron. Control of the most upstream gene target, *qseBC,* as well as the conservation of this promoter region is described in Chapter IV.

The differences between UPEC and EHEC are much greater than simply the QseBC signals and downstream gene regulation. These bacteria occupy different niches in the host, and therefore have different pathogenic strategies during infection. Thus it is possible that evolutionary pressure is responsible for the divergence in signaling mechanisms. Chapter IV outlines sequence variants in *qseBC* regulatory regions, which group to the different *E. coli* pathotypes, supporting this hypothesis. For additional insight as to the physiological relevance of ferric iron responses that are specific to UPEC, we began to investigate the UTI89 global regulon in response to ferric iron, which is described in Chapter V.

CHAPTER II

# STRONG CROSS-SYSTEM INTERACTIONS DRIVE THE ACTIVATION OF THE QSEB RESPONSE REGULATOR IN THE ABSENCE OF ITS COGNATE SENSOR

A portion of this work has been published in the "Proceedings of the National Academy of the Sciences" journal as **Guckes KR***, Kostakioti M*, Breland EJ, Gu AP, Shaffer CL, Martinez CR 3rd, Hultgren SJ, Hadjifrangiskou M. 2013 Oct 8;110(41):16592-16597.

PMID: 24062463

*Both authors contributed equally to this work

## Introduction

As UPEC infect the urinary tract, the bacteria perform a complex pathogenic cascade, which requires elegant detection of and response to both extracellular and intracellular cues to accomplish. Prior to this work, it had been reported that deletion of the sensor kinase *qseC* in UPEC leads to misregulation of gene expression and/or virulence attenuation (Hadjifrangiskou et al., 2011; Kostakioti et al., 2009). The Δ*qseC*-related defects in UPEC are a result of increased activity of the QseB response regulator, which results in increased *qseB* expression, misregulation of conserved metabolic pathways and downregulation of virulence-associated genes (Hadjifrangiskou et al., 2011; Kostakioti et al., 2009). Therefore, presumably, *qseC* deletion interferes with QseB de-phosphorylation; however, the source of QseB activation in the absence of its cognate sensor QseC was undefined. In the data outlined in this chapter, we

present evidence that UPEC QseB becomes phosphorylated, by a non-cognate sensor histidine kinase, PmrB.

## Methods

*Strains and constructs*

Experiments here were performed in *E. coli* cystitis isolate UTI89 and isogenic derivatives. UTI89Δ*qseC*, UTI89Δ*qseB* and UTI89Δ*qseBC* were created previously (Kostakioti et al., 2009). UTI89Δ*qseC*Δ*pmrB*, UTI89Δ*qseC*Δ*pmrA* and UTI89Δ*pmrA* were created following the recombineering method of Murphy & Campellone using λ Red recombinase (Murphy & Campellone, 2003). pPmrB was created using vector pTrc99A (Invitrogen) as a backbone and inserting the *pmrB* (UTI89_C4706) coding sequence downstream of its native promoter. To create pPmrB_H155A, site-directed mutagenesis was performed on pPmrB, using *Pfu* Ultra DNA polymerase (Stratagene). Tagged constructs pPmrB-mycHis and pPmrB_H155A-mycHis were created by amplifying the *pmrB* gene from pPmrB or pPmrB_H155A, and subsequently cloned into backbone vector pBADmyc-HisA (Invitrogen). Constructs pQseC, pQseC-mycHis, and the transcriptional reporter plasmid pP*qse*::GFP were previously constructed (Kostakioti et al., 2009).

*Transposon mutatgenesis, suppressor screening, and Congo red uptake assays*

Electro-competent UTI89Δ*qseC* cells and transposon mutagenesis were performed as previously described (Hadjifrangiskou et al., 2012). Briefly, 260ng of the EZ-Tn5™ <R6Kγori/KAN-2>Tnp Transposome™ (Epicentre) was electroporated in 100 μl of UTI89Δ*qseC* electro-competent cells, followed by a 60 minute recovery in SOC media at 37°C.

The entire transposition reaction was diluted 1 : 10,000 and spread on LB – Kanamycin plates in 100 µl aliquots.

Kanamycin resistant transposants were patch-plated on YESCA (1 g yeast extract, 10 g casamino acids, 20 g agar/L) agar supplemented with Congo red (CR), and incubated at 30°C for 48h. Each YESCA-CR plate included streaks of WT UTI89 and UTI89Δ*qseC* as positive and negative controls. UTI89 appears red on Yesca-CR, while UTI89Δ*qseC* appears white.

*Transposition Mapping*

UTI89Δ*qseC* transposon mutants that displayed a red (WT) phenotype on Yesca-CR media were treated for DNA isolation and subsequent transposon mapping using the multiple-round PCR procedure of Ducey and Dyer (Anriany, Sahu, Wessels, McCann, & Joseph, 2006; Ducey, Carson, Orvis, Stintzi, & Dyer, 2005) and primers Inv-1 (ATGGCTCA-TAACACCCCTTGTATTA) or Inv-2 (GAACTTTTGCTGAGTTGAAGGATCA). Resulting amplicons were purified (Qiagen) and sequenced using the KAN-2 FP-1 Forward and KAN-2 RP-1 Reverse primers supplied by Epicentre.

*Immunoblots, HA and phase assays*

For type 1 pili, bacteria were incubated in LB media at 37˚C for 4h under shaking conditions, sub-cultured (1:1000) in fresh LB media and incubated statically at 37˚C for 18h. Immunoblots (using anti-type 1 pili), HA and phase assays were performed on normalized cells ($OD_{600}$=1) as previously described (Kostakioti et al., 2009) with the exception of the FimA western blot in Fig. 5A; in this blot, the secondary antibody used was Alexa Fluor 680 donkey anti-rabbit IgG (Life Technologies), diluted 1:10,000 in Odyssey blocking buffer (Li-Cor

Biosciences) with 0.1% Tween-20, and applied for 30 minutes. Blot was then imaged on an Odyssey infrared imaging system (Li-Cor Biosciences) in the 700 nm channel.

*Motility assays*

Motility assays were performed as previously described (Wright et al., 2005). Briefly, bacteria were inoculated in LB and incubated statically at 37°C for 18 h. Bacteria from the overnight culture were stabbed in the center of 0.25% LB agar/0.001% 2,3,5-triphenyltetrazolium chloride using a sterile inoculating rod and allowed to swim outwards from the inoculation point for 7 h at 37°C. Motility diameters were recorded for 5 biological replicates with triplicate plates/strain per experiment.

*RNA extraction and qPCR*

Total RNA was isolated from *E. coli* UTI89 and isogenic mutants. Cells were broken open by enzymatic lysis using TE buffer (10 mM Tris-Cl, 1 mM EDTA, pH 8.0) containing 1 mg/ml lysozyme. RNA was extracted using the RNeasy kit (Qiagen) and DNase-treated using Turbo DNase I (Ambion). First strand cDNA synthesis was performed using 1µg DNAse treated RNA and the Superscript II Reverse Transcriptase kit (Invitrogen) following the manufacturer's protocol. For *qseB* qPCR: WT UTI89, UTI89Δ*qseC* and UTI89Δ*qseC*Δ*pmrB* cDNA was generated from RNA samples of cells grown statically at 37°C for 18h in LB. Serial cDNA dilutions (25, 12.5, 6.25, 3.125 and 1.5625 ng/µl) were used for qPCR, with *qseB*- and *rrsH*-specific primers (Kostakioti et al., 2009) according to the manufacturer's instructions (BioRad). Relative fold difference was determined by the ΔΔCt method (Pfaffl, 2001). Experiment was

repeated with five separately obtained biological replicates with triplicate reactions/cDNA dilution.

For *gfp* qPCR, samples for RNA extraction and reverse transcription were obtained from cells grown statically at 37°C for 18 h in N-minimal media (0.1% casamino acids, 38 mM glycerol, 22 mM glucose, and 10 μM $MgCl_2$, pH 7.7) with and without 100 mM $FeCl_3$. Quantitative real time PCR was executed in triplicate on an ABI StepOne Plus Real Time PCR machine, using multiplexed TaqMan MGB chemistry. Two dilutions of cDNA (25 ng and 6.25 ng) were analyzed per isolate for each experimental condition. Abundance of *gfp* transcripts (probe: 5'6FAM-ACGTGCTGAAGTCAAG3') in UTI89 isogenic mutant strains was calculated using the ΔΔCT method, with each transcript signal normalized to the abundance of the *rrsH* (probe: 5'VIC-CGTTAATCGGAATTACTG3') internal control and comparison to the normalized transcript levels of WT UTI89. Abundance of *pmrB* transcripts (probe: 5'6FAM-ACGCCCATTGCCA) was calculated as above, but normalized to the abundance of the *gyrB* internal control (probe: 5'VIC-ACGAACTGCTGGCGGA). As a control, DNAse-treated RNA samples not subjected to reverse transcription were analyzed by qPCR in parallel.

*Mouse infections*

Female C3H/HeN mice (Harlan), 7–9 weeks old, were transurethrally infected with $10^7$ bacteria carrying the plasmid pANT4 as previously described (Kostakioti et al., 2009). IBC enumeration was performed using confocal microscopy as described by Kostakioti *et al*. Experiments were repeated three times and statistically analyzed using two-tailed Mann-Whitney ($P<0.05$, considered significant).

*Microscopy*

For fluorescence microscopy, bacteria were grown without shaking, in modified N-minimal media (5 mM KCl, 7.5 mM $(NH_4)_2SO_4$, 0.5 mM $K_2SO_4$, 1 mM $KH_2PO_4$, 0.1 mM Tris-HCl pH 7.4, 10 mM or 10 mM $MgCl_2$, 0.2% glucose, 0.1% Casamino acids, 38 mM glycerol /L) pH 7.6 and visualized using a Zeiss fluorescence microscope.

*PmrA and QseB purification*

The pQseB-mycHis construct used for QseB expression and purification was previously constructed (Kostakioti et al., 2009). The pPmrA-mycHis was constructed for this study by amplifying the *pmrA* gene and cloning into the pBAD-mycHisA vector. Protein expression was induced with 0.1% arabinose and the proteins were affinity-purified using a Talon column (Clontech), followed by anion exchange chromatography through a MonoQ column (GE Healthcare), as described in (Kostakioti et al., 2009).

*Electrophoretic mobility shift assays*

Purified QseB and PmrA was incubated with DNA fragments in binding buffer (final concentration: 20mM Tris-HCl, 5mM $MgCl_2$, 5mM KCl, 10% glycerol) for 20 minutes at room temperature. Reactions were loaded onto a 5% acrylamide non-denaturing gel. Electrophoresis was performed for 2.5 hours at 50V. Gels were dried at 80°C for 2 hours before being exposed to X-ray film at -80°C.

*Preparation of QseC- and PmrB-enriched membranes*

UTI89Δ*qseC*Δ*pmrB*/pPmrB-mycHis, UTI89Δ*qseC*Δ*pmrB*/pPmrB_H155A-mycHis, UTI89Δ*qseC*/pQseC-mycHis and UTI89Δ*qseC*Δ*pmrB*/pBAD-mycHisA were grown to an $OD_{600}$ = 0.6, in LB with shaking at 37°C and induced with 0.02% arabinose for 2 h. Cells were mechanically lysed by French Press (1000 p.s.i) and total membranes were isolated by 1 h ultra-centrifugation at 15,000 r.p.m., and re-suspended in 20 mM Tris (pH 8.0)/1 mM $MgCl_2$.

*Phosphotransfer and phosphatase assays*

Membranes from UTI89Δ*qseC*/pQseCmyc-His or UTI89Δ*qseC*/pBADmyc-HisA (7 μg) were incubated in the absence or presence of purified QseB (14 μg) with 0.7 mCi [$\gamma$-$^{32}$P]-ATP, in 1x TBS/0.5 mM DTT/0.5 mM $MgCl_2$ per reaction. A 10-reaction master-mix was prepared and 10 μl aliquots were removed at different time points, mixed with SDS loading buffer and kept on ice until SDS-PAGE. For the phosphatase assays, beads were prepared and used to *in vitro* phosphorylate QseB according to (Kato & Groisman, 2004). QseB~P (0.2 nmol, equal to 9,000 c.p.m) was incubated at room temperature with 7 μg of membrane vesicles in 1x TBS/0.5 mM DTT/0.5 mM $MgCl_2$. Aliquots (10 μl) were withdrawn from the reaction master-mix and treated as described above. Gels were dried and exposed to X-ray film for 48h at -80°C. Band intensities corresponding to QseB~P over time were quantified using ImageJ software and normalized to QseB~P at time=0. All experiments were repeated at least 3 times with biological replicates.

## Results

*Transposon mutagenesis identifies suppressors of the qseC deletion*

To identify the primary QseB activating source, we performed a suppressor screen using a library of UTI89Δ*qseC* transposon mutants and a phenotypic assay that assesses curli

production based on colony morphology. Deletion of *qseC* downregulates expression of curli adhesive fibers; thus, when grown on Yeast Extract-Casamino Acids (YESCA) agar, supplemented with the Congo Red dye (CR), UTI89Δ*qseC* forms white and smooth colonies indicative of diminished curli production, in contrast to WT UTI89 which exhibits a red, dry and rough morphotype (Kostakioti et al., 2009). Screening a UTI89Δ*qseC* transposon library on YESCA-CR agar, identified 37 suppressor mutants with WT- or near-WT morphology. Subsequent transposition mapping of the mutants with WT morphology identified 7 unique genes (Fig. 4A). Among those, *qseB* served as a robust internal control, since we have previously shown that UTI89Δ*qseBC* produces WT levels of curli (Kostakioti et al., 2009). The other identified targets included the PmrB (also known as BasS) sensor kinase, the SdiA regulatory protein, the cold-shock DEAD box protein A, the hypothetical YfiR protein, as well as FadD and CyoA, involved in respiration (Fig. 4A).

The identified disruptions may restore curli expression by affecting the activation state of QseB, or by impacting regulation of curli gene expression in a QseB-independent manner. We have previously shown that UTI89Δ*qseC* is non-motile and exhibits reduced type 1 pili expression (Hadjifrangiskou et al., 2011; Kostakioti et al., 2009). Given that disruption of the true QseB phospho-donor should suppress all Δ*qseC*-related defects, we also tested for restoration of motility and type 1 pili expression in each of the identified transposon mutants. Western blot analysis probing for the major type 1 pili subunit FimA, and motility assays revealed that only disruption of either *qseB*, or *pmrB* fully restored UTI89Δ*qseC* FimA expression and motility to WT levels (Fig. 4B-C, respectively). Based on these observations, we further investigated the potential contribution of PmrB to QseB activation.

*Disruption of pmrB in the absence of qseC suppresses the ΔqseC phenotypes*

We generated a clean *pmrB* deletion in the UTI89Δ*qseC* strain background to verify that the effects we saw with Tn::*pmrB* were specific to *pmrB* disruption and not an artifact of transposition. Indeed, the resulting mutant, UTI89Δ*qseC*Δ*pmrB*, behaved like the corresponding transposon mutant, being restored for motility, curli and type 1 pili expression (Fig. 5A). Subsequent qPCR analysis showed that *qseB* transcript levels in UTI89Δ*qseC*Δ*pmrB* were similar to WT UTI89, indicating that disruption of *pmrB* abrogates the increased *qseB* transcription observed in UTI89Δ*qseC* (Fig 5B). These phenotypes are specific to *pmrB* deletion as complementation of UTI89Δ*qseC*Δ*pmrB* with PmrB under its native promoter (plasmid pPmrB) resulted in a Δ*qseC* phenotype (Fig 5A).

UTI89Δ*qseC* is severely attenuated *in vivo*, forming considerably fewer IBCs and being less fit during acute and chronic infection (Kostakioti et al., 2012; Kostakioti et al., 2009). Given that deletion of *pmrB* restored type 1 pili expression, we tested the ability of UTI89Δ*qseC*Δ*pmrB* to establish acute UTI. Female C3H/HeN mice were transurethrally inoculated with $10^7$ UTI89, UTI89Δ*qseC* or UTI89Δ*qseC*Δ*pmrB*. Bladder colony forming units (CFU) and IBC numbers were assessed at 6 h post infection (h.p.i), marking the middle of IBC development, and 16 h.p.i, marking the end of the first IBC cycle at which time bacteria disperse from the biomass, spreading to neighboring cells (Justice et al., 2004). In contrast to UTI89Δ*qseC,* UTI89Δ*qseC*Δ*pmrB* formed WT-levels of IBCs, and was able to establish acute infection as efficiently as WT UTI89 (Fig 5C). Based on these data we further tested the hypothesis that PmrB is the primary QseB phospho-donor in the absence of QseC and that its deletion abrogates QseB-mediated gene dysregulation.

A

| Suppressor mutations imparting wt curli morphology in UTI89Δ*qseC* | |
|---|---|
| **Gene locus** | **Predicted function** |
| UTI89_C3450, *qseB* | QseB response regulator |
| UTI89_C2117-18, *sdiA-yecF* | DNA-binding transcriptional activator with autoinducer-binding domain |
| **UTI89_C4706, *pmrB/basS*** | **Sensor kinase-phosphotransferase** |
| UTI89_C2936, *yfiR* | Hypothetical protein |
| UTI89_C3255-56, *ygeXW* | Predicted transport system, metabolism |
| UTI89_C0456, *cyoA* | Cytochrome o ubiquinol oxidase subunit II; involved in aerobic respiration |
| UTI89_C1999, *fadD* | Enzyme involved in small-molecule/fatty acid degradation; contains AMP-binding site |
| UTI89_C3590, *deaD* | ATP-dependent RNA helicase with a DEAD-box; involved in cold shock response; |

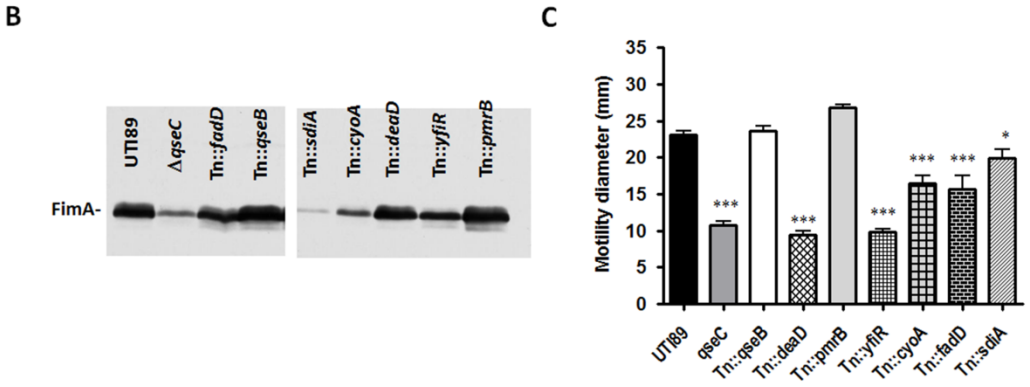


**Figure 4. Random mutagenesis screening identifies suppressors of the *qseC* deletion phenotype**

A) Table depicting factors the disruption of which restored wild-type (WT) curli morphology in the *qseC* deletion mutant. Transposon mutagenesis was performed as described in (Hadjifrangiskou et al., 2012). B) Western blot probing for FimA protein abundance in suppressor mutants shown in (A). A representative of 2 experiments is shown. C) Bar graph depicting average motility diameters (in mm) of each suppressor mutant compared to WT UTI89 and UTI89Δ*qseC* after 7h of groWTh in soft LB-agar (0.25%). Average motility diameters were calculated using data from 3 independent experiments. Statistical analyses were performed using unpaired, two-tailed Student's t-test. *, P≤0.01, ***, P<0.0001.

*PmrB cannot efficiently de-phosphorylate QseB*

If PmrB phosphorylates QseB in the absence of QseC, then ablating the PmrB kinase activity by site-directed mutagenesis should yield the same outcome as the *pmrB* deletion. We thus altered the PmrB phospho-accepting histidine (H155) to alanine. The resulting construct, pPmrB_H155A, was introduced to UTI89Δ*qseC*Δ*pmrB* and the generated strain UTI89Δ*qseC*Δ*pmrB*/pPmrB_H155A was tested for motility. Motility assays indicated that in contrast to the non-motile UTI89Δ*qseC*Δ*pmrB*/pPmrB (Fig. 5A and 6A), UTI89Δ*qseC*Δ*pmrB*/pPmrB_H155A exhibited WT motility (Fig 6A), indicating that the kinase activity of PmrB is linked to QseB activation. Subsequent *in vitro* phosphotransfer assays confirmed that PmrB phosphorylates QseB (Fig. 6B). For these assays, membrane vesicles (MV) were generated from UTI89Δ*qseC*Δ*pmrB*/pPmrB_mycHisA (PmrB-enriched MV), UTI89Δ*qseC*Δ*pmrB*/p-BAD_mycHisA (MV lacking PmrB), or UTI89Δ*qseC*/pQseC_mycHis (QseC-enriched MV) as described in materials and methods. We observed that phosphorylation of purified QseB occurred upon 15 min incubation with PmrB-enriched MV (Fig. 6B, left panel), but not upon incubation with MV lacking PmrB (Fig. 6B, right panel). PmrB-enriched vesicles incubated in the absence of QseB (Fig. 6B, middle panel), were used as a control for PmrB auto-kinase activity.

Given that QseB~P requires the QseC phosphatase activity for de-phosphorylation and de-activation (Kostakioti et al., 2009), we tested the hypothesis that PmrB cannot de-phosphorylate QseB as efficiently as QseC. We performed a time-course, assessing de-phosphorylation of *in vitro*-phosphorylated QseB (QseB~P) incubated with PmrB-enriched MV, MV lacking PmrB or QseC-enriched MV. Using ImageJ analysis, we determined that, after 5 minutes of incubation 25% of QseB was de-phosphorylated by PmrB. After 60 minutes of

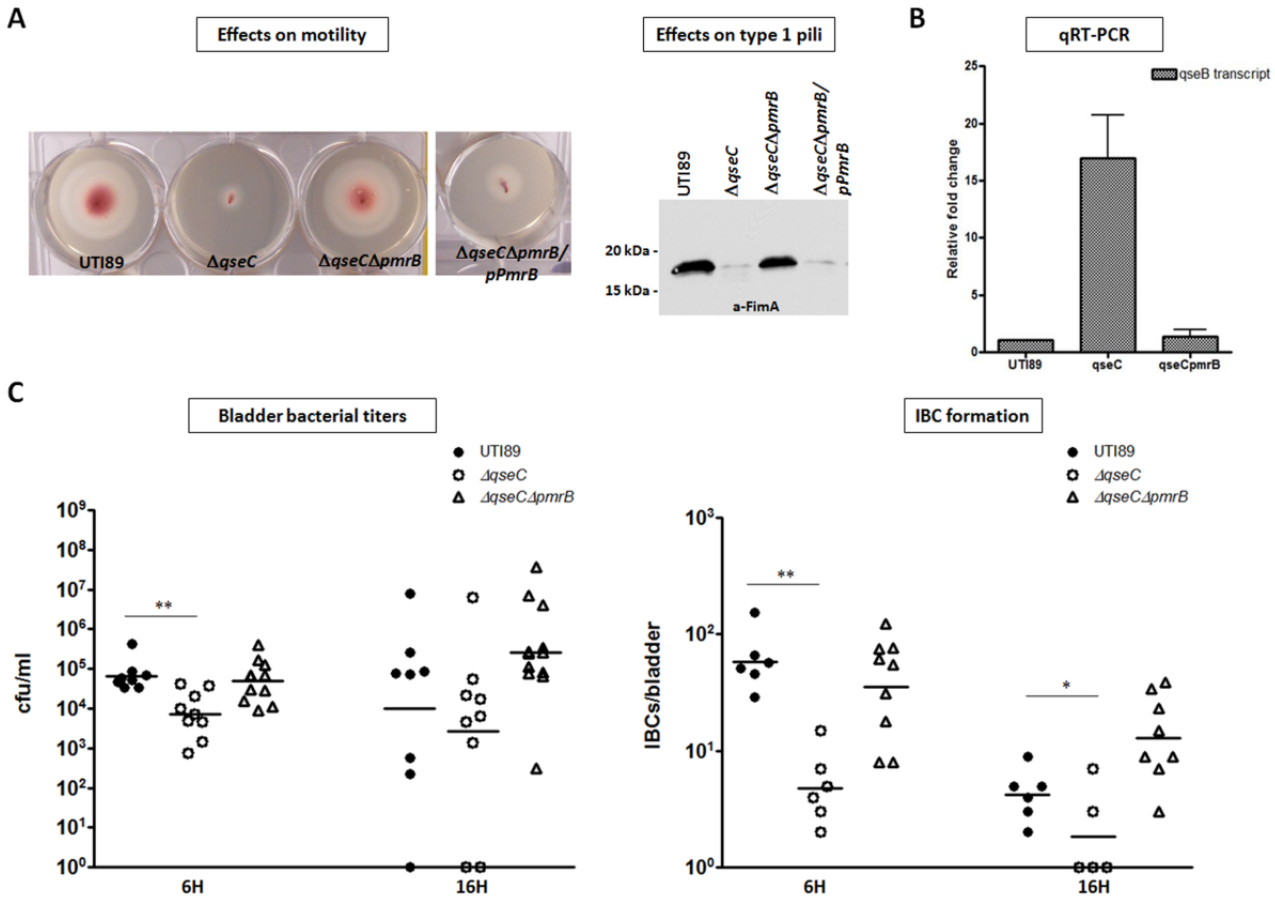


**Figure 5. Deletion of *pmrB* in UTI89Δ*qseC* restores *in vitro* and *in vivo* phenotypes**

A) Motility and FimA Western blot assays demonstrating that UTI89Δ*qseC*Δ*pmrB* exhibits WT motility and expresses WT-levels of type 1 pili. Both phenotypes are suppressed upon complementation with *pmrB*. B) Relative-fold change of *qseB* in WT UTI89, UTI89Δ*qseC,* UTI89Δ*qseC*Δ*pmrB*, measured by qPCR. Values are normalized to the *rrsH* gene. An average of 3 independent experiments is shown; error bars represent SEM. C) Graphs showing bladder titers and IBC numbers recovered at 6 and 16 h.p.i. for WT UTI89, UTI89Δ*qseC* and UTI89Δ*qseC*Δ*pmrB*. *, P P≤0.027; **, P≤0.0024, determined by two-tailed Mann-Whitney.

incubation 60% of QseB remained phosphorylated (Fig. 6C. left panel). In striking contrast, 44% of QseB was de-phosphorylated after 5 minutes of incubation in the presence of QseC, and by 60 min of incubation, only 2.5% of QseB~P remained phosphorylated (Fig. 6D). Incubation of QseB~P with MV lacking PmrB or QseC or incubation of QseB in the absence of MV altogether did not significantly impact the QseB phosphorylation state (Fig. 6C, middle and right panels), indicating that QseB~P does not get de-phosphorylated by other kinases/phosphatases in the MV and it does not undergo significant spontaneous de-phosphorylation. These findings demonstrate that, remarkably, PmrB exhibits phosphatase activity towards QseB~P, but de-phosphorylation occurs considerably slower than with QseC. Collectively, our data show that although PmrB can phosphorylate QseB at rates relatively comparable to QseC, it is significantly less efficient in its ability to dephosphorylate QseB~P, resulting in the disproportionate activation of QseB in the *qseC* mutant.

*The PmrA response regulator contributes to qseBC induction in the absence of QseC*

Given the involvement of PmrB in activating UPEC QseB at the protein level, we wondered whether the PmrB cognate response regulator, PmrA, is involved in the observed *qseBC* induction in the Δ*qseC* mutant. Scanning the *qseBC* promoter region for the PmrA binding sequence (5'-(C/T)TTAA(G/T)-N5-(C/T)TTAA(G/T)-3') (Kato, Latifi, & Groisman, 2003; Tamayo, Prouty, & Gunn, 2005; Wosten & Groisman, 1999), revealed the presence of a PmrA binding consensus (Fig. 7A) overlapping the previously reported QseB-dependent promoter (Clarke & Sperandio, 2005).

Therefore, we investigated the hypothesis that, in addition to PmrB activating QseB at the protein level (via phosphorylation), PmrA is involved in mediating *qseBC* transcription. We used

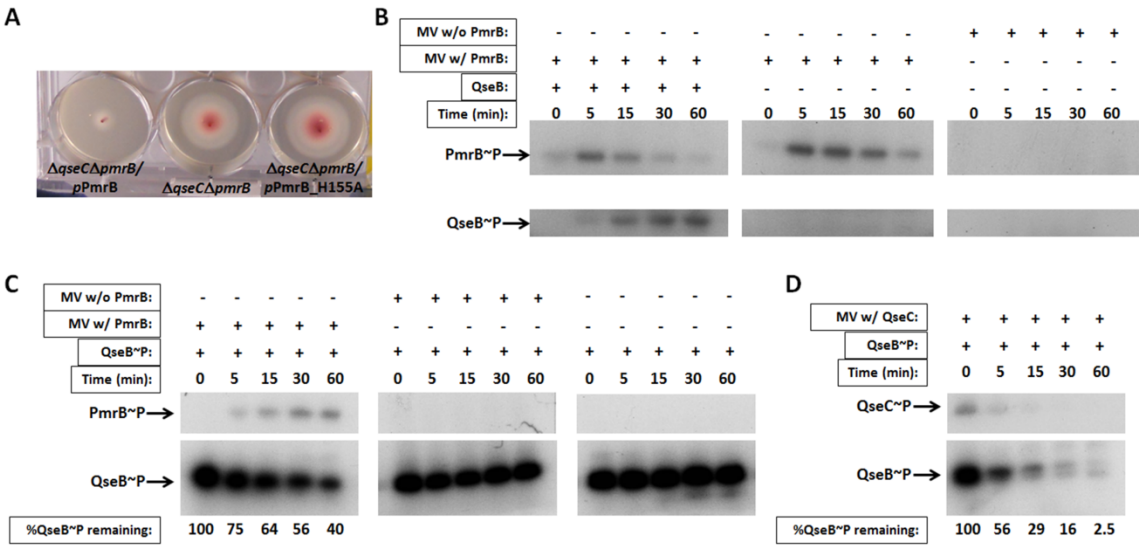


**Figure 6. PmrB phosphorylates QseB in the absence of QseC**

A) Effects of inactivating PmrB kinase activity on the motility of UTI89Δ*qseC*Δ*pmrB*/pPmrB, UTI89Δ*qseC*Δ*pmrB* and UTI89Δ*qseC*Δ*pmrB*/pPmrB_H155A. Motility diameters were measured after a 7h of incubation at 37°C. B) Phosphotransfer assays with PmrB-enriched membrane vesicles (MV) and purified QseB. Middle panel demonstrates PmrB autokinase activity in the absence of QseB. The last panel depicts a mock phosphotransfer assay using MV without PmrB to verify that phosphotransfer to QseB occurs specifically by PmrB. A representative of 3 independent experiments is shown. C-D) *In vitro* phosphatase assays with PmrB-enriched membrane vesicles (MV) and *in vitro* phosphorylated QseB~P. Percent QseB~P was calculated based on peak intensity analysis of each band normalized to the sample at t=0, using the ImageJ software. A representative of 3 independent experiments is shown.

a previously constructed *qseBC* promoter-GFP reporter plasmid, P*qse*::GFP (Kostakioti et al., 2009) in combination with qPCR to assess the contribution of PmrA on promoter activity. We had previously shown that, although P*qse*::GFP was robustly active in UTI89Δ*qseC*, there was no promoter activity recorded in WT UTI89 or UTI89Δ*qseBC* during growth in either LB or N-minimal media (Kostakioti et al., 2009). Here, we constructed a non-polar *pmrA* deletion in UTI89 and UTI89Δ*qseC*, introduced P*qse*::GFP in the resulting mutants and sampled *gfp* steady-state transcript and GFP fluorescence as a proxy to *qseBC* expression. This allowed us to assess *qseBC* promoter activity in a panel of mutants, including those lacking *qseB* (in which a *qseB*-specific probe would not be informative). Consistent with our above observations, *qseBC* expression in UTI89Δ*qseC*Δ*pmrB* was similar to WT UTI89 and UTI89Δ*qseBC* and was significantly lower than UTI89Δ*qseC* (Fig. 7B and Fig. 8). However, deletion of *pmrA* in the absence of QseC (UTI89Δ*qseC*Δ*pmrA*) resulted in a 2-fold reduction of *gfp* steady-state transcript (Fig. 7B and Fig. 8), indicating that PmrA contributes to *qseBC* transcription. Previous studies showed and PmrA induces *pmrAB* expression in response to ferric iron (Wosten et al., 2000). Despite the absence of the PmrAB activating signal, it is possible that deletion of *pmrA* affects transcription of *pmrB*, resulting in less PmrB protein, which would impact levels of phosphorylated QseB. To test this hypothesis, we sampled *pmrB* expression in the absence of *pmrA* using qPCR, and found that *pmrB* levels in fact increased in the *pmrA* mutants under the tested conditions (Fig. 7C). Therefore, the observed reduction in *qseBC* transcript in UTI89Δ*qseC*Δ*pmrA* is not the result of lower PmrB and QseB~P levels, but rather a result of the PmrA absence.

We therefore tested if PmrA directly binds to the *qseBC* promoter using electrophoretic mobility shift assays (EMSAs). As a positive control, we tested PmrA binding to the *yibD*

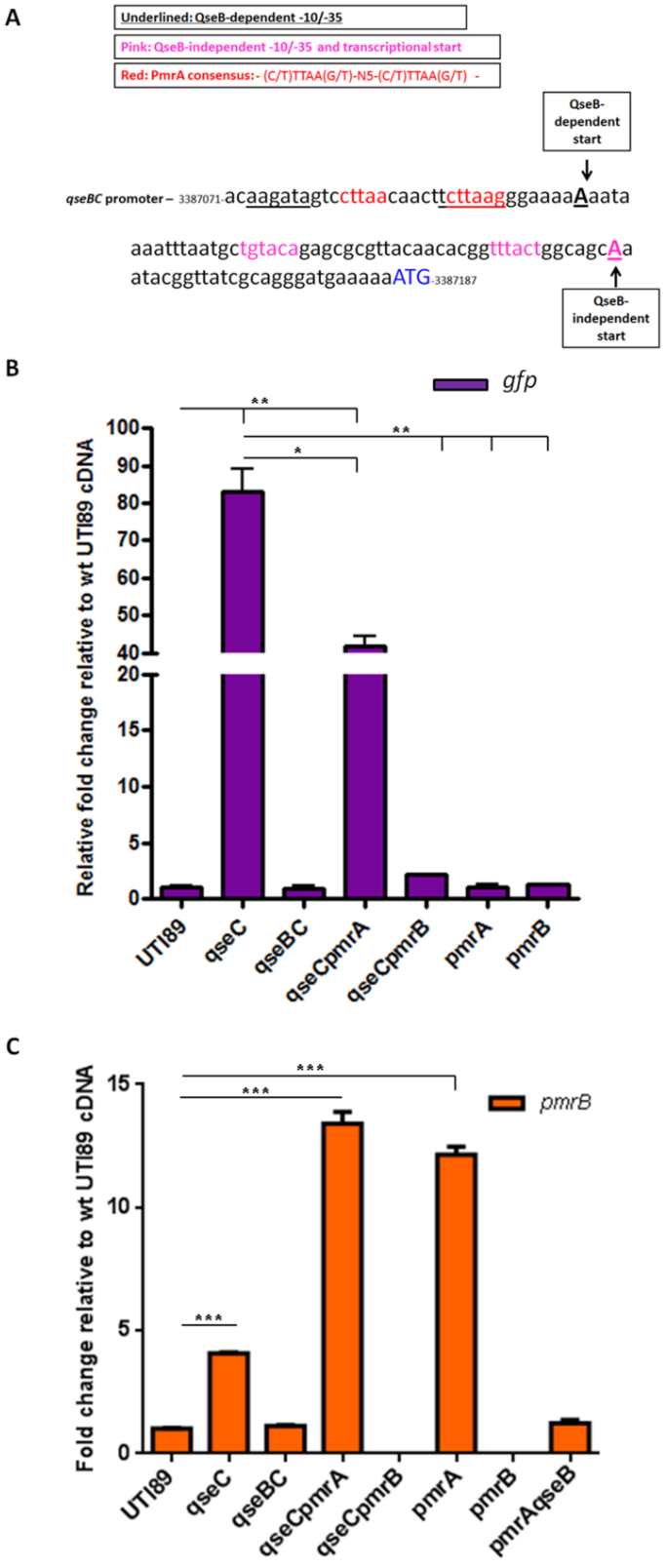
A
Underlined: QseB-dependent -10/-35
Pink: QseB-independent -10/-35 and transcriptional start
Red: PmrA consensus: - (C/T)TTAA(G/T)-N5-(C/T)TTAA(G/T) -
QseB-dependent start
qseBC promoter – 3387071 acaagatagtccttaacaacttcttaaggaaaaAaata
aaatttaatgctgtacagagcgcgttacaacacggtttactggcagcAa
atacggttatcgcagggatgaaaaaATG 3387187
QseB-independent start
B
gfp
Relative fold change relative to wt UTI89 cDNA
UTI89
qseC
qseBC
qseCpmrA
qseCpmrB
pmrA
pmrB
C
pmrB
Fold change relative to wt UTI89 cDNA
UTI89
qseC
qseBC
qseCpmrA
qseCpmrB
pmrA
pmrB
pmrAqseB

**Figure 7. PmrA contributes to *qseBC* upregulation in the absence of QseC**

A) The *qseBC* promoter region from UTI89 (spanning nt 3387071-3387110) harbors a PmrA binding consensus that precedes the previously described (Clarke et al., 2005) QseB-dependent start site. B) Relative-fold change of *gfp* driven by the *qseBC* promoter in WT UTI89, UTI89Δ*qseC,* UTI89Δ*qseBC,* UTI89Δ*qseC*Δ*pmrA*, UTI89Δ*qseC*Δ*pmrB*, UTI89Δ*pmrA* and UTI89Δ*pmrB* measured by qRT-PCR. C) Relative-fold change of *pmrB* in WT UTI89, UTI89Δ*qseC,* UTI89Δ*qseBC,* UTI89Δ*qseC*Δ*pmrA*, UTI89Δ*qseC*Δ*pmrB*, UTI89Δ*pmrA*, UTI89Δ*pmrB* and UTI89Δ*qseB*Δ*pmrA* measured by qPCR. Quantitative real time PCR was executed in triplicate on an ABI StepOne Plus Real Time PCR machine, using multiplexed TaqMan MGB chemistry. Two dilutions of cDNA (25 ng and 6.25 ng) were analyzed per isolate. Abundance of *gfp* transcripts (probe: 5'6FAM-ACGTGCTGAAGTCAAG3') in UTI89 isogenic mutant strains was calculated using the ΔΔCT method, with each transcript signal normalized to the abundance of the *rrsH* internal control (probe: 5'VIC-CGTTAATCGGAATTACTG3') and comparison to the normalized transcript levels of WT UTI89. Abundance of *pmrB* transcripts (probe: 5'6FAM-ACGCCCATTGCCA) was calculated as above, but normalized to the abundance of the *gyrB* internal control (probe: 5'VIC-ACGAACTGCTGGCGGA). Error bars for both graphs represent SEM. Statistical analyses were performed by two-tailed unpaired t-test, where *, $P<0.03$; **, $P\leq0.0053$.

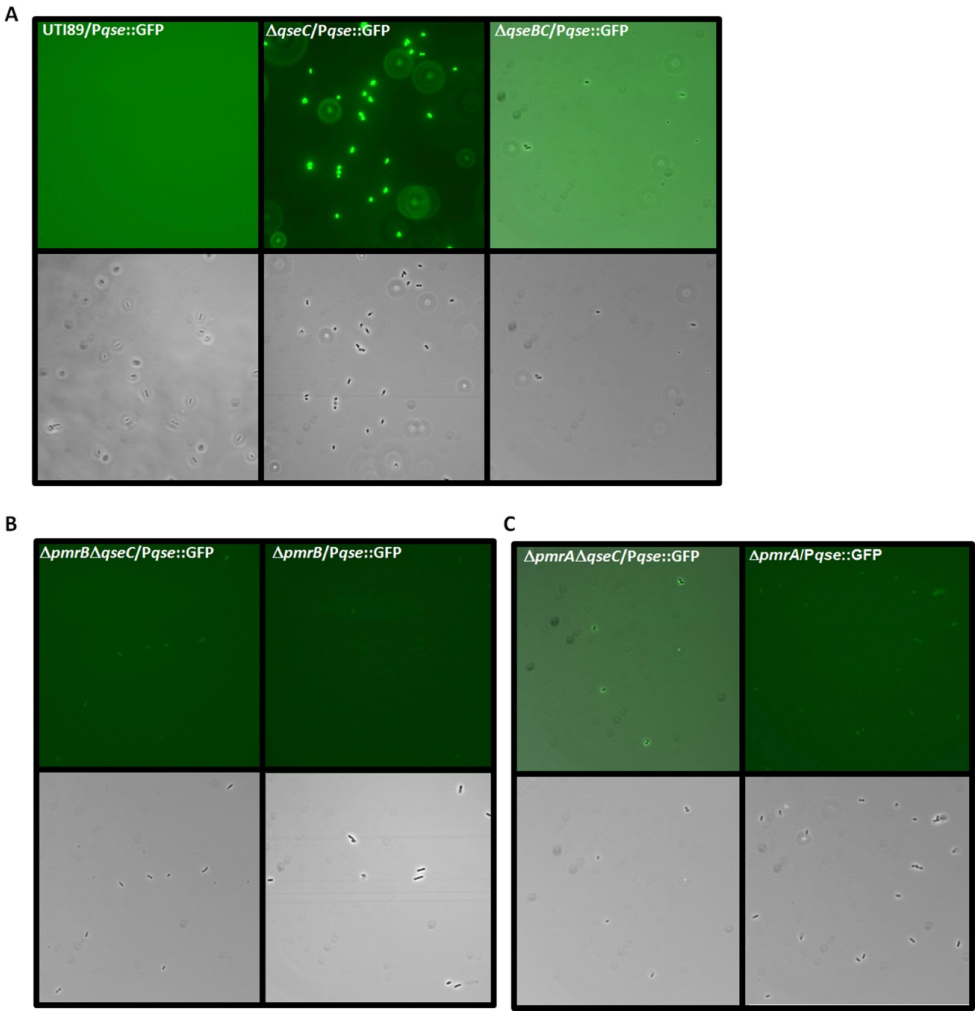


**Figure 8. Q*seBC* upregulation in the absence of QseC involves both PmrB and PmrA**

A-C) Fluorescence microscopy, tracking *qseBC* promoter-driven GFP expression. Duplicate slides per strain were scanned for fluorescence per experiment. Data shown are representative of three independent experiments. Images shown are representative of the bacterial populations sampled per slide.

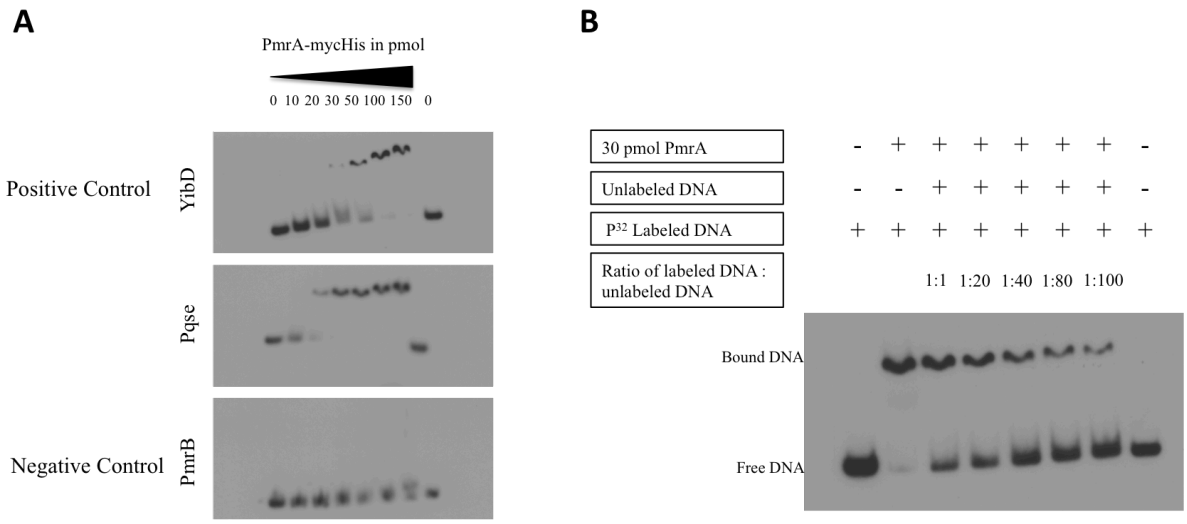


**Figure 9. PmrA directly binds to the *qseBC* promoter**

A) Electrophoretic mobility shift assays (EMSAs) with purified PmrA and $^{32}$P end-labeled *qseBC* promoter fragment. The internal region of *pmrB* was amplified and used as a negative control for PmrA binding, while the previously identified *yibD* promoter (Tomayo et. al., 2002) was used as a positive control for PmrA binding. B) EMSA using 30 pmol purified PmrA and indicated ratios of *qseBC* promoter as $^{32}$P end-labeled: unlabeled.

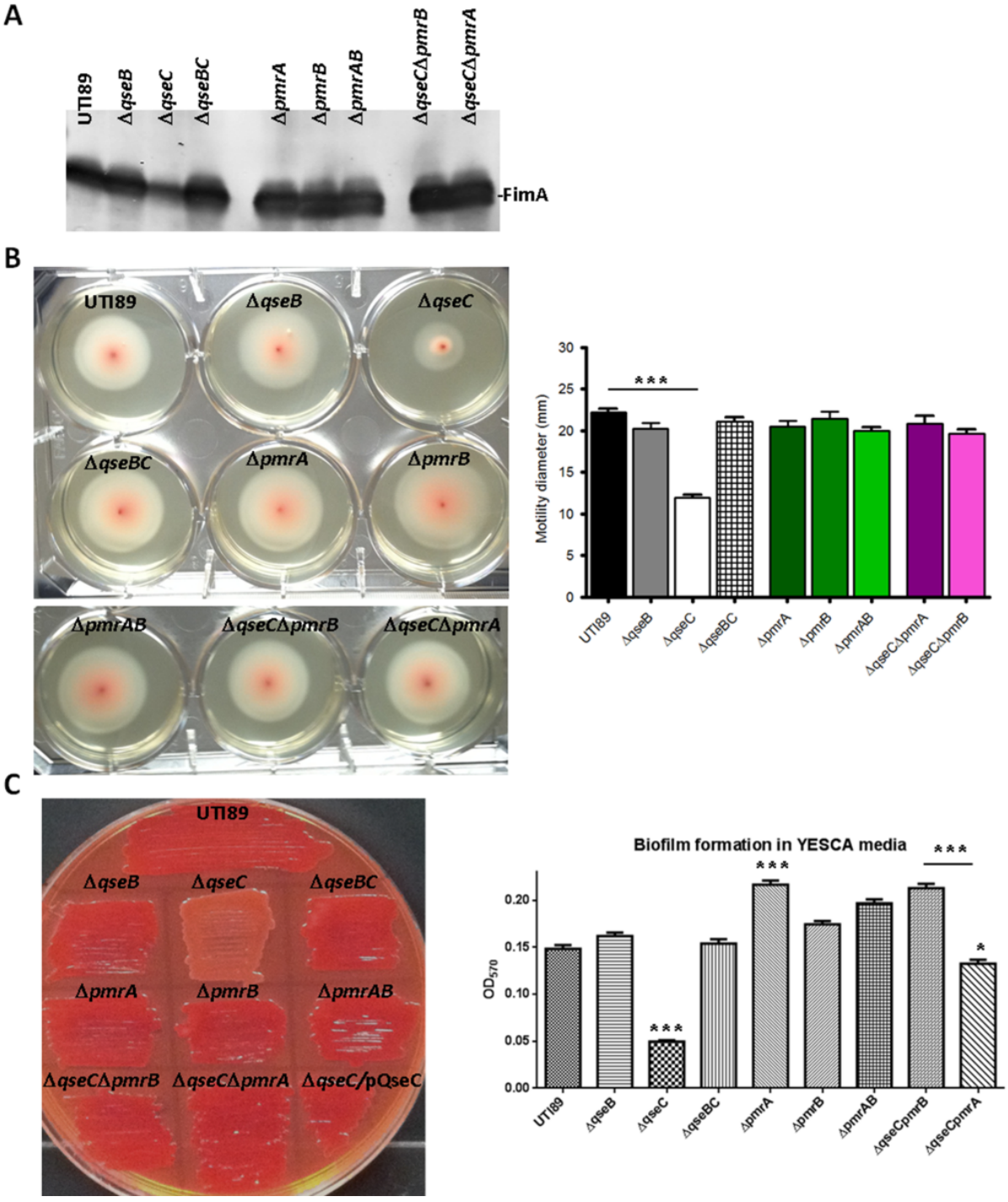
A
UTI89
ΔqseB
ΔqseC
ΔqseBC
ΔpmrA
ΔpmrB
ΔpmrAB
ΔqseCΔpmrB
ΔqseCΔpmrA
FimA
B
UTI89
ΔqseB
ΔqseC
ΔqseBC
ΔpmrA
ΔpmrB
ΔpmrAB
ΔqseCΔpmrB
ΔqseCΔpmrA
Motility diameter (mm)
***
C
UTI89
ΔqseB
ΔqseC
ΔqseBC
ΔpmrA
ΔpmrB
ΔpmrAB
ΔqseCΔpmrB
ΔqseCΔpmrA
ΔqseC/pQseC
Biofilm formation in YESCA media
OD570
***
*

**Figure 10. Deletion of *pmrA* abolishes some of the *qseC* deletion defects**

A) FimA Western blot probing total cell lysates from a panel of *qse/pmr* mutants. Blot was imaged on an Odyssey infrared imaging system (Li-Cor Biosciences, Lincoln, NE) in the 700 nm channel. B) Motility phenotypes of the *qse/pmr* mutants; bacteria were inoculated into 0.25% LB agar/0.001% 2,3,5-triphenyltetrazolium chloride and incubated at 37°C for 7 h. Motility (depicted in the photo panels for each mutants) was evaluated by measuring the motility diameters (presented in the accompanying graph). Experiment was repeated 2 times with triplicate plates/strain. ***, $P \leq 0.0001$, determined by two-tailed unpaired Student's t-test. C) Yeast Extract/Casamino Acid (YESCA) agar plate supplemented with Congo Red (CR) dye serving as a proxy to curli fiber expression. Curli positive bacteria appear bright red on these media, while curli-negative bacteria appear white and smooth. Biofilm formation after 48h in YESCA media is depicted in the graph on the right hand panel. Quantitation of biomass was performed using the colorimetric method of O'Toole as previously described (Hadjifrangiskou et al., 2012). Experiment was repeated twice with three technical replicates per biological repeat. *, $P < 0.05$, ***, $P \leq 0.0001$, as determined by two-tailed unpaired Student's t-test. Asterisks directly above bars depicting significance compared to WT UTI89.

promoter, a previously identified direct PmrA target (Tamayo, Ryan, McCoy, & Gunn, 2002). Using a previously established protocol with increasing concentrations of PmrA, we detected binding to *qseBC* promoter at concentrations lower than those observed for *yibD* (Figure 9A). Competition assays with unlabeled *qseBC* promoter DNA titrated PmrA binding from the $^{32}$P-labeled *qseBC* promoter fragments, validating specificity for this sequence (Figure 9B). Taken together, our findings indicated that in the absence of QseC, *qseBC* upregulation comes from a possible synergistic effect of high levels of activated QseB~P and the activity of PmrA (the phosphorylation state of which for this function remains unknown) likely on the *qseBC* promoter.

Over 500 genes are differentially expressed in the absence of QseC, due to aberrant *qseB* induction (Hadjifrangiskou et al., 2011). The observed 50% reduction in *qseBC* expression in UTI89Δ*qseC*Δ*pmrA* may be sufficient to abrogate some of the known QseC defective phenotypes, and in particular expression of type 1 pili, curli and flagella. As was the case for UTI89Δ*qseC*Δ*pmrB*, UTI89Δ*qseC*Δ*pmrA* expressed WT-levels of type 1 pili (Fig. 10A), and regained motility (Fig. 10B). However, despite the WT-levels of CR uptake, UTI89Δ*qseC*Δ*pmrA* was defective in YESCA biofilm formation, compared to WT UTI89 and UTI89Δ*qseC*Δ*pmrB* (Fig. 10C), suggesting that deletion of *pmrA* is not sufficient to suppress all of the Δ*qseC* phenotypes. Thus, PmrA and QseB contribute to *qseBC* upregulation in the absence of QseC, revealing a previously uncharacterized link between PmrAB and QseBC that may be of physiological significance.

## Discussion

Signal integration through TCS is among the means exploited by bacteria to sample environmental changes and tailor their gene expression profile in a manner that enables survival in a specific condition. Bacterial genomes can harbor multiple TCSs, which regulate most aspects of bacterial physiology, spanning chemotaxis, central metabolism, stress responses and virulence.

It was previously reported that in UPEC, the absence of the QseC sensor leads to aberrant and robust phosphorylation of the cognate response regulator QseB by a non-cognate sensor or phosphor-donor molecule (Kostakioti et al., 2009). This aberrant cross-talk imparts pleiotropic gene expression changes that negatively impact bacterial physiology and attenuate virulence (Hadjifrangiskou et al., 2011; Kostakioti et al., 2009). The work presented in this chapter revealed the identity of the phosphodonor protein responsible for activating QseB in the absence of QseC. Our data indicated that the PmrB sensor kinase, which is canonically paired with the PmrA response regulator, can robustly phosphotransfer to QseB. PmrB-mediated phosphotransfer event to QseB is kinetically comparable to the phosphotransfer rate between QseC and QseB. This observation lies outside the established paradigm in the field, which states that interaction between non-cognate pairs is disfavored and thought to only occur weakly upon cognate sensor disruption.

As discussed in Chapter I, molecular determinants, both sequence and structure-based, between sensor kinase and response regulator proteins ensure fidelity between cognate partners (Capra & Laub, 2012). Upon a gene duplication event yielding a new TCS, these molecular determinants normally unique between cognate pairs, would be the same between the new and old TCSs. This presents the opportunity for TCSs to cross-interact, potentially preventing the bacteria from responding appropriately to specific stimuli. If this is the case, evolutionary

pressure will cause the TCSs to diverge, allowing each system to sense and respond to a specific signal by restricting molecular interactions between cognate pairs. PmrB is the closest homolog of QseC in UTI89, with 37% sequence identity and 70% coverage, suggesting that one system gave rise to the other by a gene duplication event. This also suggests that the interacting interfaces of PmrB and QseC share common features, or co-evolving residues, that enable similar protein-protein interactions with QseB. Therefore, there are two explanations for the robust cross-interactions between QseBC and PmrAB: Either these systems are in the process of diverging and we are observing them in the midst of evolution, or there is a physiological reason that these systems cross-interact and there is evolutionary pressure to maintain this interaction.

Our study documents a strong interaction between a RR and a non-cognate sensor: PmrB readily phosphorylates QseB, with kinase reaction kinetics similar to those of QseC. PmrB phosphatase activity towards QseB is slow, thus providing a potential explanation for the observed QseB over-activation when QseC is not present. Although PmrB phosphatase activity is slow towards QseB, the presence of any phosphatase activity between these non-cognate proteins is intriguing because phosphatase activity is one of the main mechanisms for preventing cross-talk between systems (Alves & Savageau, 2003). This provides further evidence to suggest a physiological link between the QseBC and PmrAB TCSs.

In addition to identifying PmrB and investigating its phosphotransfer kinetics in relation to QseC, we have discovered that in the absence of QseC, the PmrB cognate response regulator, PmrA contributes to aberrant expression of the *qseBC* operon, possibly by augmenting *qseB* gene expression. The current analyses have shown that, while the Δ*qseC*Δ*pmrB* double mutant suppresses aberrant *qseB* expression back to WT levels (Fig. 7B and 7B) deletion of *pmrA* in UTI89Δ*qseC* only results in a 50% reduction of *qseB* steady-state transcript (Fig. 7B). These

data demonstrate that in addition to cross-talk between PmrB and QseB there is a potential synergistic effect of the two RR on *qseBC* promoter activation. Previous analyses by Clarke *et al.*, had mapped QseB-dependent and –independent start sites within the *qseBC* promoter of the EHEC strain 86-24 (Clarke & Sperandio, 2005). Clarke *et al.* had reported that the QseB-dependent start site disappears in the *qseC* deletion mutant, while, a QseB-independent start site exists downstream of the QseB-dependent start. Interestingly, the mapped QseB-independent transcriptional start reported by this group, is very highly prominent in the *qseC* deletion mutant (Clarke & Sperandio, 2005). It is thus possible that PmrA contributes to transcriptional control from this start site in the absence of QseC, augmenting *qseB* upregulation in the *qseC* mutant and driving the increase in QseB levels. The involvement of PmrA in the transcriptional control of the *qseBC* operon is further evidence that there is a physiological reason for the cross-interactions between QseBC and PmrAB, suggesting that these systems may be engaging in cross-regulation. The mechanism of transcriptional control orchestrated by these two response regulators is described in chapter IV.

Collectively, this work demonstrates that the bi-functional nature of sensors is crucial in maintaining an optimal ratio of cognate RR phosphorylated and unphosphorylated states to prevent aberrant RR activity and fine-tune physiological TCS cross-talk, facilitating proper responses to signal. PmrA involvement in *qseBC* transcriptional control, coupled with PmrB phosphatase activity towards QseB, suggests that cross-interactions between QseBC and PmrAB are evolutionarily selected for and may result in beneficial cross-regulation, which is the focus of Chapter III.

CHAPTER III

# PMRA AND QSEB MEDIATE TOLERANCE TO POLYMYXIN B IN UROPATHOGENIC *ESCHERICHIA COLI*

A portion of this work has been published in the journal "Science Signaling" as **K. R. Guckes***, E. J. Breland*, E. W. Zhang, S. C. Hanks, N. K. Gill, H. M. S. Algood, J. Schmitz, C. Stratton, and M. Hadjifrangiskou. 2016 Jan 10;10(461).

PMID: 28074004

*Both authors contributed equally to this work

## Introduction

In *Salmonella enterica*, PmrAB directs the expression of a regulon that ultimately alters LPS composition and confers tolerance or intrinsic resistance to cationic polypeptides, such as polymyxin B (PMB) (Kato et al., 2012; Richards et al., 2012; Wosten et al., 2000). Activation of PmrAB in *Salmonella* occurs via elevated ferric iron ($Fe^{3+}$), which is directly detected by PmrB, or via cationic polypeptides that are detected by the PhoQ sensor of the PhoPQ system. Previous studies in K12 *E. coli* suggested that indirect stimulation of PmrB by cationic polypeptides does not occur, leading to the conclusion that PhoPQ signaling is not implicated in mediating *E. coli* tolerance to PMB (Winfield & Groisman, 2004).

PMB mimics polymyxin E, otherwise known as colistin, in terms of antibiotic mechanism of action, clinical use, and toxicity, and it has become a last resort antibiotic, to treat multidrug resistant *Enterobacteriaceae* (Kwa, Kasiakou, Tam, & Falagas, 2007; Mediavilla et al., 2016). Increase in antibiotic resistance has become a serious issue in the treatment of UTIs.

Carbapenem resistant *Enterobacteriaceae* (CRE) have become such a serious public health issue that the Center for Disease Control elevated these pathogens to an urgent threat level. Recently there was a report of a woman with a UTI that was caused by UPEC that was classified as CRE, which was additionally resistant to colistin, via a plasmid, which contains the colistin resistance conferring *mcr-1* gene (Mediavilla et al., 2016). This gene is an ortholog to *pmrC*, one of the PmrA target genes that modifies lipid A of the LPS in *Salmonella* (Chen & Groisman, 2013).

Data presented in Chapter II suggested a physiological link between the PmrAB and QseBC systems, the molecular mechanism and the significance of which remains undetermined. We therefore wondered whether QseBC-PmrAB interactins have evolved in E. coli to mediate intrinsic tolerance to PMB.

Here we present evidence that elevated ferric iron induce PmrB activation, which then phosphorylates PmrA and QseB, both of which are required to mediate resistance to PMB. This response is different from the PmrAB stimulus response established for *Salmonella* spp., because in UPEC, the PhoPQ TCS plays a minor role in PmrAB activation ((Winfield & Groisman, 2004; Wosten et al., 2000) and Fig. 18). Biochemical analyses demonstrated that PmrB kinase activity was enhanced toward both its cognate (PmrA) and non-cognate (QseB) response regulators in the presence of ferric iron, leading to an activation surge in transcription of the *qseBC* locus that was PmrA/QseB-dependent. QseB and PmrA response regulators were both necessary to mediate optimal transcription of downstream target genes in response to ferric iron. These data describe a unique example in which activation of a single bacterial receptor (PmrB) leads to the co-opting of a non-cognate response regulator (QseB) to elicit a physiologically relevant response.

## Methods

*Bacterial strains and growth conditions*

Cultures were grown in Lysogeny broth (Fisher) or N minimal broth with or without ferric iron (Fisher) or epinephrine (Sigma) at 37°C with shaking. UTI89Δ*qseC*, UTI89Δ*pmrB*Δ*qseC*, and the corresponding, pQseC, pQseC-mycHis, pPmrB, and pQseC-mycHis plasmid constructs harboring the corresponding wild-type *qseC* and *pmrB* gene sequences were created previously (Guckes et al., 2013; Kostakioti et al., 2009). Promoter activity for the *qseBC* operon was measured using a previously created *qseBC* promoter transcriptional reporter construct, P*qse*::*gfp* (Guckes et al., 2013; Kostakioti et al., 2009).

*Phosphotransfer assays*

Membranes from each strain (7 μg) were incubated with purified QseB (14 μg) and 0.7 μCi [γ-$^{32}$P]-ATP, in the absence or presence of signal, with 1x TBS, 0.5 mM DTT, and 0.5 mM $MgCl_2$ per reaction. A 7 reaction master-mix was prepared and 10 μl aliquots were removed at different time points, mixed in a 1:1 ratio with 2X SDS loading buffer and kept on ice until SDS-PAGE. Aliquots (10 μl) were withdrawn from the reaction master-mix and treated as described above. Gels were dried and exposed to X-ray film for 48 h at -80°C. Band intensities corresponding to QseB~P over time were quantified using ImageJ software and normalized to QseB~P at time=0. All experiments were repeated 2-4 independent times, with different biological samples.

*Phosphatase assays*

Beads were prepared and used to *in vitro* phosphorylate QseB as described in (Kato & Groisman, 2004). QseB~P (0.2 nmol) was incubated at room temperature with 7 μg of membrane

vesicles, harboring QseC, PmrB, or neither kinase, in the presence or absence of signal in a reaction buffer comprising 1x TBS, 0.5 mM DTT, and 0.5 mM $MgCl_2$. Aliquots (10 µl) were withdrawn from the reaction master-mix and treated as described above. Gels were dried and exposed to X-ray film at -80°C. Band intensities corresponding to QseB~P over time were quantified using ImageJ software and normalized to QseB~P at time=0.

*QseB and PmrA purification*

The pQseB-mycHis and pPmrA-mycHis constructs used for QseB and PmrA expression respectively and purification was previously constructed (Kostakioti et al., 2009). QseB expression was induced with 0.1% arabinose and QseB was affinity-purified using a Talon column (Clontech), followed by anion exchange chromatography through a MonoQ column (GE Healthcare), as described in (Kostakioti et al., 2009).

*Electrophoretic mobility shift assays*

Purified and *in vitro* phosphorylated response regulators were incubated with 105bp fragment of the *yibD* promoter region. Proteins were *in vitro* phosphorylated using beads fused to the cytosolic portion of PmrB, as described previously (Guckes et al., 2013). Post-phosphorylation, response regulators were incubated with DNA in binding buffer (final concentration: 20mM Tris-HCl, 5mM $MgCl_2$, 5mM KCl, 10% glycerol) for 20 minutes at room temperature. Reactions were loaded onto a 5% acrylamide non-denaturing gel. Electrophoresis was performed for 2.5 hours at 50V. Gels were dried at 80°C for 2 hours before being exposed to X-ray film at -80°C.

*qPCR*

Cultures were grown to log phase at 37°C with shaking before adding 100μM ferric iron. To collect samples at various time points after the stimulus, the culture was temporarily moved to room temperature, statically and subsequently returned to shaking at 37°C between time points. RNA was extracted from bacteria using the RNeasy kit (Qiagen), DNase-treated using Turbo DNase I (Ambion), and reverse transcribed using Superscript II Reverse Transcriptase (Invitrogen). DNAse-treated RNA samples not subjected to reverse transcription were used as negative controls. qPCR was performed in triplicate with two different amounts of cDNA (50 ng and 25 ng per reaction). cDNA was amplified using *gfp* and *rrsH* specific primers. Relative fold change was determined by the ΔΔCt method where transcript abundances were normalized to *rrsH* abundance (Pfaffl, 2001). Quantitative real time PCR was performed using an ABI StepOne Plus Real Time PCR machine, using multiplexed TaqMan MGB chemistry. Experiments were performed with at least three independent biological replicates.

*Polymyxin B sensitivity assay*

Bacteria were grown overnight at 37°C with shaking. Overnight cultures were then sub-cultured into N-minimal media with or without 100 μM ferric chloride. Once N-minimal cultures reached mid-logarithmic phase of growth, cultures were normalized to an $OD_{600}$ of 0.3 in 1X PBS and incubated with or without 2.5 μg/mL polymyxin B at 37°C for 1.5 hours. Cultures were plated on LB agar to determine CFU/mL. Percent survival was calculated by dividing the number of bacteria that grew post-exposure to polymyxin B by the number of bacteria that grew after incubation in PBS alone, and multiplying by 100. Statistical analysis comparing percent survival between strains were performed using a non-parametric one-way

analysis of variance by the Kruskal-Wallis test, $P<0.01$. All statistical analyses were performed using GraphPad Prism software.

## Results

*All components of the QseBC and PmrAB TCSs are required for proper response to ferric iron*

Signal detection by bacterial sensor histidine kinases, typically leads to a surge in phosphorylated response regulator, which in turn alters the expression of target genes within a very short timeframe (Shin et al., 2006). In response to an incoming stimulus, there is a rapid phosphotransfer event from the cognate sensor kinase, which within 5-10 minutes, culminates to maximal phosphorylation of the cognate response regulator. For TCSs that are able to auto-regulate their expression, the phosphorylated response regulator is able to act as an activator of transcription, and this series of events is referred to an activation surge (Shin et al., 2006). The changes in transcription of known target genes over time can be followed using qPCR.

We have previously reported that in UPEC, stimulation with ferric iron induces the *qseBC* operon, in a manner that appears to involve PmrA and QseB (Guckes et al., 2013). To better define this transcriptional control, we measured the activity of the *qseBC* promoter immediately prior and immediately after exposure to 100 μM ferric iron in UPEC strain UTI89 and various isogenic *pmr* and *qse* mutants using qPCR. Samples from bacteria grown in N-minimal media were obtained from 0 to 60 minutes post exposure to ferric iron, and qPCR analysis was performed measuring the transcriptional surge of the *qseBC* promoter over time (Fig. 11). These experiments revealed that in wild-type UTI89, a robust surge in steady-state transcript was observed by 15 minutes post stimulus addition (Fig. 11). These results corroborated previous reports tracking the transcription of PmrA-regulated targets in *Salmonella*

(Shin et al., 2006). However, contrary to what has been reported for *Salmonella* (Merighi et al., 2009), the absence of QseB, QseC, PmrB, or PmrA abolished the transcriptional spike seen at 15 minutes (Fig. 11). These data implied that in the case of UPEC, all components are required to drive expression of *qseBC* in response to the ferric iron stimulus.

Previous studies indicated that QseC kinase activity is enhanced in response to epinephrine, norepinephrine and auto-inducer 3, a bacterial putative quorum signaling molecule of unknown structure (Clarke et al., 2006). We have demonstrated QseC readily auto-phosphorylates and phosphotransfers to QseB, even in the absence of signal, a behavior that is unlike typical histidine kinases (Fig. 12A and (Guckes et al., 2013; Kostakioti et al., 2009). *In vitro* phosphotransfer assays indicated that the addition of epinephrine (Fig. 12A), norepinephrine, or spent UPEC supernatant fractions did not increase QseC kinase activity towards QseB under the conditions tested, contrary to what would be expected if epinephrine were a signal for this system. Furthermore, it appears that epinephrine decreased the rate of phosphotransfer or increases the rate of de-phosphorylation by QseC under the conditions tested (Fig. 12A-C). Subsequent analyses probing for changes in *qseB* gene transcript in the presence of epinephrine indicated no differences in *qseB* steady-state transcript in the presence or absence of epinephrine in wild-type UTI89 or in a strain lacking the *qseC* gene (Fig. 12D). The *qseC* deletion mutant, UTI89Δ*qseC,* consistently had high *qseB* transcript levels, consistent with unregulated PmrB phosphotransfer to QseB (Guckes et al., 2013). Together, these results indicated that in UPEC, epinephrine and norepinephrine do not stimulate the kinase activity of the QseC sensor kinase and that QseBC is involved in proper stimulus response to ferric iron in conjunction with PmrAB.

We then probed whether PmrA- or QseB- mediated the activation surge in Fig. 11 was specific to stimulation with ferric iron, or whether other cations would elicit the same response. To test the specificity of the coordinated response to ferric iron, zinc chloride and copper sulfate were used as sources of zinc ($Zn^{2+}$) and copper ($Cu^{2+}$). These metal cations were chosen, based on previous studies listing high concentrations of extracellular zinc (II) as a putative signal for *E. coli* PmrB (Lee, Barrett, & Poole, 2005) and toxic ions including cesium, cobalt, copper, nickel, and ruthenium causing hypersensitivity in *E. coli* strains lacking QseBC (Zhou, Lei, Bochner, & Wanner, 2003). We tested the steady-state transcript abundance of *qseB* using a probe-based TaqMan qPCR approach that was similar to the approach employed to measure the responses to ferric iron (Fig. 11). Only the presence of ferric iron resulted in observed typical transcriptional surge (Fig. 11), while zinc cations led to a modest and consistent increase in the abundance of *qseB* transcript, that were maintained overtime and did drop to baseline levels (Fig. 13**,** green squares). Addition of copper cations steadily increased the amount of *qseB* transcript overtime, reaching maximal transcription at 60 minutes post-stimulation (Fig. 13**,** blue circles), suggesting that *qseBC* may be downstream of a different copper-responsive regulator. Based on these observations, we evaluated protein-protein interactions and downstream regulatory events in response to ferric iron.

*PmrB phosphotransfers to PmrA and QseB upon stimulation with ferric iron*

The studies summarized in Fig. 11 indicated a strong surge in *qseBC* transcript in response to ferric iron that only occurs when the QseBC and PmrAB systems are intact. These studies also suggested that signal interception occurs through PmrB and likely transduced by phosphorylation to the two response regulators. We have previously shown that PmrB

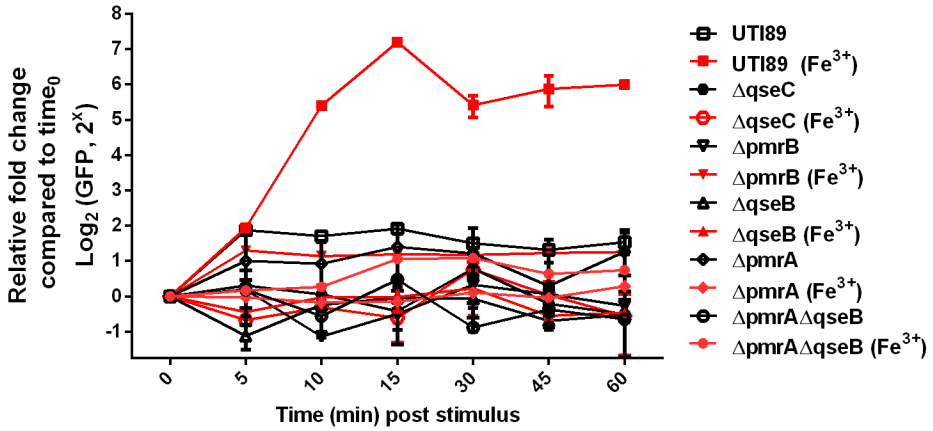


**Figure 11. All components of both TCSs are required for *qseBC* transcriptional surge in response to ferric iron.**

Graph depicts quantitative real-time PCR (qPCR) measuring *gfp* steady-state transcript abundance, which reports *qseBC* promoter activity using a P*qse*::*gfp* fusion construct. *gfp* mRNA abundances were measured by TaqMan qPCR. Fold changes were calculated using the ΔΔCT method, where *rrsH* was used as an endogenous control and samples were normalized to $time_0$. Fold changes are graphed on a $log_2$ scale. Error bars indicate SEM; experiment performed at least three times.

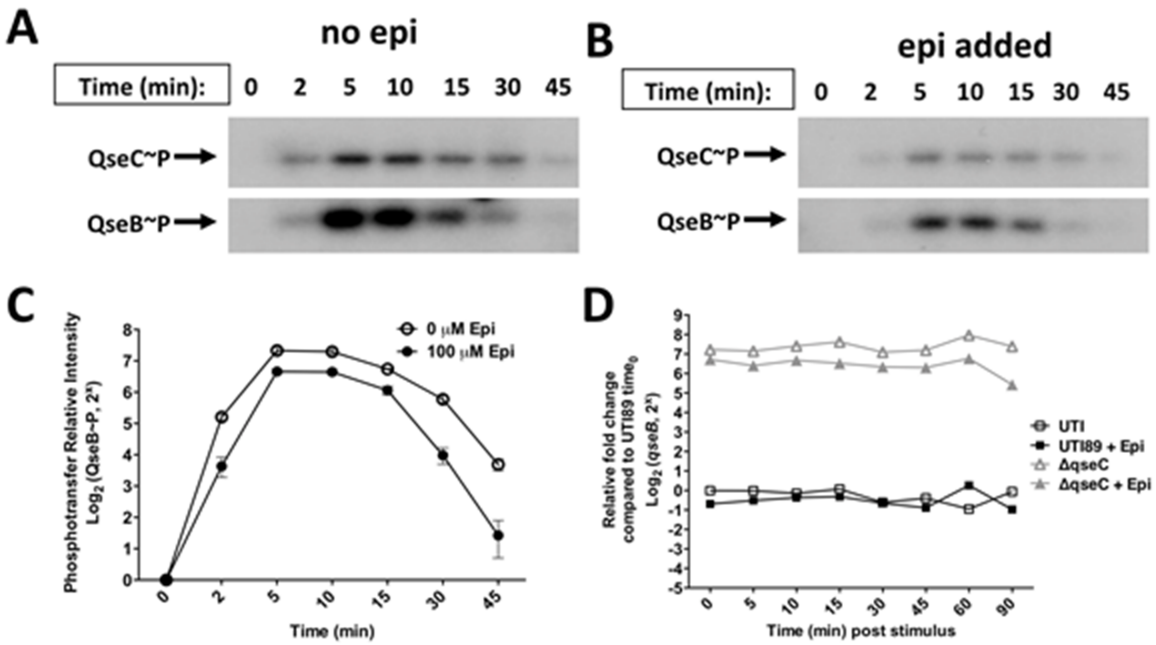


**Figure 12. QseC activity is not enhanced in the presence of epinephrine.**

**(A-B)** Panels depict radiographs that track auto-phosphorylation and subsequent phosphotransfer of $^{32}$P-γATP to QseB by QseC in the absence (**A**) and presence (B) of 100 μM epinephrine (Epi). Images are representative of at least 3 biological replicates. Detailed methods regarding the phosphotransfer experiments are described in the materials and methods section. **(C)** Representative quantitation of phosphorylated QseB (QseB~P) in the presence (Closed circle) and absence (open circle) of 100 μM epinephrine (Epi) using image J. **(D)** Representative qPCR analysis tracking the relative fold change of *qseB* transcript for wild type UTI89 (squares) and UTI89Δ*qseC* (triangles) in the presence (closed shape) and absence (open shape) of 100 μM epinephrine (Epi). Fold changes are graphed on a $Log_2$ scale.

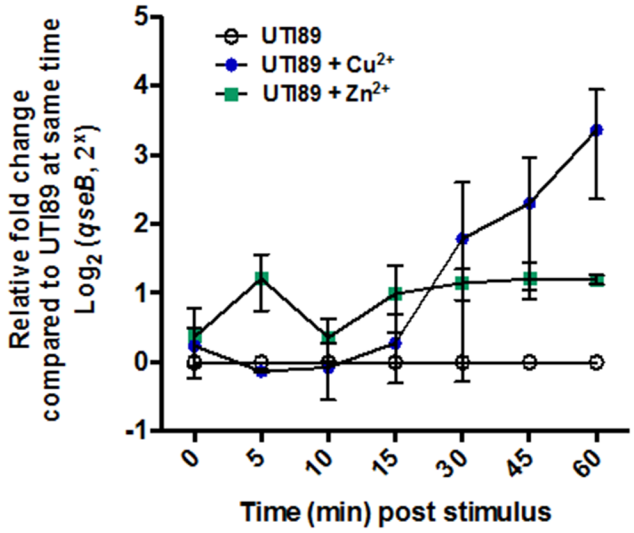


**Figure 13. The *qseBC* transcriptional surge is specific to ferric iron.**

Graph depicts qPCR measuring *qseB* steady-state transcript levels for UTI89 in N-minimal medium without any additional metals (open circles), UTI89 in the presence of copper (blue circle $Cu^{2+}$), and UTI89 in the presence of zinc (green square $Zn^{2+}$). Fold changes were calculated by the ΔΔCT method, where *rrsH* was used as an endogenous control and samples were normalized to matching time points of UTI89 in the absence of signal. Fold changes are graphed on a $Log_2$ scale. Error bars indicate SEM between 3 biological replicates.

indiscriminately phosphotransfers to QseB in the absence of signal (Chapter II; (Guckes et al., 2013). Here we evaluated how the kinetic activity of UPEC PmrB towards PmrA and QseB inthe presence of ferric iron. For these studies, tagged PmrB was expressed in strain UTI89 and membrane fractions were prepared as previously described (Kostakioti et al., 2009). Notably, UTI89 PmrB sequence harbors 98% nucleotide identity and 99% protein sequence identity to previously tested, non-pathogenic *E. coli* strain K12 (Table 1**,** Clustal Omega). In the absence of signal, UPEC PmrB exhibited strong phosphatase activity towards PmrA (Fig. 14A and Fig. 14E), consistent with previous reports evaluating PmrB activity in non-pathogenic *E. coli,* and consistent with the typical mechanism of action for signal-responsive kinase-phosphatases. PmrB indiscriminately phosphorylated the non-cognate response regulator QseB, in the absence of signal (Fig. 14C, and Fig. 14E), as we previously reported, indicating that in the absence of signal, PmrB can interact appropriately only with its cognate partner (Guckes et al., 2013).

When the phosphotransfer assays were repeated with 100μM ferric iron added to the reaction buffer, enhanced PmrB phosphotransfer was observed towards both PmrA and QseB (Fig. 14B, Fig. 14D, and Fig. 14F). On average, maximal phosphorylation of the response regulators was observed 10 minutes following addition of stimulus, with the highest rate of phosphorylation occurring within the first 2 minutes of the reaction (Fig. 14F). These data indicated that presence of stimulus changes the kinetic behavior of PmrB towards both the cognate (PmrA) and the non-cognate (QseB) partners.

*QseB and PmrA co-direct the expression of ferric iron-regulated targets*

We then assessed whether PmrA and QseB are both required for optimal expression of *yibD*, another ferric iron-stimulated target that has been shown to influence LPS modification in

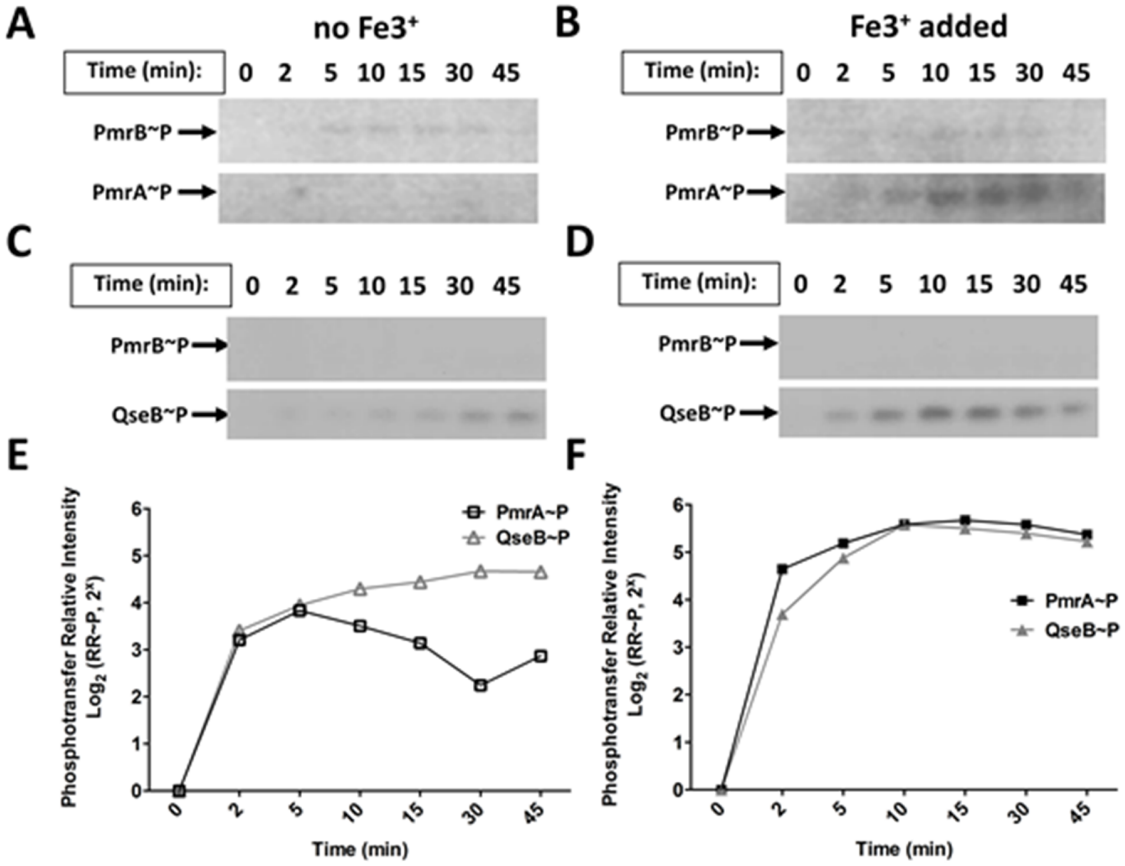


**Figure 14. PmrB phospho-transfer activity is enhanced in the presence of ferric iron.**

(A-B) Panels depict radiographs that track auto-phosphorylation and subsequent phosphotransfer of $^{32}$P-γATP to PmrA by PmrB in the absence (**A**) and presence (**B**) of 100 μM ferric iron ($Fe^{3+}$). Images are representative of at least 3 biological replicates. **(C-D)** Panels depict radiographs that track auto-phosphorylation and subsequent phosphotransfer of $^{32}$P-γATP to QseB by PmrB in the absence (**C**) and presence (**D**) of 100 μM ferric iron ($Fe^{3+}$). Images are representative of at least three biological replicates. Detailed methods regarding the phosphotransfer experiments are described in the materials and methods section. **(E-F)** Graphs depict representative quantitation of phosphorylated response regulators (RR) PmrA (PmrA~P, squares) and QseB (QseB~P, triangles) using image J in the absence (**E** open shapes) or presence (**F,** closed shapes) of 100 μM ferric iron ($Fe^{3+}$). Relative intensities are graphed on a $Log_2$ scale. Details on the analysis are provided in the materials and methods.

**Table 1: QseB and QseC protein sequence identity amongst *E. coli* strains and other enteric bacteria.**

| Strain | QseB protein sequence identity (%) | GenBank accession number | QseC protein sequence identity (%) | GenBank accession number |
|---|---|---|---|---|
| *E. coli* | | | | |
| UPEC str. UTI89 | 100 | ABE08897.1 | 100 | ABE08898.1 |
| APEC O1K1 str. O1 | 100.00 | ABJ02530.1 | 100.00 | ABJ02531.1 |
| B2 phylogenetic group: O83:H1 | 100.00 | YP_006121348.1 | 98.89 | YP_006121349.1 |
| D1 phylogenetic group: UMN026 | 100.00 | YP_002414171.1 | 98.89 | YP_002414172.1 |
| D2 phylogenetic group: IAI39 | 100.00 | YP_002409426.1 | 98.22 | YP_002409427.1 |
| UPEC str. CFT073 | 99.54 | AAN82208.1 | 98.89 | AAN82209.1 |
| K12 str. MG1655 | 99.54 | NP_417497.1 | 98.89 | NP_417498.1 |
| B1 phylogenetic group: O104:H4 | 99.54 | AFS72693.1 | 98.22 | AFS72692.1 |
| EAEC str. E55989 | 99.54 | CAU99558.1 | 98.22 | CAU99560. |
| EHEC str. EDL933 | 99.54 | AIG70396.1 | 98.22 | AIG70397.1 |
| EPEC O55:H7 str. CB9615 | 99.54 | ADD58237.1 | 98.22 | ADD58238.1 |
| O157:H7 str. Sakai Sakai* | 99.54 | NP_311934.1 | 97.13 / 98.55 | NP_3909913-3910437 NP_3910431-3911261 |
| ETEC O139:H28 str. E24377A | 99.07 | ABV19769.1 | 98.22 | ABV17955.1 |
| Additional enteric bacteria | | | | |
| *Shigella sonnei* str. Mosely | 100.00 | EJL13232.1 | 99.11 | EJL13233.1 |
| *Salmonella enterica* Typhumurium str. LT2 | 87.67 | NP_462092.1 | 79.29 | NP_462093.1 |

| | | | | |
|---|---|---|---|---|
| *Salmonella enterica* Typhumurium str. 14028S | 87.67 | ACY90252.1 | 79.29 | ACY90253.1 |
| *Klebsiella pneumoniae* str. 342 | 83.11 | ACI08570.1 | 67.04 | ACI08526.1 |
| *Edwardsiella tarda* | 74.89 | ADO13165.1 | 56.35 | ADO24152.1 |

***Sakai has a stop codon in the middle of this putative QseC sequence rendering QseC non-functional in this strain.**

*Salmonella enterica* (Merighi et al., 2009; Tamayo et al., 2002). The promoter of UPEC-encoded *yibD* also contains a PmrA binding consensus and is bound by PmrA in *in vitro* assays (Guckes et al., 2013). Analysis of *yibD* expression in response to ferric iron revealed that, compared to wild-type UTI89, deletion of *pmrA* abolished expression, while deletion of *qseB* reduced the *yibD* transcriptional surge by five-fold (Fig. 15). Subsequent electrophoretic mobility shift assays (EMSAs) indicated that PmrA and QseB could each physically engage the *yibD* promoter, albeit with different binding affinities (Fig. 16). *In vitro* phosphorylated PmrA (PmrA~P) caused a discernible shift in DNA at a concentration of 30pmol of purified protein, while *in vitro* phosphorylated QseB (QseB~P) was able to directly bind the *yibD* promoter at a concentration of 100 pmol (Fig. 16). This binding was shown to be specific as unlabeled *yibD* promoter was able to titrate both QseB and PmrA protein from labeled promoter (Fig. 16).

*PmrA and QseB mediate UPEC tolerance to polymyxin B*

In *Salmonella enterica*, the PmrAB TCS was shown to mediate lipopolysaccharide (LPS) modifications to buffer against damage due to antimicrobial peptides like polymyxin B (PMB) (Kato et al., 2012). Another TCS, PhoPQ, has been shown to coordinate with PmrAB to contribute to the control of LPS modifications in response to increased decreased magnesium ions (Kato et al., 2012). However, the same coordination between PmrAB and PhoPQ has not been shown in *E. coli* (Winfield & Groisman, 2004). *E. coli* strains not harboring the *mcr-1* plasmid typically show susceptibility to PMB and colistin. When we tested UTI89 and mutants deleted for components of QseBC, PmrAB and PhoPQ for PMB sensitivity in the absence of pre-stimulation with ferric iron, we observed that minimum inhibitory concentrations (MICs) to PMB were similar between wild-type and mutants lacking the entire QseBC, PmrAB, or PhoPQ

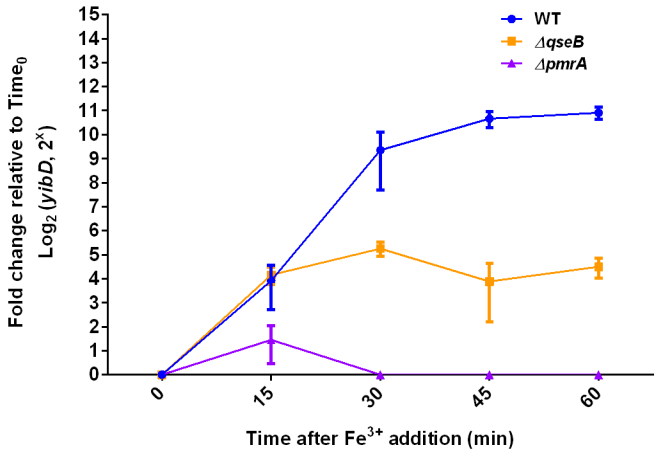


**Figure 15. Additional targets controlled by both PmrA and QseB response regulators**. qPCR depicting transcriptional surge of *yibD* in response to ferric iron. *gyrB* was used as an endogenous control to calculate ΔΔCT values compared to each strain's $time_0$. Error bars indicate the SEM of three biological replicates.

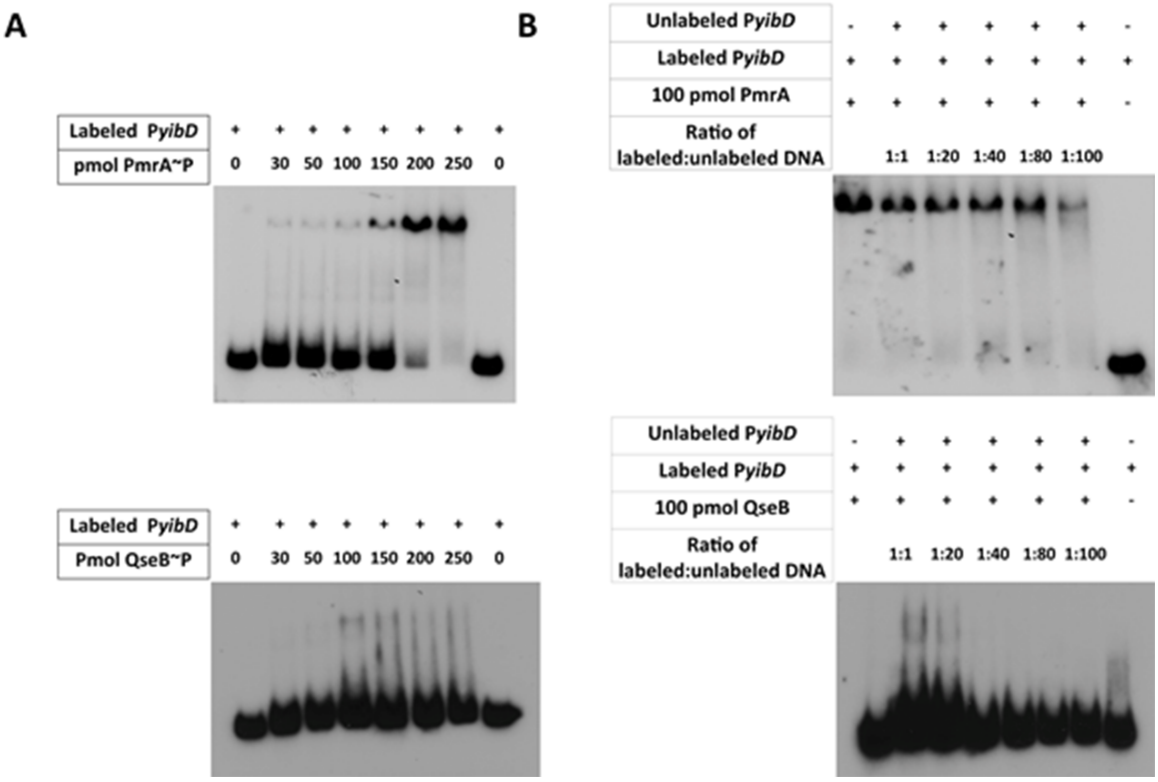


**Figure 16. PmrA and QseB binding to the *yibD* promoter is specific.**

**(A)** EMSA using labeled *yibD* promoter DNA using indicated amounts of *in vitro* phosphorylated PmrA and QseB. (B) EMSA showing 100 pmol of *in vitro* phosphorylated PmrA or QseB binding to the labeled *yibD* promoter DNA with increasing concentrations of unlabeled promoter. Blots are representative of at least three biological replicates.

TCSs (Fig. 17) indicative of overall baseline susceptibility of UPEC to PMB. However, strain UTI89Δ*qseC*Δ*pmrA*, which positively biases cross-interaction between PmrB and QseB, had a statistically significant increase in PMB tolerance (Fig. 17). This increase in MIC observed with the Δ*qseC*Δ*pmrA* mutant was unchanged with the additional deletion of *phoPQ* (Fig. 17). However, when *qseB* was additionally removed from the Δ*qseC*Δ*pmrA* mutant, the MIC returned to wild-type susceptibility concentrations.

Previous studies by Winfield and Groisman indicated that pre-treatment of *E. coli* with sub-lethal concentrations of ferric iron boosted tolerance to PMB (Winfield & Groisman, 2004). Given the increased tolerance when PmrB and QseB were isolated (Δ*qseC*Δ*pmrA* mutant), and the observed ability of PmrB to phosphorylate both PmrA and QseB in response to ferric iron, we asked whether pre-treatment of ferric iron would prime UPEC to prevent damage due to PMB in a PmrA-QseB-dependent manner. To test this, wild-type UTI89 and isogenic *pmr* and *qse* mutants were grown in the presence or absence of ferric iron for two hours, after which they were exposed to 2.5 μg/mL PMB, and subsequently assessed for survival. As a control, *Salmonella enterica* serovar Typhimurium strain 14028 was included in the studies, since it has previously been shown that *Salmonella* tolerance to PMB increases after incubation with ferric iron in a PmrAB-PhoPQ dependent manner (Winfield & Groisman, 2004). These studies revealed that, consistent with previous observations, *Salmonella* had a higher overall tolerance to PMB, even in the absence of ferric iron conditioning. Conditioning with ferric iron prior to exposure to PMB resulted in 75% survival for WT UTI89, a value that is comparable to tolerance exhibited by *Salmonella* (Fig. 18). In contrast, the Δ*pmrA* mutant exhibited decreased survival to 20%, while the mutant lacking QseB exhibited even greater reduction in survival, declining to about 10% compared to pre-treated WT UTI89. The mutants lacking both *pmrA* and

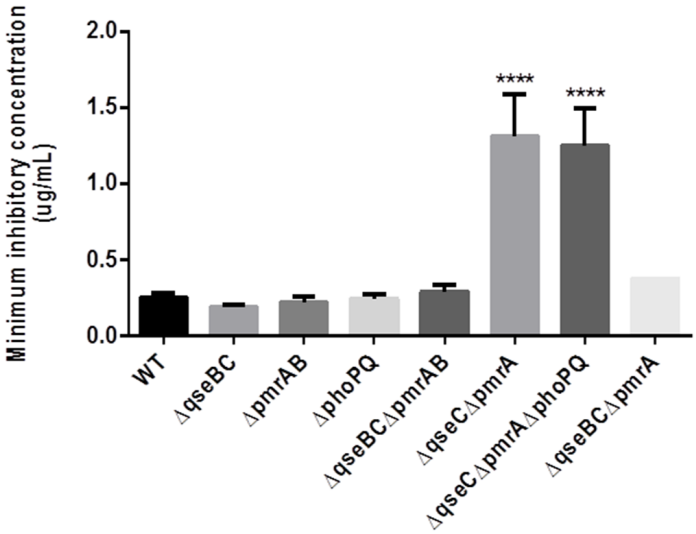


**Figure 17. Minimum inhibitory concentrations of polymyxin B.**

Minimum inhibitory concentrations for polymyxin B without pre-treatment of bacteria with ferric iron were calculated for indicated strains using Etest strips (Biomerieux). Experiments were performed a minimum of four times, where error bars represent standard error of the mean (SEM). Statistical analyses were performed using a two-way ANOVA with a Tukey multiple comparison test, where ****, $P \leq 0.0001$.

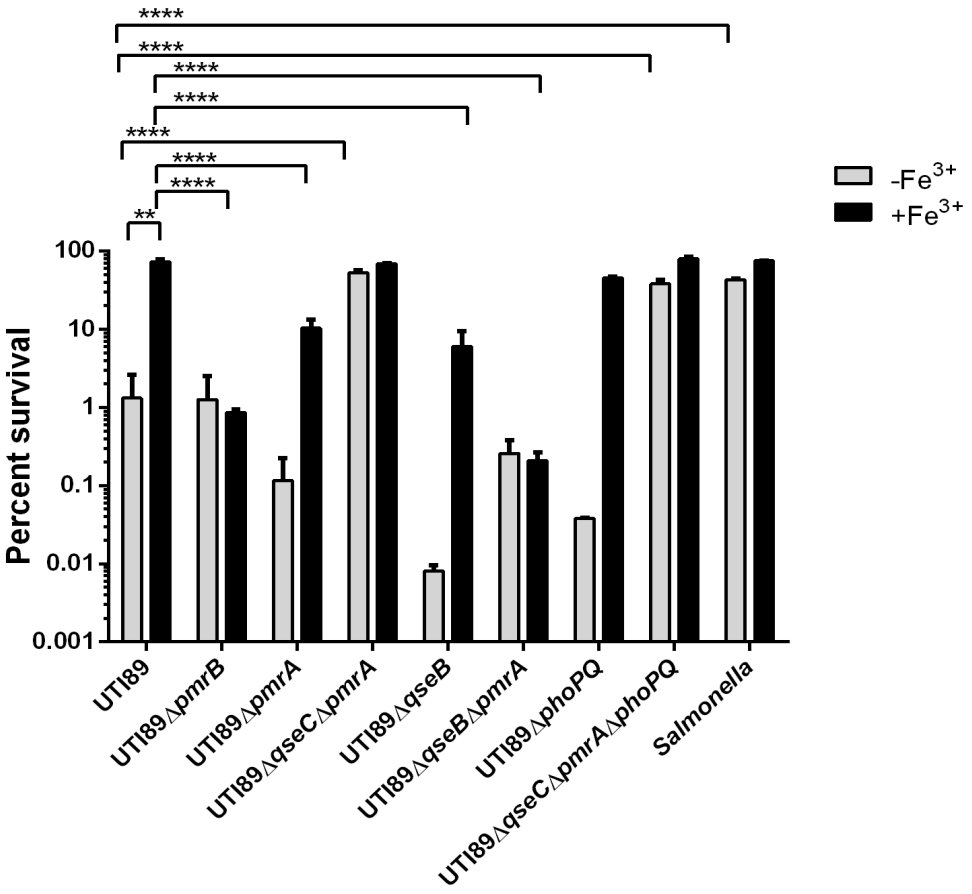


**Figure 18. Polymyxin B resistance is enhanced in a PmrAB and QseB dependent manner**.

Graph reports UPEC tolerance to 2.5 μg/mL polymyxin B with or without ferric iron pre-conditioning. "-$Fe^{3+}$" indicates cells grown in N-minimal media without additional ferric iron before exposure to polymyxin B. "+$Fe^{3+}$" indicates cells grown in N-minimal media with 100μM ferric iron before exposure to polymyxin B. Survival was calculated by dividing the number of CFUs recovered after polymyxin B incubation by the number of CFUs recovered after incubation in PBS alone. Error bars represent SEM of three biological replicates. Statistical analyses were performed using Two-Way ANOVA with Bonferroni post-test. P values indicated: *, $P<0.05$; **, $P\leq0.01$; ***, $P\leq0.001$; ****, $P<0.0001$. Additionally, the survival ratio between paired batches of pre-conditioned and non-conditioned bacteria were compared across strains and were shown to be statistically significant using a non-parametric one-way analysis of variance by the Kruskal-Wallis test, $P<0.01$. All statistical analyses were performed using GraphPad Prism software.

*qseB* genes had survival percentages comparable to those seen in the Δ*pmrB* mutant. Deletion of *phoPQ* did not significantly alter UTI89 survival (Fig. 18), indicating that pre-conditioning with ferric iron raises UPEC tolerance to PMB through coordinated regulation of downstream targets by PmrAB and QseBC and without regulatory input by PhoPQ.

To determine if this phenotype was strain-specific, we tested various other strains of extraintestinal *E. coli* (ExPEC), including well-characterized strains EC958 and CFT073, as well as urinary isolates collected from the Vanderbilt University Hospital. PMB tolerance post-ferric iron conditioning was variable among the different strains. Vanderbilt urinary tract isolates (VUTI) 39, 47, 61 and 77, as well as CFT073 exhibited increases in tolerance post-ferric iron treatment, with VUTI77 and CFT073 having the highest tolerance (Figure 19). However, VUTI61 and EC958 exhibited no difference in PMB susceptibility, suggesting that the observed effects with PMB are not strain-specific, but are also not universally conserved among urinary isolates. Taken together, our analyses have uncovered a previously uncharacterized interaction between PmrA and QseB that mediates resistance to polymyxin B in a subset of *E. coli* strains.

## Discussion

In work described in this chapter, we sought to determine whether there is a condition in which PmrAB and QseBC physiologically interact. We found that in contrast, to the previously reported cross-interacting TCSs (Matsubara et al., 2000; Howell et al., 2006; Rabin et al., 1993; Drepper et al., 2006; Schröder et al., 1994), QseBC-PmrAB interactions are mediated by a single stimulus, which culminates in kinetically equivalent phosphorylation of two response regulators, at least based on *in vitro* phosphotransfer assays (Figs. 14 and 20).

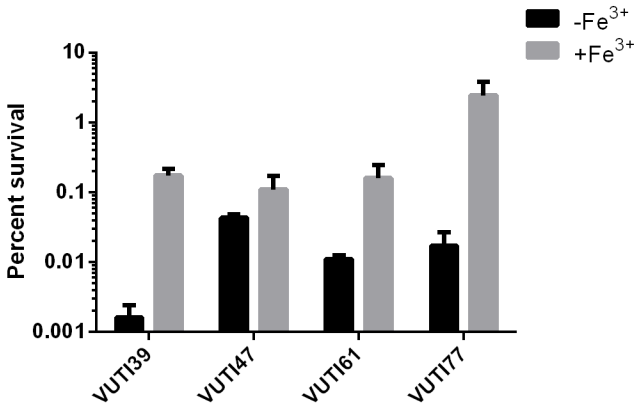


**Figure 19. Polymyxin B tolerance post-ferric iron conditioning is variable among ExPEC strains.**

Graph depicts UPEC tolerance to 2.5ug/mL polymyxin B with or without ferric iron pre-conditioning. "-$Fe^{3+}$" indicates cells grown in N-minimal media without additional ferric iron before exposure to polymyxin B. "+$Fe^{3+}$" indicates cells grown in N-minimal media with 100μM ferric iron before exposure to polymyxin B. Survival was calculated by dividing the number of CFUs recovered after polymyxin B incubation by the number of CFUs recovered after incubation in PBS alone, and multiplying by 100. Error bars represent SEM of three biological replicates.

Here, there was an equally rapid increase in phosphotransfer from PmrB to PmrA and QseB in the presence of ferric iron (Fig. 14). This response was specific to ferric iron and did not appear to involve PhoPQ, which has been proposed to physically interact with cationic polypeptides such as PMB ((Figs. 17 and 18 and (Gunn et al., 1998; Hicks et al., 2015). Notably, no QseBC- (PreAB-) independent (Merighi et al., 2009), it is important to note that epinephrine, and other interaction between the two TCSs was observed with the reported QseC signal, epinephrine (Fig. 12). While the effects of epinephrine on motility in *Salmonella* were previously rendered catechols, can chelate ferric iron. Previous studies by Sánchez *et al*. and Merighi *et al.* have suggested that effects on *Salmonella* motility could be a product of iron availability rather than catecholamine presence, and our data in UPEC support this hypothesis.

Combined our data also point to PmrB being the primary signal receptor, the activation of which leads to downstream activation of QseB and PmrA, at least in the case of UPEC. Therefore, as expected, deletion of *pmrB* abolished the *qseBC* transcriptional surge, consistent with PmrB being the sole ferric iron sensor in the QseBC-PmrAB circuit (Figs. 11 and 14). The involvement of QseC in mediating the proper surge and decline of the transcriptional responses to ferric iron is not yet clear; when QseC is absent, any *qseBC* transcriptional surge is obscured by constitutively high *qseB* expression (Fig. 14E). This suggests that QseC physically prevents PmrB-QseB interactions or resets the system via dephosphorylation. How these types of control are overridden when PmrB detects the ferric iron signal remains unknown. QseC could be sequestering QseB from interacting with and being phosphorylated by PmrB unless signal is present. Both possibilities by which QseC could be contributing to this "four-component" system deviate from the current standard of bacterial two-component system biology. Another possible mechanism for QseC-mediated control of the ferric iron response is QseC hetero-dimerization

with PmrB, which would prevent aberrant phosphotransfer between PmrB and QseB until signal is detected and sensor kinase homodimers preferably form. Sensor hetero-dimerization in bacterial pathogens has been reported at least once in the literature (Goodman et al., 2009), raising the possibility that pathogenic strains of bacteria have evolved distinct mechanisms for integrating signals and/or mediating distinct responses to an incoming stimulus that may be of import during infection. For example, in acute urinary tract infection, bacteria are starved for iron, as many studies have previously shown (Henderson et al., 2009), yet, at the same time, they have to be able to distinguish between the need for metals and detrimental cations deployed by the innate immune response that are catastrophic to bacterial membrane integrity. It is also possible that ferric iron in this study merely acts as a proxy to the signal that is detected *in vivo*. This could emcompass a molecule produced by the bacteria in the gut or the host immune response. UPEC infect the urinary tract, but can persist for long periods of time in the gut. QseBC-PmrAB interactions may mediate survival in the gastrointestinal niche or the urinary environment. Further in vivo analysis are required to address these possibilities. Future studies will also focus on delineating the potential protein-protein interactions that could be contributing to the tight control of QseBC-PmrAB responses to ferric iron.

While our transcriptional studies mostly focused on the *qseBC* operon, we observed similar interactions for an additional shared target, *yibD*. This gene target was previously reported to be part of the extensive PmrAB regulon in *Salmonella* (Merighi et al., 2009; Kato et al., 2003). To date, the only gene targets reported for QseB have been *qseBC* and *flhDC* (Clarke et al., 2005; Sperandio et al., 2002). Deletion of either response regulator attenuated the *yibD* and *qseBC* transcriptional surge in response to ferric iron (Fig. 15), suggesting that both of these gene targets are part of the QseBC-PmrAB regulon and that QseB augments transcription of *yibD* in

the presence of PmrA. This is critical, given our studies investigating resistance mechanisms to PMB after ferric iron treatment increased survival of several *E. coli* urinary isolates. Colistin is a last resort antibiotic for treating UTIs. Our data suggest that in at least a portion of urinary isolates, intrinsic colistin resistance can be coaxed by ferric iron, and perhaps an unidentified bacterial or host derived molecule. Ongoing studies described in Chapters IV and V of this thesis dissect the QseBC-PmrAB regulon in UPEC strain UTI89 and investigate single nucleotide polymorphisms (SNPs) in the *qseBC* promoter that contribute to signal response divergence among *E. coli* pathotypes and strains.

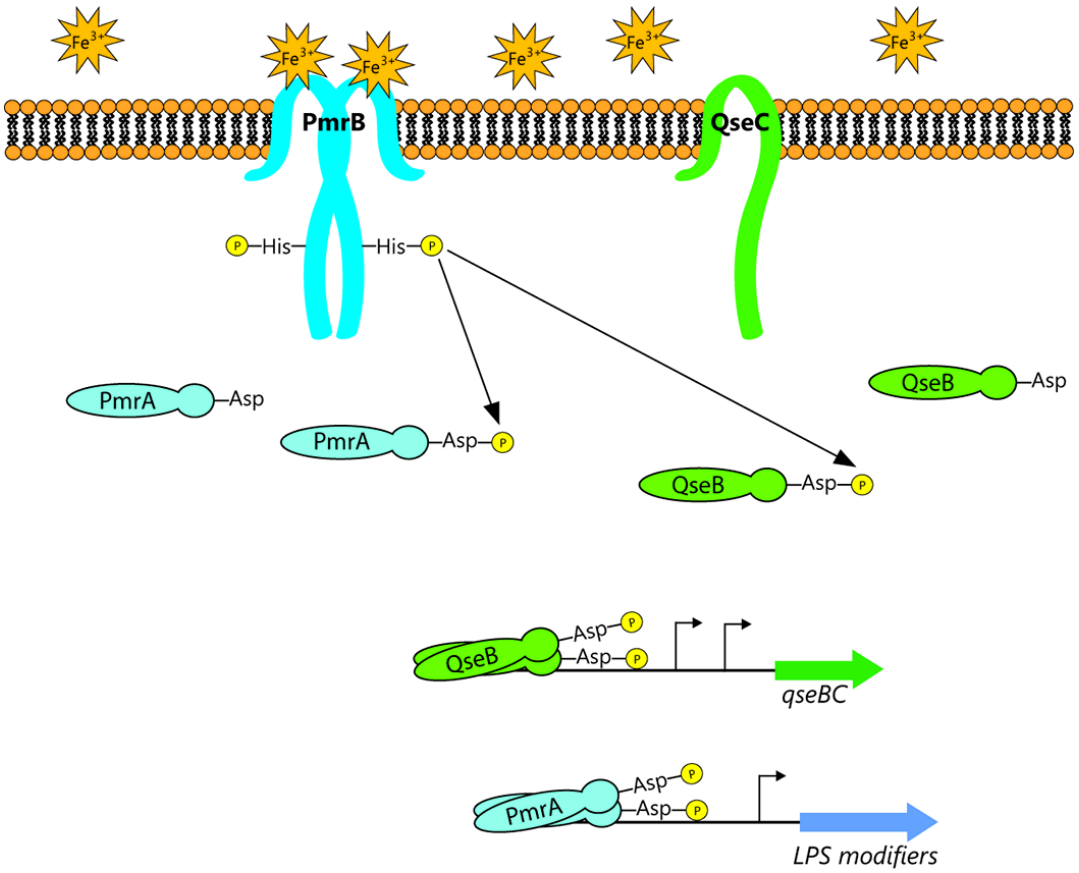


**Figure 20. Model of QseBC-PmrAB signal transduction in response to ferric iron.**

Ferric iron is sensed by the PmrB sensor kinase, which in turn, phosphorylates both the cognate PmrA response regulator and the non-cognate QseB response regulator.

CHAPTER IV

# QSEB AND PMRA RESPONSE REGULATORS COORDINATE TO MEDIATE QSEBC TRANSCRIPTIONAL CONTROL IN UPEC STRAIN UTI89

## Introduction

*E. coli* are classified into 5 major phylogenetic groups or clades: A, B1, B2, D, and E (Clermont et al., 2000). These groups have been defined based on nucleotide sequence comparisons among a core set of housekeeping genes (Sims & Kim PNAS 2011). However, extensive horizontal gene transfer in different *E. coli* strains has led to the acquisition and loss of numerous genes, including those involved in virulence. Therefore, some phylogroups are separated by as little as 3% nucleotide identity between housekeeping genes but as much as 50% of total genes contained within the genome (Sims & Kim, 2011). Phylogenetic group A is comprises strains that are non-pathogenic (Rijavec et al., 2008; Johnson et al., 2001). The extra-intestinal pathogenic *E. coli* (ExPEC) strains mostly belong to the phylogenetic group B2, with some strains within the phylogroup D (Johnson & Stell, 2000; Picard et al. 1999). The majority of intestinal pathogenic *E. coli* strains are found within phylogroups B1, D, and E (Pupo et al., 1997; Gordon et al., 2008). No studies have been performed to evaluate diversity in the signaling pathways of the different *E. coli* pathotypes and/or among the different *E. coli* phylogroups.

As explained in Chapter I, differences in the QseBC signaling cascade and output responses have been reported extensively between UPEC and EHEC (Guckes et al., 2013; Kostakioti et al., 2009; Clarke et al., 2006; Clarke et al., 2005). One explanation for these

discrepancies may be the variations in responses and signals that are important to the survival of the bacteria in the urinary tract versus the gut. Therefore, variations in the evolutionary pressures the different *E. coli* experience may manifest as divergence among *E. coli* QseBC signaling cascades. Additionally, Figure 19 depicts differences in the ability of ferric iron to induce increased PMB tolerance in clinical urinary tract isolates including UPEC and asymptomatic strains, demonstrating that the variation in QseBC signaling may also exist among ExPEC isolates, including UPEC and asymptomatic strains. Therefore, with the help of collaborators at the Broad Institute, we have begun mapping

To address this gap in the field, we collaborated with Dr. Ashlee Earl's group at the Broad Institute to begin mapping single nucleotide polymorphisms (SNPs) within the *qseBC* promoter among different *E. coli* strains, spanning all major phylogroups. In parallel studies, we undertook a thorough analysis of the *cis*-elements of the *qseBC* promoter in UPEC strain UTI89. We have shown that PmrA and QseB upregulate *qseBC* transcription in response to ferric iron, and that this increase in transcription is an important upstream target of a pathway that leads to increased antibiotic tolerance (Fig. 16). Although our previous studies demonstrated that QseB and PmrA could individually bind the qseBC promoter, we have not extensively interrogated the interplay of the two proteins together in association with *qseBC* promoter DNA. Here we describe studies that begin to dissect interactions PmrA,QseB, and promoter DNA.

## Methods

*Strains and Constructs*

All studies have been performed in the uropathogenic *Escherichia coli* strain UTI89 (Mulvey et al., 2001) and isogenic mutants. Deletion strains UTI89Δ*pmrA*, UTI89Δ*pmrB*,

UTI89Δ*pmrAB*, UTI89Δ*qseC*, UTI89Δ*qseB*, UTI89Δ*pmrAB* and the quadruple mutant UTI89Δ*pmrAB*Δ*qseBC* have been previously created (Guckes et al., 2013; Kostakioti et al., 2009; Hadjifrangiskou et al., 2011), using the method of Murphy and Campellone (2003).

The previously constructed transcriptional reporter plasmid pP*qse*::GFP (Kostakioti et al., 2009) was used as a template for site-directed mutagenesis to generate the PmrA binding site variants. Site-directed mutagenesis accomplished using an adapted method from the Agilent QuikChange II protocol as previously described (Kostakioti et al., 2009).

*Electrophoretic Mobility Shift Assays (EMSAs)*

EMSAs were performed as described as in Chapter III. A representative of at least 3 biological replicates is presented in each figure.

*Motility Assays*

Motility assays were performed as described in previous chapters where motility diameters were recorded for at least 5 biological replicates with at least 3 technical replicates per experiment. Statistical analysis was performed using one-way ANOVA with $P<0.05$ considered significant.

*Transcriptional Profiling by qPCR*

RNA was extracted using the Qiagen RNeasy kit and DNAse-treated as described in previous chapters. One microgram of DNAse-treated RNA was subjected to reverse transcription, using Superscript II Reverse transcriptase and random hexamers (Life Technologies). qPCR was performed on 6.25 and 3.125 ng of cDNA to probe for relative transcript levels. Relative-fold change was determined using the $\Delta\Delta C_T$ method of Pfaffl *et al.*

(2001), and statistical analyses on the expression levels obtained from at least three biological replicates were performed using one-way ANOVA, with $P<0.05$ considered significant.

*Genomic alignments*

Forty-nine high-quality genomes representing pathogenic and non-pathogenic strains from each major clade (A, B1, B2, D, E, and *Shigella*) were used to construct phylogenetic trees using FastTree and RAxML (Price, Dehal, & Arkin, 2010; Stamatakis, 2014). Alignments were made using UTI89 genome nucleotide coordinates shown in Table 2.

**Table 2. Nucleotide coordinates used in P*qse* alignments.**

| | nt coordinates from UTI89 genome (NC_007946.1) |
|---|---|
| QseB | 3387184-3387843 |
| QseC | 3387840-3389189 |
| Pqse | 3387024-3387183 |

## Results

*QseB and PmrA co-direct the expression of qseBC*

The binding consensus for PmrA is well described (Tamayo et al., 2002) and found within the *qseBC* promoter (Guckes et al., 2013). Analyses by Clarke *et al*. elucidated a loose QseB binding consensus within the *qseBC* promoter and this binding sequence lies 5 nucleotides away from the PmrA consensus (Fig. 21A). To ascertain the molecular interplay between QseB and PmrA on the *qseBC* promoter, we first examined the binding affinity of phosphorylated and un-phosphorylated QseB and PmrA on the *qseBC* promoter. Phosphorylation of response regulators allows the protein to assume a conformation that allows for more stable DNA binding

(Stock, 2000). Previously constructed phospho-mimetic (QseB_D51E) and phospho-inactive (QseB_D51A) QseB variants (Kostakioti et al., 2009) were used, as well as corresponding phospho-inactive (PmrA_D51A) and phospho-mimetic (PmrA_D51E) variants in PmrA, which were generated for this study.

EMSAs revealed that in its un-phosphorylated form, QseB did not bind the *qseBC* promoter region (Fig. 21B), whereas productive binding could be seen with the phospho-mimetic variant, QseB_D51E, at concentrations as low as 50 pmol per reaction (Fig. 21C). This observation was consistent with typical response regulator binding ability activated by phosphorylation. Unlike QseB, PmrA did not require phosphorylation to bind the *qseBC* promoter (Fig. 21D-E), although PmrA_D51E had a higher affinity for the promoter causing a notable shift at 20 pmol of protein (Fig. 21D), compared to the 50 pmol required for PmrA_D51A (Fig. 21E). Combined, our results indicate that QseB requires phosphorylation to bind the promoter, while PmrA binds the *qseBC* sequence regardless of phosphorylation state. Because PmrB has been shown to phosphorylate PmrA and QseB in response to ferric iron (Fig. 14), we also tested binding activity of phospho-mimetic PmrA when incubated with phospho-mimetic QseB, simulating the situation that would occur in the presence of signal (Fig. 21F). Interestingly, the co-incubation of 30 pmol PmrA_D51E and an equimolar concentration of QseB_D51E with labeled *qseBC* promoter resulted in a DNA shift that was identical to the QseB-promoter migration pattern (Fig. 21F). Collectively, these data indicate the presence of PmrA~P somehow enhances QseB~P binding to its own promoter.

*QseB and PmrA stoichiometry dictates qseBC promoter control*

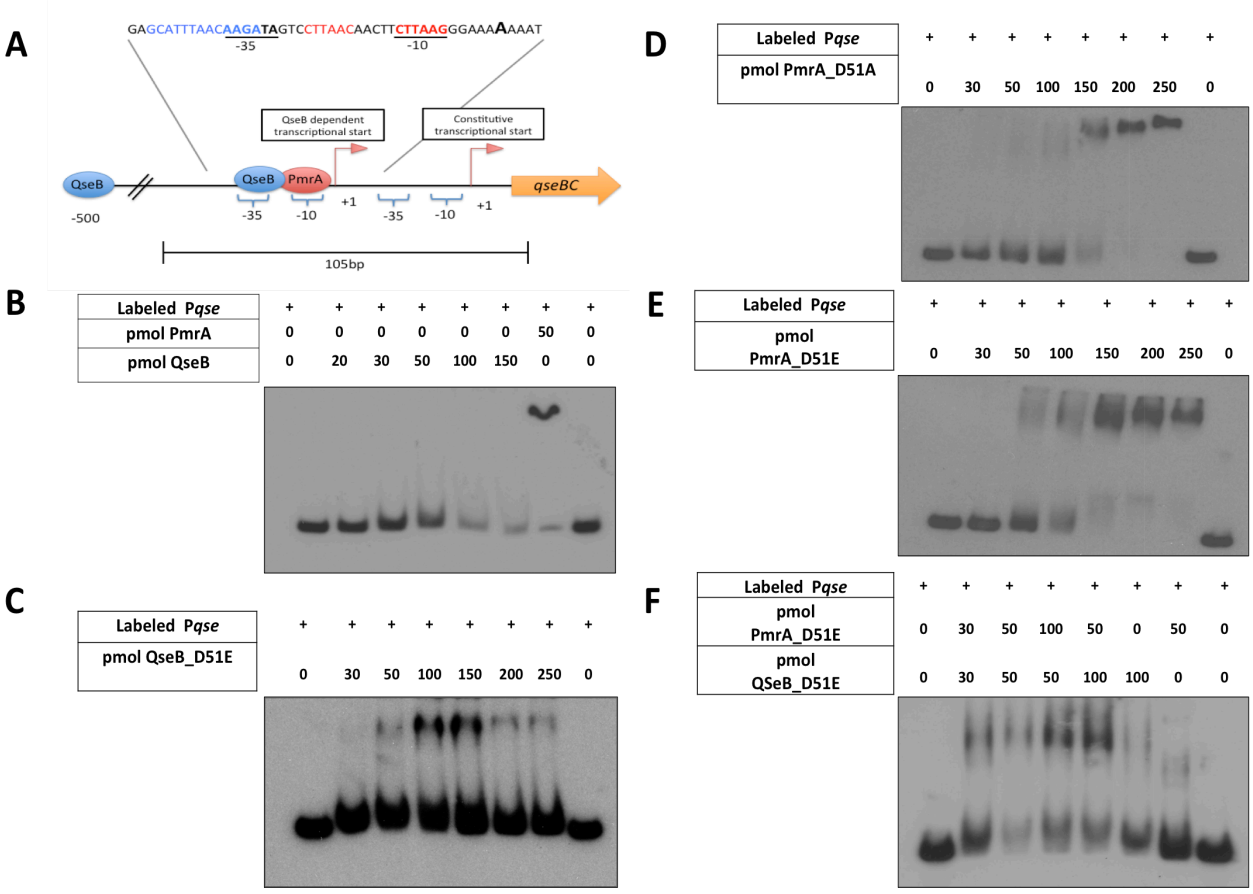


**Figure 21. PmrA stabilizes QseB-promoter interactions.**

A) Schematic depicting the reported binding sites for QseB (blue; Clarke et al., 2005) and hypothesized binding site for PmrA (red). Numbers indicate distance from the transcriptional start sites. Bracket at the bottom indicates the portion of the promoter used for EMSAs in B-F. B) EMSA using radiolabeled *qseBC* and purified PmrA or QseB as indicated. C) EMSA using radiolabeled *qseBC* and purified QseB_D51E (conformationally phosphorylated) D) EMSA using radiolabeled *qseBC* and purified PmrA_D51A (conformationally unphosphorylated) E) EMSA using radiolabeled *qseBC* and purified PmrA_D51E (conformationally phosphorylated). F) EMSA using radiolabeled *qseBC* promoter and both purified QseB_D51E and PmrA_D51E in pmol amounts indicated.

The baseline expression levels of *pmrAB* and *qseBC* have not been determined. Therefore how QseB and PmrA stoichiometry influences protein-DNA interactions in the presence and absence of signal remains unknown. To determine how altered PmrA levels would influence *qseBC* expression, we introduced *pmrA* extra-chromosomally and evaluated *qseB* steady-state transcript levels by qPCR. Consistent with previous observations, (Figure 7B), Δ*qseC* had significantly higher *qseB* transcript than WT, while the Δ*qseC*Δ*pmrA* strain had intermediate transcript levels between those of WT and Δ*qseC* (Fig. 22A). Surprisingly, over-expression of *pmrA* in the Δ*qseC*Δ*pmrA* strain reduced the *qseB* transcript levels closer to WT, suggesting a suppressive effect when abundant (Fig. 22A).

Given the lack of QseB phosphor-specific antibodies, motility were used as a proxy for active QseB levels. Phosphorylated QseB is a known repressor of the *flhDC* flagella regulator (Kostakioti et al., 2009); therefore, an increase in *qseB* expression manifests as a motility decrease in soft agar. Consistent with the qPCR data, we observed and inverse relationship between motility and *qseB* expression (Figure 22). The over-expression of PmrA_D51E or PmrA_D51A led to a reduction in *qseB* transcript and increase in motility, indicative that less QseB was produced in the presence of high levels of PmrA (Fig. 22B). Together, these data suggest that a complete lack of PmrA or over-expression of PmrA leads to decreased *qseBC* expression (Fig. 22).

*PmrA and QseB binding sites overlap*

*In silico* analysis and EMSAs demonstrating binding sites for PmrA and QseB, which appear to overlap. This overlap is likely to influence productive protein-DNA interactions and/or interactions of RNA polymerase with the promoter. The PmrA binding site is made up of two

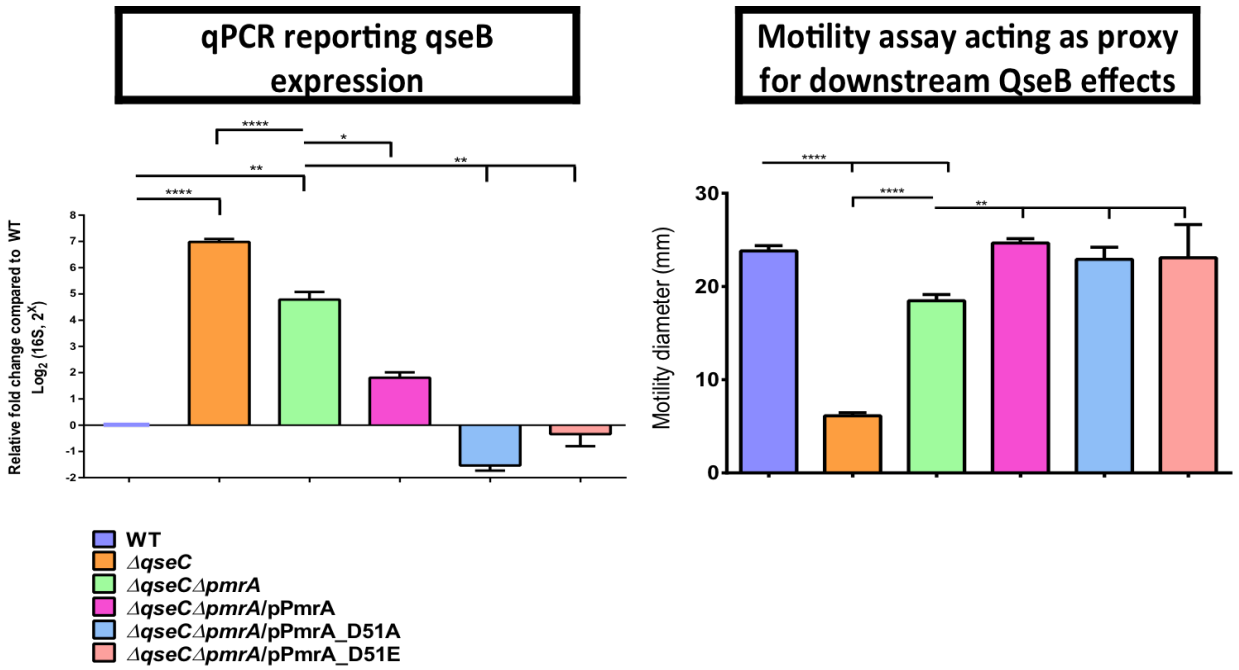


**Figure 22. PmrA contributes to *qseBC* transcriptional control.**

A) qPCR measuring *gfp* mRNA in strains containing a *gfp* fusion to the *qseBC* promoter. *rrsh* was used as an endogenous control to calculate ΔΔCT values compared to the WT strain. B) Motility assay reporting flagella expression via the distance bacteria swim through soft agar. Strains either contain an empty pTrc99a plasmid or a pTrc99a plasmid containing indicated phospho-variants of *pmrA*. Error bars represent SEM. Statistical analyses were performed by two-way ANOVA, where *, P<0.05; **, P≤0.01;***, P<0.001; ****, P<0.0001 where *, P<0.05; **, P≤0.01;***, P<0.001; ****, P<0.0001.

direct repeats, which is bound by PmrA dimers. To further investigate this possibility, we altered the PmrA binding site consensus sequence, creating six different promoter mutants in which one or both of the direct repeats of the PmrA consensus sequence are altered (Figure 23A). Alterations in sequence were made to the repeat most proximal or distal to the QseB dependent transcriptional start, as well as both repeats (Figure 23A). Figure 23A depicts the different promoter mutants, with mutations that affect sequence alone are shown in orange and mutations that affect both sequence and DNA topology are shown in pink.

Binding of the resulting sequences with purified PmrA or phosphomimetic QseB was evaluated using EMSAs (Fig. 23B-D). As expected, PmrA binding affinity was decreased with any alteration to the consensus sequence (Figure 23B-D). Interestingly, alterations affecting DNA topology and sequence at the most proximal repeat also decreased QseB affinity, suggesting that QseB binds closest to the proximal repeat within the PmrA consensus sequence (Fig. 23 B-C). However, alterations to sequence alone at the most distal repeat was able to increase QseB affinity (Fig. 23D). Mutations to the PmrA consensus sequence was able to alter both QseB and PmrA binding affinities, suggesting that binding sites for both proteins overlap (Fig. 23).

*Mutations in Pqse cluster within distinct E. coli phylogroups*

After evaluating rationally designed P*qse* mutations (Fig. 23), we sought to identify naturally occurring variations in the *qseBC* promoter region among *E. coli* isolates. To do this we worked with collaborators Ashlee Earl and Abigail Manson at the Broad Institute to align P*qse* nucleotide sequences from 49 different *E. coli* strains. The strains were chosen based on their genomic sequence quality as well as their diversity among the five different *E. coli*

phylogroups. Figure 24 shows the generated phylogeny, which outlines the strain, pathotype, pathogenicity, and phylogroup. The tree also shows the four mutations that were identified within the P*qse* sequence for each strain. Of these mutations, mutations "1" and "2" were found only 4 strains, which suggests that these SNPs are less phylogenetically significant and less representative of the phylogroup as a whole (Fig. 24). However, mutation "3" is found in all of the group B2 strains, as well as three group D strains, which harbor the majority of UPEC strains, and *Shigella*. Remarkably, mutation "4" clusters exclusively in group E strains, which typically harbor EHEC (Fig. 24). The location of these mutations within the P*qse* sequence is shown in Figure 25. Mutation "3", which is associated with the ExPEC in this phylogeny, lies just 4 nucleotides upstream of the -35 region of the previously reported constitutive transcriptional start site of *qseBC* (Fig. 25 and (Clarke et al., 2005)), while the EHEC associated mutation "4" lies directly downstream of the -10 region of the same transcriptional start site (Fig. 25 and Clarke et al., 2005)). These data show that there are naturally occurring SNPs within the *qseBC* promoter region that cluster with specific pathotypes of *E. coli*. We are in the process of evaluating how these SNPs influence *qseBC* expression and PmrA and/or QseB interactions with the promoter.

## Discussion

PmrA and QseB are both capable of binding the *qseBC* promoter *in vitro*; however, PmrA is able to bind in either the phospho-mimetic or phospho-inactive state (Fig. 21), suggesting that it could possibly be acting as a repressor of *qseBC* in the absence of signal. QseB was able to cause a discernible shift in the DNA in its phosphorylated state, suggesting that only QseB~P productively engages the *qseBC* promoter. Moreover, stoichiometric amounts of

PmrA~P somehow enhanced QseB~P binding (Fig. 21F), suggesting that, in stoichiometric amounts, PmrA aids in stabilizing QseB – DNA interactions. This could be due to differential binding of PmrA and PmrA~P. PmrA~P may be positioned such that QseB~P interactions with the DNA are stabilized. However, data in Figure 22 suggest that over-expression of PmrA leads to a decrease in *qseBC* transcript, potentially because PmrA has an inherently higher affinity for P*qse* (Fig. 21B-D), out-competing QseB when in excess. Congruent with this hypothesis, mutations made to the PmrA consensus sequence affect the binding of both response regulators suggesting that the proteins may hinder each other stoichiometrically and would not be able to bind P*qse* simultaneously (Fig. 23).

The precise mechanism by which PmrA modulates *qseBC* transcription in conjunction with QseB~P remains unclear. Absence of PmrA or QseB ablates the *qseBC* transcriptional surge (Fig. 11), and intermediate *qseBC* expression levels are observed in the Δ*qseC*Δ*pmrA* mutant (Figs. 7B and 22), suggesting an activating role for PmrA, yet overexpression of PmrA shuts down *qseBC* transcription. This paradox could be explained by the position of the PmrA binding consensus. One of the tandem repeats precedes the -35 region for the more proximal transcription start site, while the other repeat is found within the -10 region. If only the repeat at the -35 region is bound, then PmrA may act as a class I activator, stabilizing RNA polymerase on the promoter to initiate transcription. If the proximal repeat is occupied at the -10 region, this could inhibit RNA polymerase-promoter interactions, preventing transcription initiation. Future efforts will focus on dissecting protein-protein interactions between PmrA and QseB, as well as PmrA and RNA polymerase. Additional experiments are needed to determine how PmrA affects transcription of the two transcriptional start sites. These experiments are outlined in detail in Chapter VI.

Naturally occurring SNPs within the *qseBC* promoter region suggest that the mechanism of *qseBC* transcriptional control may vary among different pathotypes of *E. coli*. Notably, these SNPs cluster within distinct phylogroups associated with ExPEC and EHEC strains, which could potentially contribute to our understanding of how the QseBC signaling cascades may differ between UPEC and EHEC. We are in the process of determining how SNPs in the *qseBC* promoter may influence QseB and PmrA interactions with the DNA and therefore affect downstream stimulus responses.

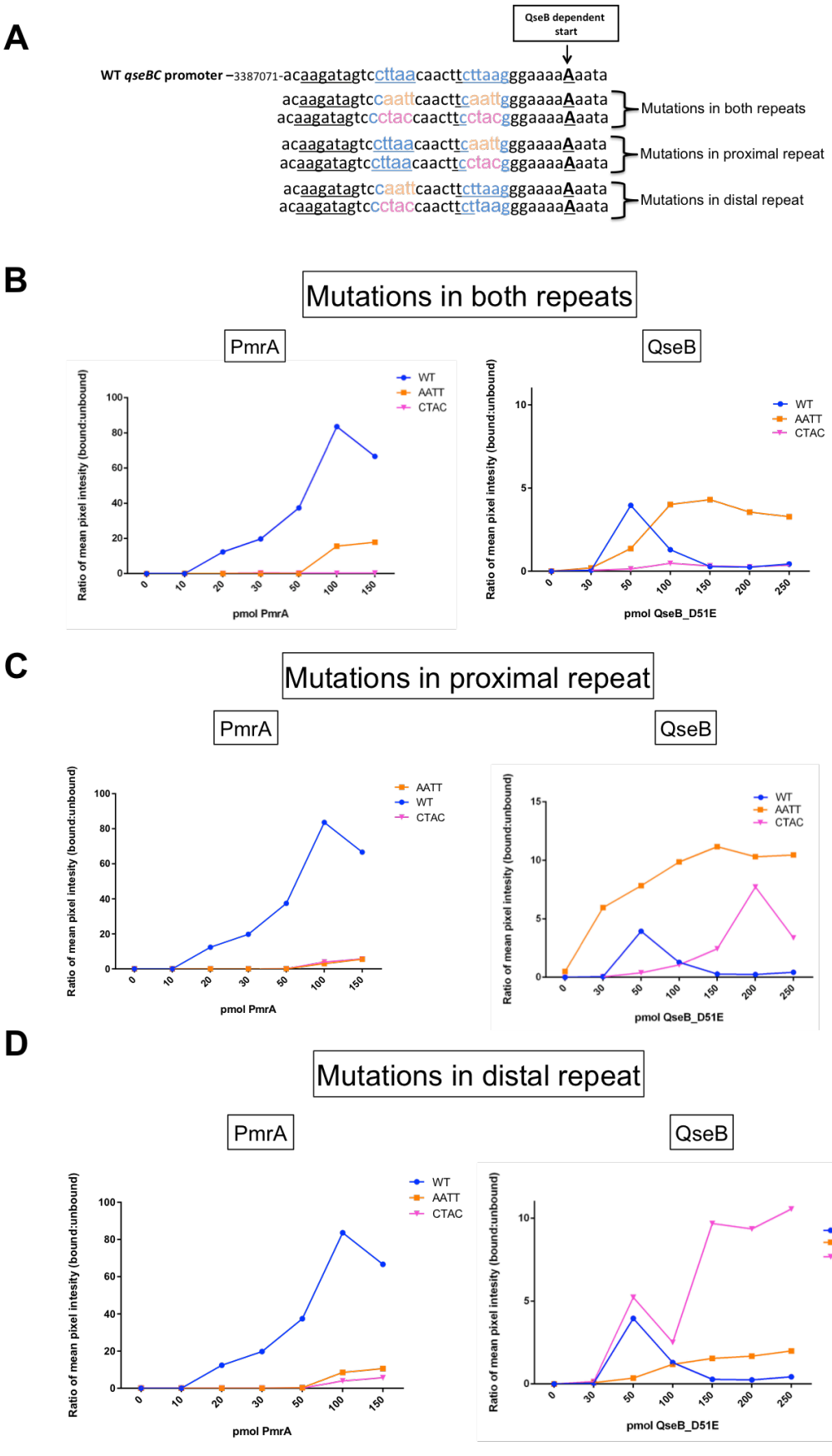
A
QseB dependent start
WT qseBC promoter –3387071-acaagatagtccttaacaacttcttaaggaaaaAaata
acaagatagtccaattcaacttcaattggaaaaAaata
acaagatagtcctacaacttcctacggaaaaAaata
Mutations in both repeats
acaagatagtccttaacaacttcaattggaaaaAaata
acaagatagtccttaacaacttcctacggaaaaAaata
Mutations in proximal repeat
acaagatagtccaattcaacttcttaaggaaaaAaata
acaagatagtcctacaacttcttaaggaaaaAaata
Mutations in distal repeat
B
Mutations in both repeats
PmrA
QseB
Ratio of mean pixel intesity (bound:unbound)
pmol PmrA
pmol QseB_D51E
WT
AATT
CTAC
C
Mutations in proximal repeat
PmrA
QseB
D
Mutations in distal repeat
PmrA
QseB

**Figure 23. PmrA and QseB binding sites overlap.**

A) Schematic showing the mutations made in proximal *qseBC* promoter. The QseB dependent transcriptional start site is shown in bold. The -10 and -35 regions are underlined. The PmrA binding consensus sequence is shown in blue. Binding site variants are shown in varying colors (orange and pink). B-D) EMSAs using purified WT PmrA or phospho-mimetic QseB with radiolabled *qseBC* promoter containing various mutations in the predicted PmrA binding site. Graph represents binding as a ratio of mean pixel intensity of bound versus unbound.

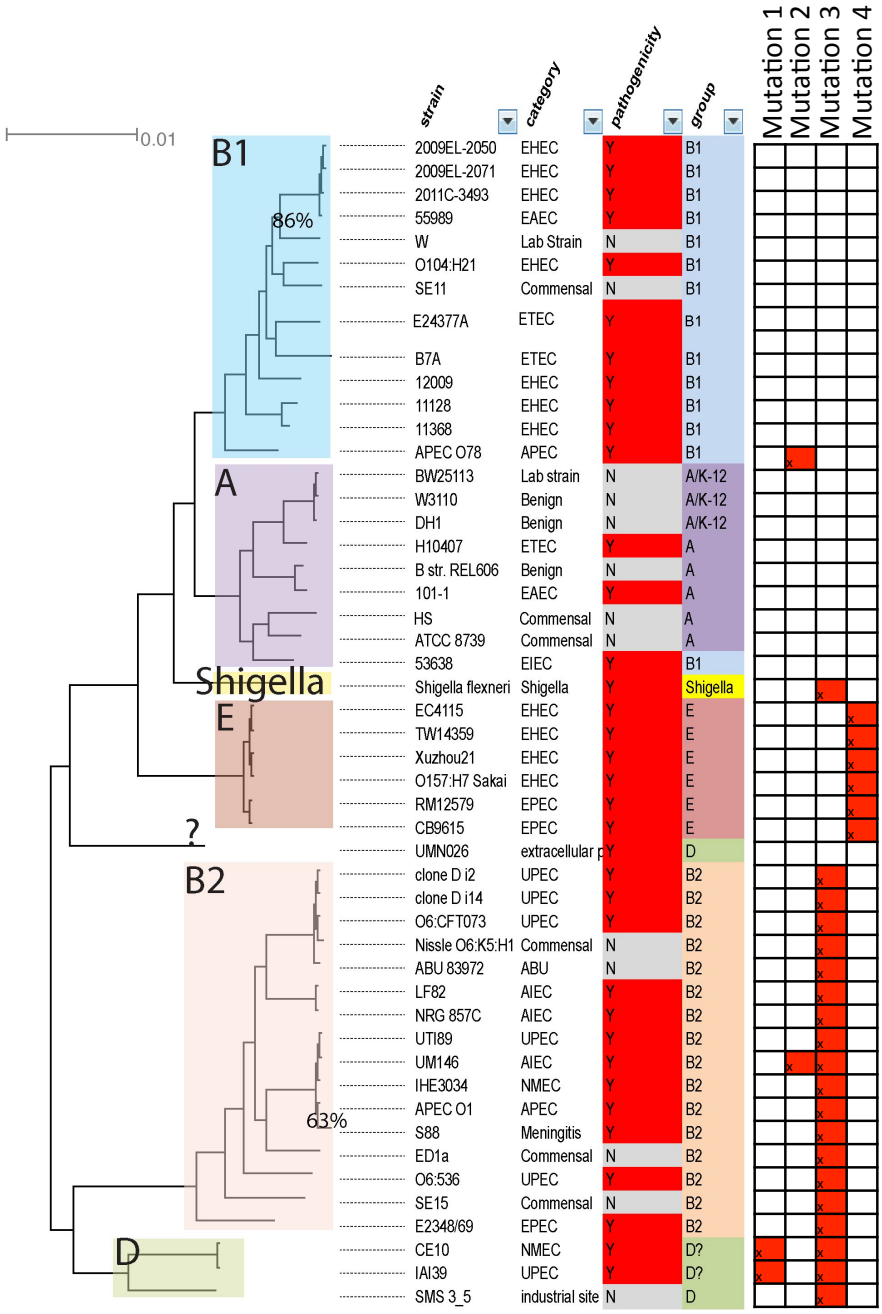


**Figure 24. P*qse* mutations cluster to distinct phylogroups.**

Phylogeny of *E. coli* strains with corresponding P*qse* mutations deviating from the consensus shown to the right. All bootstrap values were above 90%, except for the two nodes indicated on the tree.

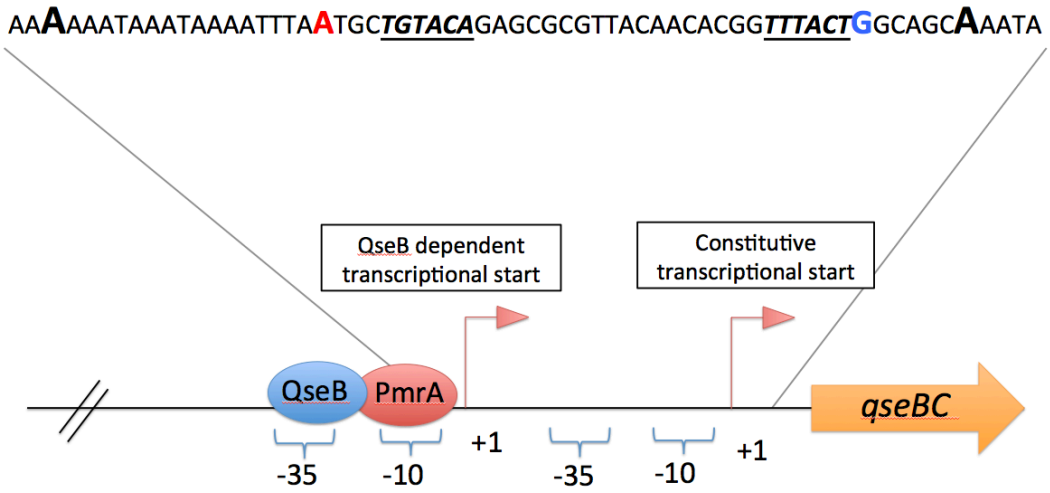


**Figure 25. Schematic of naturally occurring P*qse* mutations.**

The sequence shown is the UTI89 sequence. Transcriptional start sites are shown in larger font. The -10 and -35 regions for the constitutive transcriptional start site are shown in bold, italics, and underlined. The location of mutation 3 is shown in red, while the location of mutation 4 is shown in blue. The nucleotide at mutation 3 is a guanine in the A, B1, and E groups, and the nucleotide at mutation 4 is an adenine in group E strains.

# CHAPTER V

# DELINEATING THE UPEC QSEBC-PMRAB REGULON IN RESPONSE TO FERRIC IRON

## Introduction

The previous chapters investigated the signal transduction pathway between PmrAB and QseBC in response to ferric iron. The outcome of this signal transduction pathway is increased tolerance to PMB in several urinary *E. coli* isolates. While the PmrAB regulon has been thoroughly delineated in *Salmonella*, downstream target genes regulated by QseB and PmrA that contribute to this phenotype in UPEC have yet to be elucidated. In this chapter we used RNA sequencing (RNA-seq) to begin to delineate gene targets that are QseB- and PmrA-regulated in response to the ferric iron signal.

## Methods

### *Bacterial strains*

All studies have been performed in the uropathogenic *Escherichia coli* strain UTI89 (Mulvey et al., 2001) and isogenic mutants. UTI89Δ*pmrA*, UTI89Δ*pmrB*, UTI89Δ*qseC*Δ*pmrA*, UTI89Δ*qseC*, UTI89Δ*qseB*, and UTI89Δ*qseB*Δ*pmrA* (Guckes et al., 2013 PNAS; Hadjifrangiskou et al., 2011; Kostakioti et al. 2009).

### *Sample collection*

Cultures were grown to logarithmic phase in N-minimal media at 37°C with shaking before adding 100μM ferric iron. To collect samples at various time points after the stimulus,

the culture was temporarily moved to room temperature, statically and subsequently returned to shaking at 37°C between time points. Four milliliters were collected for each time point and subsequently used for RNA extraction via the RNeasy kit (Qiagen) and DNase-treatment using Turbo DNase I (Ambion). DNAse-treated RNA was then analyzed using a Qubit and Bioanalyzer. All samples had an RNA integrity number (RIN) of at least 7 before being used for cDNA library construction. Samples in this thesis are representative of one biological replicate. Analyses of a second replicate and collection of a third replicate are ongoing.

*RNA-sequencing and analysis*

DNAse-treated RNA was submitted to the Vanderbilt Technologies for Advanced Genomics (VANTAGE) core. VANTAGE performed mRNA enrichment using the Illumina Ribo-Zero kit and prepared cDNA libraries with the Illumina Tru-seq stranded mRNA sample prep kit. Sequencing was performed at Single Read 50 HT bp on the Illumina HiSeq 2500. With the help of collaborator Dr. Thomas Stricker, reads were aligned to the UTI89 genome (NC_007946.1) and subsequently subjected to *k*-means clustering analysis.

Gene lists for each cluster resulting from the *k*-means clustering analysis were generated using the Database for Annotation, Visualization, and Integrated Discovery (DAVID) (Huang da, Sherman, & Lempicki, 2009).

## Results and Discussion

Samples for RNA-seq were collected for UTI89 and six key isogenic mutants immediately prior as well as 15 and 60 minutes post-ferric iron stimulus. These time points were chosen based on the *qseBC* activation surge depicted in Figure 11, as 15 minutes post-stimulus

marks the peak of steady-state transcript levels for *qseBC* and 60 minutes post-stimulus shows a marked decrease in upregualtion, as the bacteria respond to the stressor and the TCS begins to "reset" (Shin et al., 2006). At 60 minutes post-stimulus, QseB and PmrA downstream targets, such as *yibD*, begin to peak (Fig. 15).

In addition to WT UTI89, the isogenic mutants were the following: (i) UTI89Δ*pmrA* and UTI89Δ*qseB,* lacking one of the two response regulators, (ii) UTI89Δ*qseB*Δ*pmrA*, to decipher genes whose expression is altered in response to ferric iron, but not QseB and PmrA mediated, (iii) UTI89Δ*pmrB* to identify genes that are regulated independent of PmrB mediated signal transduction, (iv) UTI89Δ*qseC* as a control as this mutant has been previously evaluated for global transcriptional and metabolomic devations from the WT strain (Hadjifrangiskou et al., 2011), (v) UTI89Δ*qseC*Δ*pmrA* to identify genes whose expression changes are solely due to PmrB-mediated QseB activation, as well as explore the transcriptional profile of a strain with inherent increased in resistance to PMB (Figure 17).

Transcript levels over time for all strains were grouped based on similar patterns of expression called clusters. Eight distinct clusters were extrapolated from the data (Figure 26). Cluster 1 mimics the pattern observed during an activation surge (Figs. 11 and 26). Consistent with the qPCR in Chapter III (Fig. 11), both *qseB* and *qseC* can be found within Cluster 1 in WT UTI89. Other cluster patterns include genes that are repressed over time (Clusters 2, 5 and 8), genes that are activated over time (Clusters 3, 4, and 7), and genes that are repressed and subsequently de-repressed (Cluster 6).

To further analyze these clusters, we began generating gene lists beginning with the WT strain using the DAVID online bioinformatics tool (Huang da, Sherman, & Lempicki, 2009). Table 3 depicts how genes from Cluster 1 were categorized into functional annotation summaries

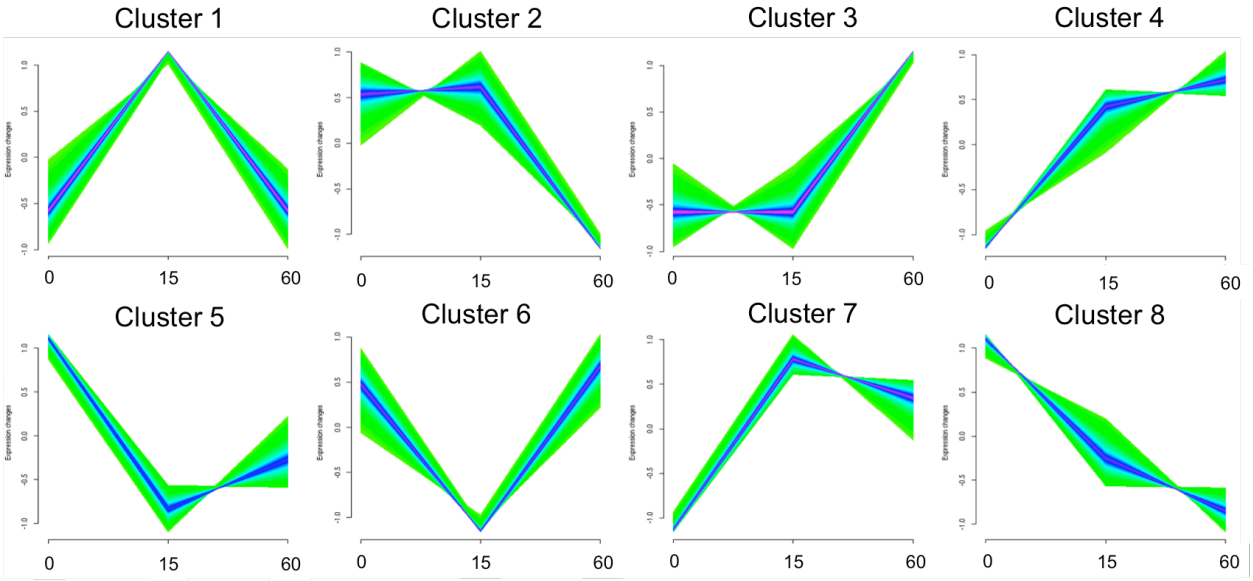


**Figure 26. Gene expression clusters resulting from RNA-seq experiment.**

Clusters were generated using k-means clustering analysis. Clusters are shown here as a type of heat map, where genes that do not fit the cluster pattern as tightly are shown in green, while those shown in blue and pink fit the cluster patter more tightly. Numbers on the X-axis of each cluster indicate the time post-ferric iron stimulus in minutes. Expression changes are shown on the Y-axis.

using this bioinformatics tool. This portion of the data was chosen for initial evaluation given that our internal control, the *qseBC* transcriptional surge, mimics the Cluster 1 expression pattern (Fig. 11), and the *qseBC* activation surge is only observed for the WT strain. DAVID generated gene lists by grouping annotated genes from another database, KEGG, using common biological pathway terms. Some genes are associated to multiple pathways, and thus appear in multiple pathway lists. There are at least 2 genes in each list. Not all genes from the WT strain within Cluster 1 are listed, only those which group with like pathway terms based on information pulled from the KEGG database.

Most gene groups are consistent with pathways that are expected to be subject to swift transcriptional changes given the experimental conditions. For example, as expected while replicating in minimal media, one of the functional gene groups is related to metabolism. Also, consistent with rapid changes in transcription, one gene group consisted of genes predicted to code for proteins, which would bind DNA and/or regulate transcription. Another expected category that appeared for WT bacteria in Cluster 1 was the 'ion-binding' pathway; however, the proteins found within this functional list are predicted to bind ions other than $Fe^{3+}$. The nucleotide-binding group is also unsurprising given most genes in that category are predicted to bind ATP; however, this group also interestingly includes a gene predicted to code for an ATPase associated with a type VI secretion system (T6SS). There was also a gene group containing genes related to bacteriophage replication.

Initial comparisons were made by evaluating the differences in gene groups between WT Cluster 1 and the other six strains tested: Δ*qseC* (Table 4), Δ*pmrB*, (Table 5), Δ*pmrA* (Table 6), Δ*qseB* (Table 7), Δ*qseB*Δ*pmrA* (Table 8), Δ*qseC*Δ*pmrA* (Table 9). Tables 4-9 contain the genes within Cluster 1 gene groups that differed from those within WT Cluster 1 gene groups. These

tables were generated with the same functional annotation gene clustering method using DAVID (Huang da, Sherman, & Lempicki, 2009).

When comparing the Δ*qseC* strain with WT, Cluster 1 contains no differences in the genes within the phage group. Though some differences were observed between the nucleotide-binding group, the most differences can be seen in the genes within the metabolism group (Table 4). These differences observed between WT and Δ*qseC* the metabolism genes were expected given the known global metabolic differences between these strains in the absence of signal (Hadjifrangiskou et al., 2011).

There were also differences observed in Cluster 1 metabolism group genes between Δ*pmrB* and WT. Specifically the differences in metabolism included the presence of phosphotransferase system (PTS) genes, which are involved in sugar transport (Table 5). Interestingly, there was also an oxidoreductase Fe-S subunit gene that appeared in the Δ*pmrB* ion-binding group (Table 5). Because Δ*pmrB* codes for the sensor that initiates the QseBC-PmrAB downstream signaling in response to ferric iron, it is likely that this oxidoreductase expression is independent of the QseBC-PmrAB signaling cascade. The same gene predicted to encode this oxidoreductase Fe-S subunit is found in Cluster 1 for the Δ*pmrA* strain (Table 6), providing further evidence that this gene expression pattern is independent of QseBC-PmrAB ferric iron responses.

The differences in Cluster 1 genes for strains deficient in the response regulators, Δ*pmrA,* Δ*qseB,* and Δ*qseB*Δ*pmrA*, were mostly in the nucleotide-binding group or the transcriptional control group. In contrast to what was observed in the strains devoid of either sensor kinase, the Δ*pmrA* strain had no differences in genes within the Cluster 1 metabolism group compared to WT. Though the Δ*pmrA* strain had no transcriptional control group differences compared to WT

within Cluster 1, Δ*qseB,* and Δ*qseB*Δ*pmrA* share the same gene predicted to encode a LysR-family transcriptional regulator (Tables 7-8).

The greatest difference between Δ*qseC*Δ*pmrA* and WT Cluster 1 gene groups are the genes contained within the phage group. While the Δ*qseC* strain had three phage group genes that differed from WT in Cluster 1 (Table 4), Δ*qseC*Δ*pmrA* had a remarkable 11 phage genes that differed from WT (Table 9). Interestingly, there were no other strains that saw any phage gene differences compared to WT.

The data shown in Tables 3-9 and Figure 26 come from a single biological experiment. A second biological replicate has been sequenced and is in the process of being analyzed and collated with the first data set. Samples will also be collected for a third biological replicate. For fear of alterations in the content of the various clusters after acquiring sequencing data for all necessary biological replicates, the pathway analysis performed for Cluster 1 will be completed for all strains and clusters after all data has been coalesced.

Additionally, it will be important to track genes of interest, such as those predicated to be involved in LPS modification, to determine if they associate with different clusters in the various isogenic mutants. We expect those genes to be in Clusters 4 or 7, following an expression pattern similar to that of *yibD*. Comparisons will be made across strains at specific time points during the ferric iron response, giving better insight as to which genes are controlled by the different QseBC and PmrAB components, either directly or indirectly. For example, given that the UTI89Δ*qseC*Δ*pmrA* has a higher PMB MIC (Fig. 17), some LPS modification genes may be upregulated at all time points compared to the other isogenic mutants.

While the PmrAB regulon has been well studied in *Salmonella enterica* (Chen & Groisman, 2013), our experiments will provide valuable information about the PmrAB regulon

in pathogenic *E. coli.* Additionally, unlike PmrA, which is predicted to bind 70 different promoters, QseB has thus far shown to directly bind only two promoter regions (Clarke et al., 2006). The full extent of the QseBC regulon is unknown, and these deep-sequencing experiments will provide insight as to which genes are directly or indirectly controlled by QseB. The most valuable insights will come from the comparisons between UTI89Δ*qseB,* UTI89Δ*pmrA,* and UTI89Δ*qseB*Δ*pmrA*, as these will help to elucidate the QseBC-PmrAB regulon overlap.

**Table 3. Cluster 1 functional gene groups from the WT UTI89 strain**

| **Metabolism group** | | |
|---|---|---|
| Locus Tag | Gene Name | Function |
| UTI89_C4639 | - | Putative phosphorelay sensor kinase |
| UTI89_C0380 | - | Putative nucleotidyltransferase |
| UTI89_C1673 | - | Putative transferase |
| UTI89_C1755 | - | Permease IIC component (Sugar phosophotransferase system) |
| UTI89_C1756 | - | D-glucosamine phosphotransferase activity |
| UTI89_C3971 | - | D-glucosamine phosphotransferase activity |
| UTI89_C4001 | - | D-glucosamine phosphotransferase activity |
| UTI89_C4003 | - | Putative xylulose kinase |
| UTI89_C4004 | - | Putative phosphocarrier protein (Serine/threonine kinase activity) |
| UTI89_C4202 | - | Putative transferase activity |
| UTI89_C4206 | - | D-glucosamine phosphotransferase activity |
| UTI89_C4207 | - | D-glucosamine phosphotransferase activity |
| UTI89_C4208 | - | Putative transcriptional antiterminator |
| UTI89_C4405 | - | Carbamate kinase (Arginine metabolic process) |
| UTI89_C4587 | - | Putative phosphotransferase |
| UTI89_C4588 | - | D-glucitol-6-phosphate dehydrogenase |
| **Nucleotide-binding group** | | |
| UTI89_C4639 | - | Putative phosphorelay sensor kinase |

| | | |
|---|---|---|
| UTI89_C0832 | *gsiA* | Glutathione import ATP-binding protein |
| UTI89_C0939 | *gpP* | Putative viral capsid assembly |
| UTI89_C1138 | - | Hypothetical protein (GTP binding) |
| UTI89_C2672 | - | Phage Nil2 gene P DnaB analogue (DNA helicase activity) |
| UTI89_C3197 | *clpB* | Putative T6SS ATPase |
| UTI89_C3693 | *rbsA* | Ribose transport ATP-binding protein |
| UTI89_C4528 | - | Hypothetical protein (nucleotide catabolism) |
| UTI89_C4634 | *sucC* | Succinyl-CoA ligase (ATP-binding) |
| **Ion-binding group** | | |
| UTI89_C3319 | - | Putative oxidoreductase (Binds $Zn^{2+}$) |
| UTI89_C4528 | - | Hypothetical protein (nucleotide catabolism) |
| UTI89_C4634 | *sucC* | Succinyl-CoA ligase (ATP-binding) |
| **Phage group** | | |
| UTI89_C0939 | *gpP* | Putative viral capsid assembly |
| UTI89_C1313 | - | Putative DNA packaging protein |
| UTI89_C1498 | - | Putative DNA packaging protein |
| **Transcriptional control group** | | |
| UTI89_C0297 | - | Transcriptional regulator (MarR-family) |
| UTI89_C2682 | - | Putative host FtsH protease inhibitor of phage Sf6 |
| UTI89_C3000 | - | Hypothetical (HTH domain) |
| UTI89_C3216 | - | Putative transcriptional antiterminator |
| UTI89_C4208 | - | Putative transcriptional antiterminator |

**Table 4. Differences in Cluster 1 between WT and Δ*qseC***

| **Metabolism group** | | |
|---|---|---|
| Locus Tag | Gene Name | Function |
| UTI89_C2218 | - | Acyl-CoA dehydrogenase |
| UTI89_C2222 | - | Peptide/polyketide synthase |
| UTI89_C2711 | - | Aminotransferase |
| UTI89_C3183 | - | Cysteine sulfinate desulfinase |
| UTI89_C3437 | - | Oxidoreductase |
| UTI89_C3971 | - | Phosphotransferase system protein |
| UTI89_C4955 | - | D-serine dehydratase 2 |
| **Nucleotide-binding group** | | |
| UTI89_C1458 | - | Excisionase |
| UTI89_C2218 | - | Acyl-CoA dehydrogenase |
| UTI89_C2257 | - | Transposase |
| **Ion-binding group** | | |
| UTI89_C5104 | - | Hypothetical protein |
| UTI89_C3274 | | Isopentenyl-diphosphate Delta-isomerase (Binds Mg2+ subunit) |
| UTI89_C5104 | - | Hypothetical protein |
| **Phage group** | | |
| None | | |
| **Transcriptional control group** | | |
| UTI89_C0227 | - | LysR family transcriptional regulator |

| | | |
|---|---|---|
| UTI89_C0683 | - | Transcriptional regulator |
| UTI89_C0912 | | Hypothetical protein |
| UTI89_C1556 | - | DEOR-type transcriptional regulator |
| UTI89_C1757 | - | Hypothetical protein |

**Table 5. Differences in Cluster 1 between WT and Δ*pmrB***

| **Metabolism group** | | |
|---|---|---|
| Locus Tag | Gene Name | Function |
| UTI89_C3671 | - | P-hydroxybenzoic acid efflux pump |
| UTI89_C4585 | - | PTS system mannose-specific transporter |
| UTI89_C4586 | - | Sorbose PTS component |
| UTI89_C1294 | - | Hypothetical protein |
| UTI89_C1481 | - | DNA adenine methyltransferase |
| UTI89_C4934 | - | Hypothetical protein |
| **Nucleotide-binding group** | | |
| UTI89_C1294 | - | Hypothetical protein |
| UTI89_C1481 | - | DNA adenine methyltransferase |
| UTI89_C2258 | - | Transposase |
| UTI89_C2913 | - | Transposase |
| UTI89_C4934 | - | Hypothetical protein |
| **Ion-binding group** | | |
| UTI89_C1863 | - | Oxidoreductase Fe-S subunit |
| UTI89_C1997 | - | Hypothetical protein |
| UTI89_C4527 | - | Hypothetical protein |
| **Phage group** | | |
| None | | |
| **Transcriptional control group** | | |
| UTI89_C2258 | - | Transposase |

| | | |
|---|---|---|
| UTI89_C2958 | - | Hypothetical protein |
| UTI89_C4417 | - | Putative transcriptional regulator |
| UTI89_C4934 | - | Hypothetical protein |
| UTI89_C4957 | - | Putative transcriptional regulator |

**Table 6. Differences in Cluster 1 between WT and Δ*pmrA***

| **Metabolism group** | | |
|---|---|---|
| Locus Tag | Gene Name | Function |
| None | | |
| **Nucleotide-binding group** | | |
| UTI89_C1386 | - | ABC transporter ATP binding protein |
| UTI89_C1458 | - | Excisionase |
| UTI89_C2218 | - | Acyl-CoA dehydrogenase |
| UTI89_C2257 | - | Transposase |
| UTI89_C1386 | - | ABC transporter ATP binding protein |
| UTI89_C1458 | - | Excisionase |
| UTI89_C2218 | - | Acyl-CoA dehydrogenase |
| UTI89_C2257 | - | Transposase |
| UTI89_C1386 | - | ABC transporter ATP binding protein |
| **Ion-binding group** | | |
| UTI89_C2567 | - | NADH dehydrogenase subunit |
| UTI89_C3253 | - | XdhC iron-sulfur-binding subunit |
| UTI89_C3463 | - | Iron compound receptor |
| UTI89_C4583 | - | Oxidoreductase |
| **Phage group** | | |
| None | | |
| **Transcriptional control group** | | |
| None | | |

**Table 7. Differences in Cluster 1 between WT and Δ*qseB***

| **Metabolism group** | | |
|---|---|---|
| Locus Tag | Gene Name | Function |
| UTI89_C1099 | - | Aminotransferase |
| UTI89_C1228 | - | PTS system protein |
| UTI89_C1786 | - | Hypothetical protein |
| UTI89_C2718 | - | Putative transport protein |
| UTI89_C2997 | - | Hypothetical protein |
| UTI89_C3214 | - | Beta-cystathionase |
| UTI89_C4399 | - | PTS system protein |
| UTI89_C4977 | - | Hypothetical protein |
| UTI89_C5103 | - | Hypothetical protein |
| **Nucleotide-binding group** | | |
| UTI89_C1131 | - | Hypothetical protein |
| UTI89_C2180 | gsiA | ABC transporter protein |
| UTI89_C2257 | gpP | Transposase |
| UTI89_C4671 | - | Oligopeptide ABC transporter protein |
| UTI89_C1131 | - | Hypothetical protein |
| UTI89_C2180 | gsiA | ABC transporter protein |
| UTI89_C2257 | gpP | Transposase |
| UTI89_C4671 | - | Oligopeptide ABC transporter protein |
| UTI89_C1131 | - | Hypothetical protein |
| **Ion-binding group** | | |

| | | |
|---|---|---|
| UTI89_C1080 | efeU | Ferrous iron permease |
| UTI89_C3459 | - | Iron ABC transporter |
| **Phage group** | | |
| None | | |
| **Transcriptional control group** | | |
| UTI89_C0317 | - | LysR family transcriptional regulator |
| UTI89_C4624 | - | Putative regulator |
| UTI89_C4653 | - | Putative transcriptional regulator |
| UTI89_C4853 | - | Hypothetical protein |
| UTI89_C4911 | - | Hypothetical protein |

**Table 8. Differences in Cluster 1 between WT and Δ*qseB*Δ*pmrA***

| **Metabolism group** | | |
|---|---|---|
| Locus Tag | Gene Name | Function |
| UTI89_C1564 | - | Bacterial cellulose biosynthesis |
| UTI89_C2157 | - | Hypothetical protein |
| UTI89_C4198 | - | Glutamate transport protein |
| UTI89_C4207 | - | PTS system protein |
| UTI89_C4387 | - | Threonine efflux system |
| UTI89_C1564 | - | Bacterial cellulose biosynthesis |
| UTI89_C2157 | - | Hypothetical protein |
| UTI89_C4198 | - | Glutamate transport protein |
| UTI89_C4207 | - | PTS system protein |
| **Nucleotide-binding group** | | |
| None | | |
| **Ion-binding group** | | |
| None | | |
| **Phage group** | | |
| None | | |
| **Transcriptional control group** | | |
| UTI89_C0317 | - | LysR family transcriptional regulator |
| UTI89_C0750 | - | Hypothetical protein |
| UTI89_C0965 | - | Bacteriophage Wphi phage protein |
| UTI89_C4853 | - | Hypothetical protein |

| | | |
|---|---|---|
| UTI89_C4973 | - | Hypothetical protein |
| UTI89_C4975 | - | Hypothetical protein |

**Table 9. Differences in Cluster 1 between WT and Δ*qseC*Δ*pmrA***

| **Metabolism group** | | |
|---|---|---|
| Locus Tag | Gene Name | Function |
| UTI89_C0019 | - | Hypothetical protein |
| UTI89_C1139 | - | Putative autotransporter |
| UTI89_C1518 | - | Hypothetical protein |
| UTI89_C2234 | - | Outer membrane receptor for iron compound |
| UTI89_C3194 | - | Hypothetical protein |
| UTI89_C4143 | - | Autotransport adhesin |
| **Nucleotide-binding group** | | |
| UTI89_C0242 | - | Hypothetical protein |
| UTI89_C2218 | - | Acyl-CoA dehydrogenase |
| UTI89_C2898 | SrmB | ATP-dependent RNA helicase |
| UTI89_C3974 | - | Phosphoglycerate dehydrogenase |
| UTI89_C4528 | - | Hypothetical protein |
| **Ion-binding group** | | |
| UTI89_C1863 | - | Oxidoreductase Fe-S subunit |
| UTI89_C4465 | - | Dehydrogenase |
| UTI89_C4528 | - | Hypothetical protein |
| UTI89_C5064 | yjjN | Zinc-type alcohol dehydrogenase |
| **Phage group** | | |
| UTI89_C0038 | - | Transposase |
| UTI89_C0563 | - | Prophage |

| | | |
|---|---|---|
| UTI89_C0683 | - | Transcriptional regulator |
| UTI89_C1267 | - | Prophage lambda integrase |
| UTI89_C1350 | - | Hypothetical protein |
| UTI89_C1437 | InsG | Transposase |
| UTI89_C1694 | - | Hypothetical protein |
| UTI89_C2204 | - | Prophage P4 integrase |
| UTI89_C3458 | - | Hypothetical protein |
| UTI89_C4475 | - | Hypothetical protein |
| UTI89_C4934 | - | Hypothetical protein |
| **Transcriptional control group** | | |
| UTI89_C0683 | - | Putative transcriptional regulator |
| UTI89_C1556 | - | DEOR-type transcriptional regulator |
| UTI89_C3458 | - | Hypothetical protein |
| UTI89_C4957 | - | Putative transcriptional regulator |

# CHAPTER VI

# FUTURE DIRECTIONS

## Introduction

One of the main questions remaining in the bacterial TCS field is how bacteria are able to adapt to an ever-changing environment, filled with an overwhelming number of signals and stressors, using only a finite number of signaling networks. The work presented in this thesis has focused on addressing this conundrum by investigating two cross-interacting TCSs, QseBC and PmrAB. In contrast to other cross-interacting systems that have been reported, PmrB robustly phosphorylates both response regulators, including the non-cognate partner, QseB, in the presence of a single signal. Uniquely, all four components of these systems are required for proper regulation in response to signal, including QseC, which to date has not been shown to be directly involved in the PmrB mediated signal cascade. Once PmrA and QseB are in their active form, they regulate genes that result in increased tolerance to PMB. Current ongoing studies are focused on evaluating the extent of the regulon that is controlled by QseB and PmrA in response to ferric iron. Additionally, questions still remain concerning the control of response regulator phosphorylation and expression, as well as the relevance of QseBC-PmrAB cross-interactions during infection. This chapter centers on the future directions of this project concerning QseBC-PmrAB regulation and their role in virulence.

## Future Directions

*QseBC-PmrAB regulon*

RNA-seq experiments to explore the QseBC-PmrAB regulon are ongoing. Once all biological replicates have been assimilated, we can evaluate how genes of interest, such as those involved LPS modification like *yibD*, move to different Cluster patterns in the different *qse*/*pmr* mutants. For example, if a subset of these LPS modification genes move from Cluster 4 in the WT to Cluster 8 in Δ*qseB*, implicating QseB as an important regulator for these genes. Genes that move to different Clusters in Δ*qseB,* but not Δ*pmrA* for example, would be considered part of the QseB regulon, and not the PmrA regulon. Gene lists will be generated based on how they change Clusters in the different isogenic mutants. Genes suspected to be part of the QseB and PmrA regulons by RNA-seq will be confirmed using qPCR and EMSAs.

*QseBC promoter control*

As discussed in Chapter IV, the exact mechanism by which PmrA contributes to *qseBC* expression remains unknown. The decrease in transcript levels in the Δ*qseC*Δ*pmrA* mutant compared to Δ*qseC* (Fig. 7), suggests that PmrA is an activator. However, over-expression of PmrA in Δ*qseC*Δ*pmrA* leads to WT levels of motility and *qseB* steady-state transcript, suggesting that PmrA is a repressor (Fig. 22). As discussed in Chapter IV, it is possible that PmrA represses one *qseBC* transcriptional start site, while activating the other, depending on which repeat is bound and/or in response to different growth conditions. To test this hypothesis, primer extension experiments should be performed for the WT, as well as the Δ*qseC*Δ*pmrA* and Δ*qseC* mutants. Additionally, primer extension should also be used to assess how the *qseBC* promoter region fires 15 minutes after WT bacteria have been exposed to the ferric iron signal, at the height of the transcriptional surge. Results from these experiments will determine which

transcriptional start site is preferred when the signal transduction cascade is impaired when a when a *qse*/*pmr* components bacteria or when the bacteria are actively responding to signal.

Another unanswered question raised by results in Chapter IV concerns the ability of the QseB and PmrA response regulators to occupy the *qseBC* promoter region simultaneously. Initial EMSAs suggest that both proteins are unable to bind the promoter at the same time, likely due to steric hindrance (Fig. 21E and Fig. 23). However, evidence shown in Chapter IV also suggests that PmrA may help to stabilize QseB interactions with its native promoter (Fig. 21). This would require QseB and PmrA to physically interact, at least temporarily, during transcription initiation. Co-immunoprecipitation with recently raised PmrA antibodies, as well as Förster resonance energy transfer (FRET) or yeast two-hybrid experiments could be used to test if PmrA and QseB directly interact with one another. Together these experiments would improve our understanding of a complex regulatory mechanism used to control the expression of components that comprise a unique bacterial signaling cascade.

*EHEC and UPEC differences in QseBC signaling*

In Chapter IV, unique SNPs in the *qseBC* promoter region were found to associate with specific *E. coli* phylogroups that largely comprise UPEC or EHEC strains. Given the differences in QseBC signaling reported between these two pathotypes of *E. coli*, studies should be conducted to test whether these SNPs contribute to the reported divergence in the QseBC signaling cascade. Site-directed mutagenesis could be utilized to alter the P*qse*::*gfp* construct to change the sequence to the EHEC sequence. If these mutations are relevant to QseBC-PmrAB mediated ferric iron responses, qPCR would capture changes in the activation surge normally observed with the native UPEC promoter. It is also possible that changes in the promoter

sequence could allow QseB or PmrA to engage the DNA differently in response to other signals, causing an activation surge in response to epinephrine.

*QseC involvement in proper signal responses*

Previous work has established that in UPEC, the absence of QseC causes a dominant misregulation of over 500 genes (Hadjifrangiskou et al., 2011). Chapter II describes that the additional deletion of the PmrB sensor kinase ablates this misregulation because PmrB would be unable to phosphorylate QseB. Delays in phosphatase function (Fig. 6) from PmrB toward QseB provide a strong suggestion that de-phosphorylation of QseB is responsible for the over activation of QseB, leading to the aberrant gene regulation. Another hypothesis for how QseC prevents an accumulation of QseB within the bacterial cell by sequestering QseB, preventing PmrB from physically interacting with QseB. Similarly, it is also possible that QseC interacts with PmrB as a heterodimer until signal is detected, freeing each sensor kinase to homodimerize and phosphorylate PmrA and QseB appropriately. Experiments using co-immunoprecipitation to pull down PmrB and evaluating associated proteins would elucidate if PmrB physically interacts with QseC in the absence of signal. FRET could also be used to detect physical interactions between QseC and PmrB *in vivo*.

*Relevance of QseBC-PmrAB interactions to virulence*

Although Chapter III provides evidence that QseBC-PmrAB cross-interactions provide a mechanism to tolerate cationic membrane stress (Fig. 18), these *in vitro* experiments do not comprehensively mimic the stressors UPEC encounter in a host. It is more likely that UPEC experience cationic stressors such as the antimicrobial peptide LL-37, rather than ferric iron, in

the bladder. Evidence provided in Chapter II shows that QseBC signaling is important to, UPEC virulence as strains lacking QseC are severely attenuated (Fig. 5). However, the extent to which QseBC-PmrAB signaling contributes to UPEC adaptation and survival during cationic stress in the host has yet to be determined.

One way to evaluate if QseBC-PmrAB interactions are vital to survival during exposure to cationic stress is to test mutants deficient in various components of the TCSs in a chronic murine model of UTI. During acute infection, UPEC are able to evade most stressors by invading the superficial umbrella cells in the bladder and forming IBCs (Anderson et al., 2003; Bower et al., 2005; Justice et al., 2004). As infection progresses, these cells are exfoliated, leaving only immature urothelial that are not conducive to IBC formation (Thumbikat et al., 2009). Therefore, during a chronic infection, the bacteria remain extracellular and exposed to the host immune responses. Additionally, recurrent UTIs are thought to partially be caused by UPEC dwelling within patient gastrointestinal tract (Yamamoto et al., 1997), making the gut another extracellular niche for UPEC.

Initial studies to determine if QseBC-PmrAB interactions were important for UPEC to occupy the gut or urinary tract niches during chronic infection were performed using either WT UIT89, as well as a mutant with increased resistance to PMB, Δ*qseC*Δ*pmrA* and a mutant deficient in both response regulators, Δ*qseB*Δ*pmrA*. Twenty female C3H/HeN mice per strain were transurethrally infected and urines and feces were collected for 13 days post-infection to track colonization and infection resolution (Figs. 27 and 28). Studies have demonstrated that urinalysis at 24 hours post-infection is predictive of chronic colonization if mice shed > $10^4$ bacteria per mL of urine. Mice with high urine titers are separated fomr those predicted to resolve to prevent mice that have resolved their infection from becoming re-infected due to

coprophagic behavior. On day 14, the mice were sacrificed and bacterial burdens were calculated for bladders, kidneys, ceca, proximal colons, and distal colons (Fig. 29).

The bacteria recovered from urine and feces fluctuated over time for each strain. Interestingly, an increase in bacteriuria was observed in the double response regulator mutant, Δ*qseB*Δ*pmrA* (Fig. 27). A mild increase in UPEC within murine feces on day 13 was also observed for this strain (Fig. 28). This increase in colonization could be due to lack of alterations in the LPS that could make the bacteria more likely to be detected by the host via Toll-like receptor (TLR)4. This hypothesis should be investigated by using the Δ*qseB*Δ*pmrA* mutant for transurethral infection of C3H/HeJ mice, which are deficient in TLR4. The only difference observed between WT and Δ*qseC*Δ*pmrA* was a defect in fecal burdens at 10 days post-infection (Fig. 28). Upon sacrifice at day 14, mice that were chronically infected with Δ*qseB*Δ*pmrA* had higher amounts of bacteria in their kidneys compared to mice chronically infected with the WT strain; no differences were observed between the mutants and WT in the gut (Fig. 29).

Although not many significant defects were observed during this two-week experiment, other chronic models have extended infections out to 4 weeks. Extending the *qse*/*pmr* experiments to the 4-week point would be informative, especially when looking at bladder burdens as the two-week experiment shows a trend where the mutants seem to colonize better. Additionally, it would be interesting to investigate differences in immune responses to these various strains via cytokine profiling. Differences in immune responses may help to explain the increase in Δ*qseB*Δ*pmrA* seen in the urine compared to WT, as well as the increase in bladder colonization, although the colonization phenotype is not statically significant (Figs. 27 and 29).

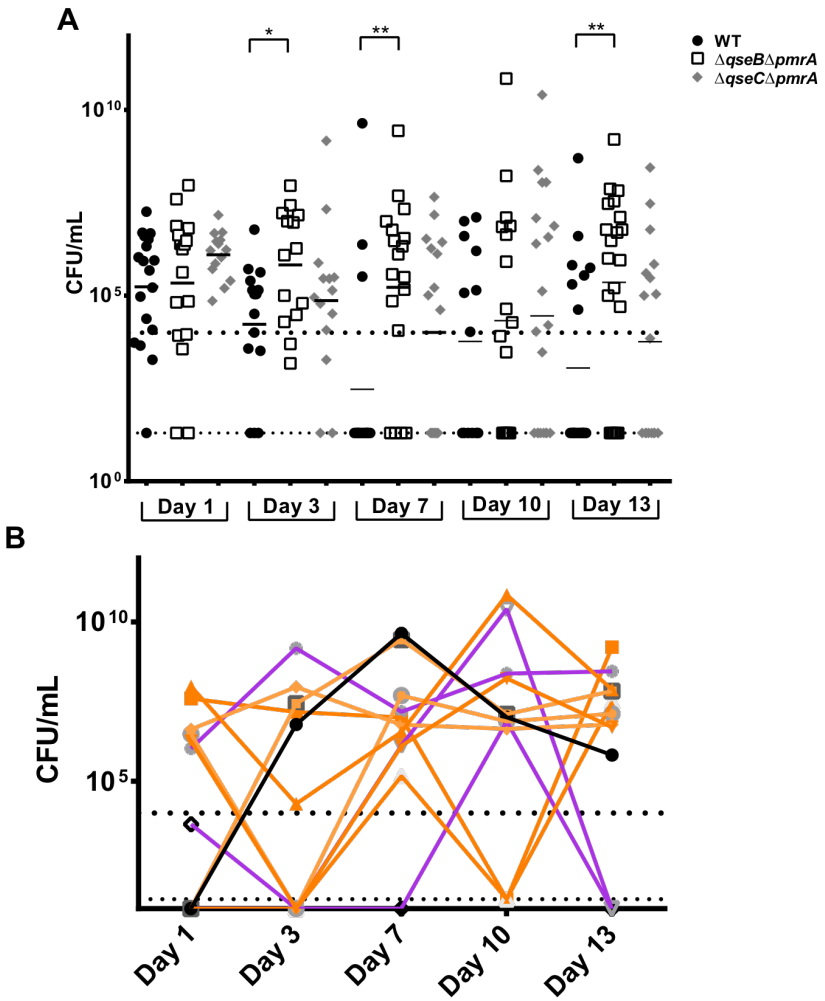


**Figure 27. Urinalysis of chronic mouse infection**

Mice were infected with $10^7$ bacterial cells from WT UTI89, UTI89Δ*qseB*Δ*pmrA*, or UTI89Δ*qseC*Δ*pmrA* via transurethral inoculation. Urines were collected from the mice on day 1, 3, 7, 10, and 13 post-infection. A) Scatter plot of colony forming units (CFUs) in urines of mice at indicated days post-infection. After day 1, mice were sorted into 'chronic' or 'resolved' cages based whether the mice had more (chronic) or less (resolved) than $10^4$ bacteria per mL in their urine. B) The same data in the scatter plot was graphed as a line plot where each line represents a mouse that was deemed chronically infected, based on final bladder burdens that exceed $10^4$ CFU/mL. Lines represent mice infected with WT (black), Δ*qseB*Δ*pmrA* (orange), and Δ*qseC*Δ*pmrA* (purple). The dotted line just above $10^1$ indicates the limit of detection for this assay. Statistical analyses were performed using non-parametric Mann-Whitney test where * represents $p \leq 0.05$; ** $p \leq 0.01$.

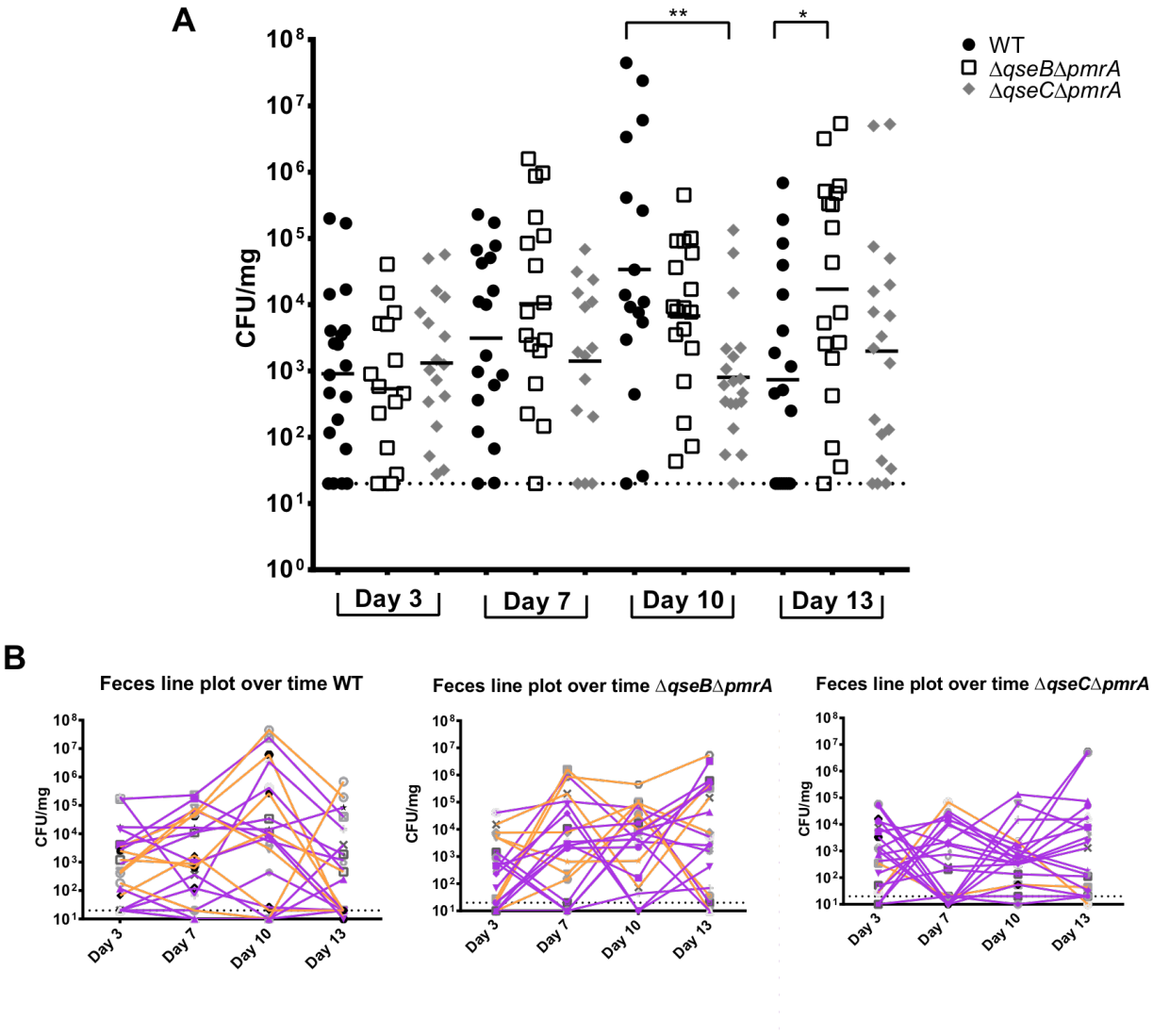


**Figure 28. Bacterial burdens in feces during chronic mouse infection**

Fecal samples were collected from the same mice depicted in Figure 27. A) Scatter plot of colony forming units (CFUs) in feces of mice at indicated days post-infection. B) The same data in the scatter plot was graphed as a line plot where each line represents a mouse. The same data in the scatter plot was graphed as a line plot where each line represents a mouse. Purple lines represent mice predicted to become chronic and orange lines represent mice predicted to resolve the infection based on day 1 urinalysis. The dotted line just above $10^1$ indicates the limit of detection for this assay. Statistical analyses were performed using non-parametric Mann-Whitney test where * represents $p \leq 0.05$; ** $p \leq 0.01$.

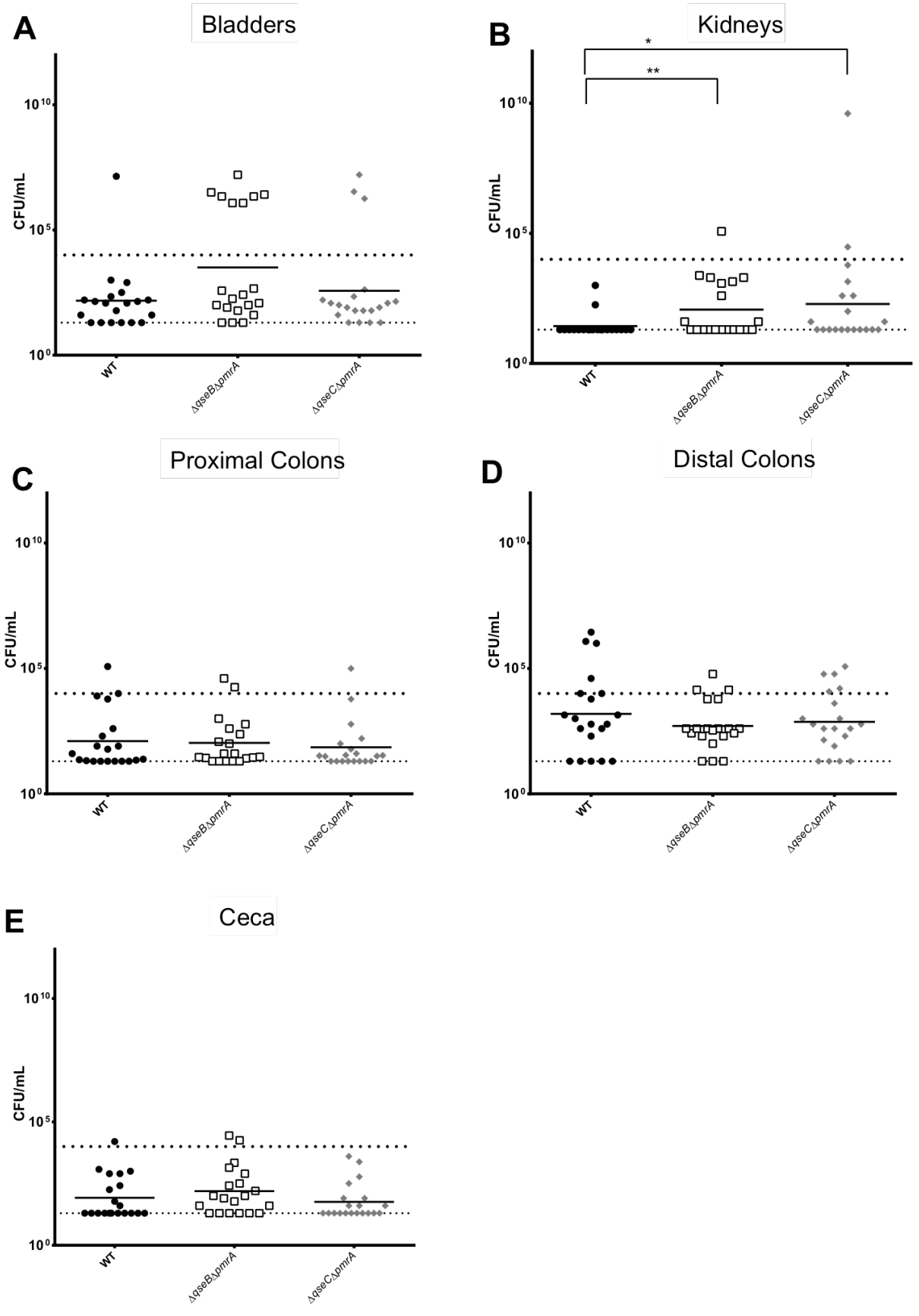
A
Bladders
B
Kidneys
C
Proximal Colons
D
Distal Colons
E
Ceca
CFU/mL
$10^{10}$
$10^{5}$
$10^{0}$
*
**
WT
ΔqseBΔpmrA
ΔqseCΔpmrA

**Figure 29. Bacterial burdens in mice 14 days post-infection**

Mice were sacrificed at 14 days post-infection. Organs were harvested and homogenized and bacterial burdens were evaluated by counting CFUs/mL A-E) Bacterial burdens for indicated organs are shown as a scatter plot with geometric mean indicated by a solid horizontal line. The dotted line just above $10^1$ indicates the limit of detection for this assay. The dotted line just above $10^4$ indicates the cutoff used to describe mice that were chronically infected. Statistical analyses were performed using non-parametric Mann-Whitney test where * represents ** $p \leq 0.01$.

Another possible contribution QseBC-PmrAB interactions may have to bacterial fitness is the ability to compete with other members of the normal microbiota. All tested strains UPEC was able to colonize the gastrointestinal tract. Despite the lack of statistical differences between bacterial burdens in the gut at two weeks post-infection, recurrent UTIs occur over the course of months or years. It is possible that QseBC-PmrAB signaling is important for maintaining colonization in these organs over a longer period of time. Some evidence to support this comes from the RNA-seq experiment presented in Chapter V. An ATPase associated with a T6SS, used for interbacterial competition, was found to have an expression pattern similar to *qseBC* in WT UTI89 during ferric iron exposure. If this and other T6SS components are found to have expression patterns that fluctuate in the different *qse*/*pmr* mutants, this would suggest that T6SS expression is controlled by QseB and/or PmrA. Interestingly, the *qseBC* operon lies within a gene cluster containing genes predicted to encode T6SS components. It would be valuable to test mutants lacking various genes predicted to encode components of the T6SS in a chronic model of UTI. These mutants would be predicted to have a colonization defect in the gut, where UPEC would have to compete with normal microbiota for nutrients and space. Together these experiments would improve our understanding of a complex, unique bacterial signaling cascade and its relevance to pathogenesis.

# REFERENCES


Alves, R., & Savageau, M. A. (2003). Comparative analysis of prototype two-component systems with either bifunctional or monofunctional sensors: differences in molecular structure and physiological function. *Mol Microbiol, 48*(1), 25-51.

Anderson, G. G., Palermo, J. J., Schilling, J. D., Roth, R., Heuser, J., & Hultgren, S. J. (2003). Intracellular bacterial biofilm-like pods in urinary tract infections. *Science, 301*(5629), 105-107. doi: 10.1126/science.1084550

Anriany, Y., Sahu, S. N., Wessels, K. R., McCann, L. M., & Joseph, S. W. (2006). Alteration of the rugose phenotype in waaG and ddhC mutants of *Salmonella enterica* serovar Typhimurium DT104 is associated with inverse production of curli and cellulose. *Appl Environ Microbiol, 72*(7), 5002-5012. doi: 72/7/5002 [pii] 10.1128/AEM.02868-05

Autret, N., Raynaud, C., Dubail, I., Berche, P., & Charbit, A. (2003). Identification of the agr locus of Listeria monocytogenes: role in bacterial virulence. *Infect Immun, 71*(8), 4463-4471.

Bearson, B. L., & Bearson, S. M. (2008). The role of the QseC quorum-sensing sensor kinase in colonization and norepinephrine-enhanced motility of Salmonella enterica serovar Typhimurium. *Microb Pathog, 44*(4), 271-278. doi: 10.1016/j.micpath.2007.10.001

Bearson, B. L., Bearson, S. M., Lee, I. S., & Brunelle, B. W. (2010). The *Salmonella enterica* serovar Typhimurium QseB response regulator negatively regulates bacterial motility and swine colonization in the absence of the QseC sensor kinase. *Microb Pathog, 48*(6), 214-219. doi: 10.1016/j.micpath.2010.03.005

Belete, B., Lu, H., & Wozniak, D. J. (2008). *Pseudomonas aeruginosa* AlgR regulates type IV pilus biosynthesis by activating transcription of the fimU-pilVWXY1Y2E operon. *J Bacteriol, 190*(6), 2023-2030. doi: 10.1128/JB.01623-07

Bijlsma, J. J., & Groisman, E. A. (2005). The PhoP/PhoQ system controls the intramacrophage type three secretion system of Salmonella enterica. *Mol Microbiol, 57*(1), 85-96. doi: 10.1111/j.1365-2958.2005.04668.x

Bower, J. M., Eto, D. S., & Mulvey, M. A. (2005). Covert operations of uropathogenic *Escherichia coli* within the urinary tract. *Traffic, 6*(1), 18-31. doi: 10.1111/j.1600-0854.2004.00251.x

Capra, E. J., & Laub, M. T. (2012). Evolution of two-component signal transduction systems. *Annu Rev Microbiol, 66*, 325-347. doi: 10.1146/annurev-micro-092611-150039

Capra, E. J., Perchuk, B. S., Ashenberg, O., Seid, C. A., Snow, H. R., Skerker, J. M., & Laub, M. T. (2012). Spatial tethering of kinases to their substrates relaxes evolutionary constraints on specificity. *Mol Microbiol, 86*(6), 1393-1403. doi: 10.1111/mmi.12064

Capra, E. J., Perchuk, B. S., Lubin, E. A., Ashenberg, O., Skerker, J. M., & Laub, M. T. (2010). Systematic dissection and trajectory-scanning mutagenesis of the molecular interface that ensures specificity of two-component signaling pathways. *PLoS Genet, 6*(11), e1001220. doi: 10.1371/journal.pgen.1001220

Chen, H. D., & Groisman, E. A. (2013). The biology of the PmrA/PmrB two-component system: the major regulator of lipopolysaccharide modifications. *Annu Rev Microbiol, 67*, 83-112. doi: 10.1146/annurev-micro-092412-155751

Clarke, M. B., Hughes, D. T., Zhu, C., Boedeker, E. C., & Sperandio, V. (2006). The QseC sensor kinase: a bacterial adrenergic receptor. *Proc Natl Acad Sci U S A, 103*(27), 10420-10425. doi: 10.1073/pnas.0604343103

Clarke, M. B., & Sperandio, V. (2005). Transcriptional autoregulation by quorum sensing *Escherichia coli* regulators B and C (QseBC) in enterohaemorrhagic *E. coli* (EHEC). *Mol Microbiol, 58*(2), 441-455. doi: 10.1111/j.1365-2958.2005.04819.x

Cotter, P. D., Emerson, N., Gahan, C. G., & Hill, C. (1999). Identification and disruption of lisRK, a genetic locus encoding a two-component signal transduction system involved in stress tolerance and virulence in *Listeria monocytogenes*. *J Bacteriol, 181*(21), 6840-6843.

Drepper, T., Wiethaus, J., Giaourakis, D., Gross, S., Schubert, B., Vogt, M., . . . Masepohl, B. (2006). Cross-talk towards the response regulator NtrC controlling nitrogen metabolism in *Rhodobacter capsulatus*. *FEMS Microbiol Lett, 258*(2), 250-256. doi: 10.1111/j.1574-6968.2006.00228.x

Ducey, T. F., Carson, M. B., Orvis, J., Stintzi, A. P., & Dyer, D. W. (2005). Identification of the iron-responsive genes of *Neisseria gonorrhoeae* by microarray analysis in defined medium. *J Bacteriol, 187*(14), 4865-4874. doi: 187/14/4865 [pii] 10.1128/JB.187.14.4865-4874.2005

Foxman, B. (2010). The epidemiology of urinary tract infection. *Nat Rev Urol, 7*(12), 653-660. doi: 10.1038/nrurol.2010.190

Foxman, B. (2014). Urinary tract infection syndromes: occurrence, recurrence, bacteriology, risk factors, and disease burden. *Infect Dis Clin North Am, 28*(1), 1-13. doi: 10.1016/j.idc.2013.09.003

Gao, R., & Stock, A. M. (2013). Evolutionary tuning of protein expression levels of a positively autoregulated two-component system. *PLoS Genet, 9*(10), e1003927. doi: 10.1371/journal.pgen.1003927

Goodman, A. L., Merighi, M., Hyodo, M., Ventre, I., Filloux, A., & Lory, S. (2009). Direct interaction between sensor kinase proteins mediates acute and chronic disease phenotypes in a bacterial pathogen. *Genes Dev, 23*(2), 249-259. doi: 10.1101/gad.1739009

Groisman, E. A. (2001). The pleiotropic two-component regulatory system PhoP-PhoQ. *J Bacteriol, 183*(6), 1835-1842. doi: 10.1128/JB.183.6.1835-1842.2001

Guckes, K. R., Kostakioti, M., Breland, E. J., Gu, A. P., Shaffer, C. L., Martinez, C. R., 3rd, . . . Hadjifrangiskou, M. (2013). Strong cross-system interactions drive the activation of the QseB response regulator in the absence of its cognate sensor. *Proc Natl Acad Sci U S A, 110*(41), 16592-16597. doi: 10.1073/pnas.1315320110

Gunn, J. S., Lim, K. B., Krueger, J., Kim, K., Guo, L., Hackett, M., & Miller, S. I. (1998). PmrA-PmrB-regulated genes necessary for 4-aminoarabinose lipid A modification and polymyxin resistance. *Mol Microbiol, 27*(6), 1171-1182.

Hadjifrangiskou, M., Gu, A. P., Pinkner, J. S., Kostakioti, M., Zhang, E. W., Greene, S. E., & Hultgren, S. J. (2012). "Transposon mutagenesis identifies uropathogenic *Escherichia coli* biofilm factors". *J Bacteriol*. doi: 10.1128/JB.01012-12

Hadjifrangiskou, M., Kostakioti, M., Chen, S. L., Henderson, J. P., Greene, S. E., & Hultgren, S. J. (2011). A central metabolic circuit controlled by QseC in pathogenic *Escherichia coli*. *Mol Microbiol, 80*(6), 1516-1529. doi: 10.1111/j.1365-2958.2011.07660.x

Hannan, T. J., Mysorekar, I. U., Hung, C. S., Isaacson-Schmid, M. L., & Hultgren, S. J. (2010). Early severe inflammatory responses to uropathogenic *E. coli* predispose to chronic and recurrent urinary tract infection. *PLoS Pathog, 6*(8), e1001042. doi: 10.1371/journal.ppat.1001042

Henderson, J. P., Crowley, J. R., Pinkner, J. S., Walker, J. N., Tsukayama, P., Stamm, W. E., . . . Hultgren, S. J. (2009). Quantitative metabolomics reveals an epigenetic blueprint for iron acquisition in uropathogenic *Escherichia coli*. *PLoS Pathog, 5*(2), e1000305. doi: 10.1371/journal.ppat.1000305

Hicks, K. G., Delbecq, S. P., Sancho-Vaello, E., Blanc, M. P., Dove, K. K., Prost, L. R., . . . Miller, S. I. (2015). Acidic pH and divalent cation sensing by PhoQ are dispensable for systemic salmonellae virulence. *Elife, 4*, e06792. doi: 10.7554/eLife.06792

Hooton, T. M., & Stamm, W. E. (1997). Diagnosis and treatment of uncomplicated urinary tract infection. *Infect Dis Clin North Am, 11*(3), 551-581.

House, B., Kus, J. V., Prayitno, N., Mair, R., Que, L., Chingcuanco, F., . . . Barnett Foster, D. (2009). Acid-stress-induced changes in enterohaemorrhagic *Escherichia coli* O157 : H7 virulence. *Microbiology, 155*(Pt 9), 2907-2918. doi: 10.1099/mic.0.025171-0

Howell, A., Dubrac, S., Noone, D., Varughese, K. I., & Devine, K. (2006). Interactions between the YycFG and PhoPR two-component systems in *Bacillus subtilis*: the PhoR kinase phosphorylates the non-cognate YycF response regulator upon phosphate limitation. *Mol Microbiol, 59*(4), 1199-1215. doi: 10.1111/j.1365-2958.2005.05017.x

Huang da, W., Sherman, B. T., & Lempicki, R. A. (2009). Systematic and integrative analysis of large gene lists using DAVID bioinformatics resources. *Nat Protoc, 4*(1), 44-57. doi: 10.1038/nprot.2008.211

Justice, S. S., Hung, C., Theriot, J. A., Fletcher, D. A., Anderson, G. G., Footer, M. J., & Hultgren, S. J. (2004). Differentiation and developmental pathways of uropathogenic *Escherichia coli* in urinary tract pathogenesis. *Proc Natl Acad Sci U S A, 101*(5), 1333-1338. doi: 10.1073/pnas.0308125100

Kato, A., Chen, H. D., Latifi, T., & Groisman, E. A. (2012). Reciprocal control between a bacterium's regulatory system and the modification status of its lipopolysaccharide. *Mol Cell, 47*(6), 897-908. doi: 10.1016/j.molcel.2012.07.017

Kato, A., & Groisman, E. A. (2004). Connecting two-component regulatory systems by a protein that protects a response regulator from dephosphorylation by its cognate sensor. *Genes Dev, 18*(18), 2302-2313. doi: 10.1101/gad.1230804

Kato, A., Latifi, T., & Groisman, E. A. (2003). Closing the loop: the PmrA/PmrB two-component system negatively controls expression of its posttranscriptional activator PmrD. *Proc Natl Acad Sci U S A, 100*(8), 4706-4711. doi: 10.1073/pnas.0836837100
0836837100 [pii]

Konyecsni, W. M., & Deretic, V. (1988). Broad-host-range plasmid and M13 bacteriophage-derived vectors for promoter analysis in *Escherichia coli* and *Pseudomonas aeruginosa*. *Gene, 74*(2), 375-386.

Kostakioti, M., Hadjifrangiskou, M., Cusumano, C. K., Hannan, T. J., Janetka, J. W., & Hultgren, S. J. (2012). Distinguishing the contribution of type 1 pili from that of other QseB-misregulated factors when QseC is absent during urinary tract infection. *Infect Immun, 80*(8), 2826-2834. doi: 10.1128/IAI.00283-12

Kostakioti, M., Hadjifrangiskou, M., Pinkner, J. S., & Hultgren, S. J. (2009). QseC-mediated dephosphorylation of QseB is required for expression of genes associated with virulence in uropathogenic *Escherichia coli*. *Mol Microbiol, 73*(6), 1020-1031. doi: 10.1111/j.1365-2958.2009.06826.x

Kwa, A., Kasiakou, S. K., Tam, V. H., & Falagas, M. E. (2007). Polymyxin B: similarities to and differences from colistin (polymyxin E). *Expert Rev Anti Infect Ther, 5*(5), 811-821. doi: 10.1586/14787210.5.5.811

Laub, M. T., & Goulian, M. (2007). Specificity in two-component signal transduction pathways. *Annu Rev Genet, 41*, 121-145. doi: 10.1146/annurev.genet.41.042007.170548

Lee, L. J., Barrett, J. A., & Poole, R. K. (2005). Genome-wide transcriptional response of chemostat-cultured *Escherichia coli* to zinc. *J Bacteriol, 187*(3), 1124-1134. doi: 10.1128/jb.187.3.1124-1134.2005

Lizewski, S. E., Lundberg, D. S., & Schurr, M. J. (2002). The transcriptional regulator AlgR is essential for *Pseudomonas aeruginosa* pathogenesis. *Infect Immun, 70*(11), 6083-6093.

Mandin, P., Fsihi, H., Dussurget, O., Vergassola, M., Milohanic, E., Toledo-Arana, A., . . . Cossart, P. (2005). VirR, a response regulator critical for *Listeria monocytogenes* virulence. *Mol Microbiol, 57*(5), 1367-1380. doi: 10.1111/j.1365-2958.2005.04776.x

Matsubara, M., Kitaoka, S. I., Takeda, S. I., & Mizuno, T. (2000). Tuning of the porin expression under anaerobic growth conditions by his-to-Asp cross-phosphorelay through both the EnvZ-osmosensor and ArcB-anaerosensor in *Escherichia coli*. *Genes Cells, 5*(7), 555-569. doi: gtc347 [pii]

Mediavilla, J. R., Patrawalla, A., Chen, L., Chavda, K. D., Mathema, B., Vinnard, C., . . . Kreiswirth, B. N. (2016). Colistin- and Carbapenem-Resistant *Escherichia coli* Harboring mcr-1 and blaNDM-5, Causing a Complicated Urinary Tract Infection in a Patient from the United States. *MBio, 7*(4). doi: 10.1128/mBio.01191-16

Merighi, M., Septer, A. N., Carroll-Portillo, A., Bhatiya, A., Porwollik, S., McClelland, M., & Gunn, J. S. (2009). Genome-wide analysis of the PreA/PreB (QseB/QseC) regulon of *Salmonella enterica* serovar Typhimurium. *BMC Microbiol, 9*, 42. doi: 10.1186/1471-2180-9-42

Mika, F., & Hengge, R. (2005). A two-component phosphotransfer network involving ArcB, ArcA, and RssB coordinates synthesis and proteolysis of sigmaS (RpoS) in *E. coli*. *Genes Dev, 19*(22), 2770-2781. doi: 10.1101/gad.353705

Moreno, E., Andreu, A., Pigrau, C., Kuskowski, M. A., Johnson, J. R., & Prats, G. (2008). Relationship between *Escherichia coli* strains causing acute cystitis in women and the fecal *E. coli* population of the host. *J Clin Microbiol, 46*(8), 2529-2534. doi: 10.1128/JCM.00813-08

Morici, L. A., Carterson, A. J., Wagner, V. E., Frisk, A., Schurr, J. R., Honer zu Bentrup, K., . . . Schurr, M. J. (2007). *Pseudomonas aeruginosa* AlgR represses the Rhl quorum-sensing system in a biofilm-specific manner. *J Bacteriol, 189*(21), 7752-7764. doi: 10.1128/JB.01797-06

Mulvey, M. A., Lopez-Boado, Y. S., Wilson, C. L., Roth, R., Parks, W. C., Heuser, J., & Hultgren, S. J. (1998). Induction and evasion of host defenses by type 1-piliated uropathogenic *Escherichia coli*. *Science, 282*(5393), 1494-1497.

Murphy, K. C., & Campellone, K. G. (2003). Lambda Red-mediated recombinogenic engineering of enterohemorrhagic and enteropathogenic *E. coli*. *BMC Mol Biol, 4*, 11.

Nairismagi, M. L., Vislovukh, A., Meng, Q., Kratassiouk, G., Beldiman, C., Petretich, M., . . . Groisman, I. (2012). Translational control of TWIST1 expression in MCF-10A cell lines recapitulating breast cancer progression. *Oncogene, 31*(47), 4960-4966. doi: 10.1038/onc.2011.650

Nakanishi, N., Tashiro, K., Kuhara, S., Hayashi, T., Sugimoto, N., & Tobe, T. (2009). Regulation of virulence by butyrate sensing in enterohaemorrhagic *Escherichia coli*. *Microbiology, 155*(Pt 2), 521-530. doi: 10.1099/mic.0.023499-0

Nguyen, Y., & Sperandio, V. (2012). Enterohemorrhagic *E. coli* (EHEC) pathogenesis. *Front Cell Infect Microbiol, 2*, 90. doi: 10.3389/fcimb.2012.00090

Noriega, C. E., Lin, H. Y., Chen, L. L., Williams, S. B., & Stewart, V. Asymmetric cross-regulation between the nitrate-responsive NarX-NarL and NarQ-NarP two-component regulatory systems from *Escherichia coli* K-12. *Mol Microbiol, 75*(2), 394-412. doi: MMI6987 [pii] 10.1111/j.1365-2958.2009.06987.x [doi]

Overhage, J., Lewenza, S., Marr, A. K., & Hancock, R. E. (2007). Identification of genes involved in swarming motility using a *Pseudomonas aeruginosa* PAO1 mini-Tn5-lux mutant library. *J Bacteriol, 189*(5), 2164-2169. doi: 10.1128/JB.01623-06

Pacheco, A. R., & Sperandio, V. (2012). Shiga toxin in enterohemorrhagic *E. coli*: regulation and novel anti-virulence strategies. *Front Cell Infect Microbiol, 2*, 81. doi: 10.3389/fcimb.2012.00081

Pfaffl, M. W. (2001). A new mathematical model for relative quantification in real-time RT-PCR. *Nucleic Acids Res, 29*(9), e45.

Price, M. N., Dehal, P. S., & Arkin, A. P. (2010). FastTree 2--approximately maximum-likelihood trees for large alignments. *PLoS One, 5*(3), e9490. doi: 10.1371/journal.pone.0009490

Rabin, R. S., & Stewart, V. (1993). Dual response regulators (NarL and NarP) interact with dual sensors (NarX and NarQ) to control nitrate- and nitrite-regulated gene expression in *Escherichia coli* K-12. *J Bacteriol, 175*(11), 3259-3268.

Rasko, D. A., Moreira, C. G., Li de, R., Reading, N. C., Ritchie, J. M., Waldor, M. K., . . . Sperandio, V. (2008). Targeting QseC signaling and virulence for antibiotic development. *Science, 321*(5892), 1078-1080. doi: 10.1126/science.1160354

Richards, S. M., Strandberg, K. L., Conroy, M., & Gunn, J. S. (2012). Cationic antimicrobial peptides serve as activation signals for the *Salmonella* Typhimurium PhoPQ and PmrAB regulons in vitro and in vivo. *Front Cell Infect Microbiol, 2*, 102. doi: 10.3389/fcimb.2012.00102

Schröder, I., Wolin, C. D., Cavicchioli, R., & Gunsalus, R. P. (1994). Phosphorylation and dephosphorylation of the NarQ, NarX, and NarL proteins of the nitrate-dependent two-component regulatory system of Escherichia coli. *J Bacteriol, 176*(16), 4985-4992.

Shin, D., Lee, E. J., Huang, H., & Groisman, E. A. (2006). A positive feedback loop promotes transcription surge that jump-starts *Salmonella* virulence circuit. *Science, 314*(5805), 1607-1609. doi: 10.1126/science.1134930

Sims, G. E., & Kim, S. H. (2011). Whole-genome phylogeny of *Escherichia coli*/*Shigella* group by feature frequency profiles (FFPs). *Proc Natl Acad Sci U S A, 108*(20), 8329-8334. doi: 10.1073/pnas.1105168108

Skerker, J. M., Perchuk, B. S., Siryaporn, A., Lubin, E. A., Ashenberg, O., Goulian, M., & Laub, M. T. (2008). Rewiring the specificity of two-component signal transduction systems. *Cell, 133*(6), 1043-1054. doi: 10.1016/j.cell.2008.04.040

Sperandio, V., Torres, A. G., Jarvis, B., Nataro, J. P., & Kaper, J. B. (2003). Bacteria-host communication: the language of hormones. *Proc Natl Acad Sci U S A, 100*(15), 8951-8956. doi: 10.1073/pnas.1537100100

Sperandio, V., Torres, A. G., & Kaper, J. B. (2002). Quorum sensing *Escherichia coli* regulators B and C (QseBC): a novel two-component regulatory system involved in the regulation of flagella and motility by quorum sensing in *E. coli*. *Mol Microbiol, 43*(3), 809-821.

Stahl, A. L., Arvidsson, I., Johansson, K. E., Chromek, M., Rebetz, J., Loos, S., . . . Karpman, D. (2015). A novel mechanism of bacterial toxin transfer within host blood cell-derived microvesicles. *PLoS Pathog, 11*(2), e1004619. doi: 10.1371/journal.ppat.1004619

Stamatakis, A. (2014). RAxML version 8: a tool for phylogenetic analysis and post-analysis of large phylogenies. *Bioinformatics, 30*(9), 1312-1313. doi: 10.1093/bioinformatics/btu033

Stock, A. M., Robinson, V. L., & Goudreau, P. N. (2000). Two-component signal transduction. *Annu Rev Biochem, 69*, 183-215. doi: 10.1146/annurev.biochem.69.1.183

Tamayo, R., Prouty, A. M., & Gunn, J. S. (2005). Identification and functional analysis of *Salmonella enterica* serovar Typhimurium PmrA-regulated genes. *FEMS Immunol Med Microbiol, 43*(2), 249-258. doi: S0928-8244(04)00186-5 [pii] 10.1016/j.femsim.2004.08.007

Tamayo, R., Ryan, S. S., McCoy, A. J., & Gunn, J. S. (2002). Identification and genetic characterization of PmrA-regulated genes and genes involved in polymyxin B resistance in *Salmonella enterica* serovar typhimurium. *Infect Immun, 70*(12), 6770-6778.

Thumbikat, P., Berry, R. E., Zhou, G., Billips, B. K., Yaggie, R. E., Zaichuk, T., . . . Klumpp, D. J. (2009). Bacteria-induced uroplakin signaling mediates bladder response to infection. *PLoS Pathog, 5*(5), e1000415. doi: 10.1371/journal.ppat.1000415

Whitchurch, C. B., Alm, R. A., & Mattick, J. S. (1996). The alginate regulator AlgR and an associated sensor FimS are required for twitching motility in *Pseudomonas aeruginosa*. *Proc Natl Acad Sci U S A, 93*(18), 9839-9843.

Winfield, M. D., & Groisman, E. A. (2004). Phenotypic differences between *Salmonella* and *Escherichia coli* resulting from the disparate regulation of homologous genes. *Proc Natl Acad Sci U S A, 101*(49), 17162-17167. doi: 10.1073/pnas.0406038101

Wosten, M. M., & Groisman, E. A. (1999). Molecular characterization of the PmrA regulon. *J Biol Chem, 274*(38), 27185-27190.

Wosten, M. M., Kox, L. F., Chamnongpol, S., Soncini, F. C., & Groisman, E. A. (2000). A signal transduction system that responds to extracellular iron. *Cell, 103*(1), 113-125.

Wright, K. J., Seed, P. C., & Hultgren, S. J. (2005). Uropathogenic *Escherichia coli* flagella aid in efficient urinary tract colonization. *Infect Immun, 73*(11), 7657-7668. doi: 10.1128/IAI.73.11.7657-7668.2005

Yamamoto, S., Tsukamoto, T., Terai, A., Kurazono, H., Takeda, Y., & Yoshida, O. (1997). Genetic evidence supporting the fecal-perineal-urethral hypothesis in cystitis caused by *Escherichia coli*. *J Urol, 157*(3), 1127-1129.

Yu, H., Mudd, M., Boucher, J. C., Schurr, M. J., & Deretic, V. (1997). Identification of the *algZ* gene upstream of the response regulator *algR* and its participation in control of alginate production in *Pseudomonas aeruginosa*. *J Bacteriol, 179*(1), 187-193.

Zhou, L., Lei, X. H., Bochner, B. R., & Wanner, B. L. (2003). Phenotype microarray analysis of *Escherichia coli* K-12 mutants with deletions of all two-component systems. *J Bacteriol, 185*(16), 4956-4972.